Title

Energy performance of air distribution systems part II: room air stratification full scale testing

Authors

Webster, Tom
Lukaschek, Wolfgang
Dickeroff, Darryl
et al.

Publication Date

2007-01-22

Peer reviewed

ENERGY PERFORMANCE OF UNDERFLOOR AIR DISTRIBUTION (UFAD) SYSTEMS PART II: ROOM AIR STRATIFICATION FULL SCALE TESTING

Tom Webster, Wolfgang Lukaschek, Darryl Dickerhoff, and Fred Bauman

Center for the Built Environment

Commission Project Manager: Norman Bourassa

PIER Buildings Program

CEC Contract 500-01-035

1 BACKGROUND[1]

Room air stratification (RAS) is one of the key features of UFAD technology that determines how the benefits of low energy, good indoor comfort and ventilation performance are achieved. Understanding, accounting for, and controlling RAS are essential to successful design, installation, and operation of these systems. Likewise, modeling RAS is essential to simulating the energy performance of these systems. Although much research has been focused on RAS for displacement ventilation systems, relatively little has been done to develop a comprehensive model for UFAD systems, and no models currently exist within energy simulation programs commonly used by design and installation practitioners. Development of a model for RAS must be based on sound physical principles as well as also accurately representing the reality of how these systems are installed and operated. That is the purpose of the full scale testing effort we describe in this report.

CBE has been involved in RAS research for several years, and the work reported here can be considered an expansion and improvement over earlier work in CBE's environmental chamber and that performed in partnership with York International at the McGrath Laboratory in St. Louis MO from 2000 and 2001. [Webster, et. al. 2001] The work reported here was conducted between January 2003 and November 2004 in the York Air Distribution Research Facility (ADRF) in York, PA. The full scale testing work was conducted in close collaboration with other elements of this project as described in the final report. [Bauman et. al. 2006] Additional material about UFAD technology can be found in the ASHRAE underfloor design guide [Bauman 2003].

2 OBJECTIVES

The primary objectives of the full scale testing were to conduct a series of tests and provide a database of test results to support the following efforts:

1. Determine sensitivity of RAS to various design, installation, and operating parameters.
2. Compare full scale idealized thermal plume tests to UCSD theoretical and empirical results from bench scale ideal plume testing.
3. Validate the final EnergyPlus models using full scale test results.

[1] Please see the project statement of work for a comprehensive overview of UFAD technology and its perceived benefits as well as an overview of other elements of the overall project in the main body of the report.

3 METHODS

3.1 THE YORK AIR DISTRIBUTION RESEARCH FACILITY (ADRF)

Since the focus of this research is on the cooling performance of UFAD systems in commercial buildings, it is important to conduct the tests in realistic Office environments. The Air Distribution Research Facility located inside a warehouse (see Figure 1) at York International headquarters in York PA provided such an opportunity. Although York originally developed this facility to support product testing and marketing efforts for their UFAD product line, beginning in late 2002, we began working with York to convert the facility to a research grade testing laboratory to support the goals of our full scale testing effort. The ADRF was configured to provide realistic simulated offices spaces for interior and perimeter zones by installing actual office furniture, computer workstations, and thermal manikins to simulate occupants. For perimeter zones, a solar simulator was created by installing high temperature quartz lamps outside a window wall on one side of the test room. For most of the testing the chamber was operated using a VAV control strategy thus simulating commonly used control methods. Controls for the test room were integrated into the air handler and chiller control system using York's ISN facility management and control products.

Included in laboratory development work were installation, setup, calibration and verification testing for instrumentation, equipment, system controls, and data acquisition and reduction tools. This was an iterative process that was not fully completed until May 2004 (test Session #6) for interior tests and November 2004 for perimeter tests (test Session #8). Over the two year period of testing during which time 124 tests were performed, York conducted marketing demonstrations between our testing sessions. This required switching the room between a demonstration and research configuration to support both types of activities.

Figure 1: Warehouse at York International in York, PA

3.1.1 FACILITY LAYOUT AND CONSTRUCTION

Figure 2 shows a layout of the ADRF. The facility consists of a test chamber, an adjoining conference room, and an environmental chamber (EC). Air handling equipment is located inside the warehouse adjacent to the EC; chillers are located outside on the East side of the test room. All walls are inside the warehouse except one wall of the test room and two walls of the conference room that are outside walls. The following sections describe the test facility in more detail.

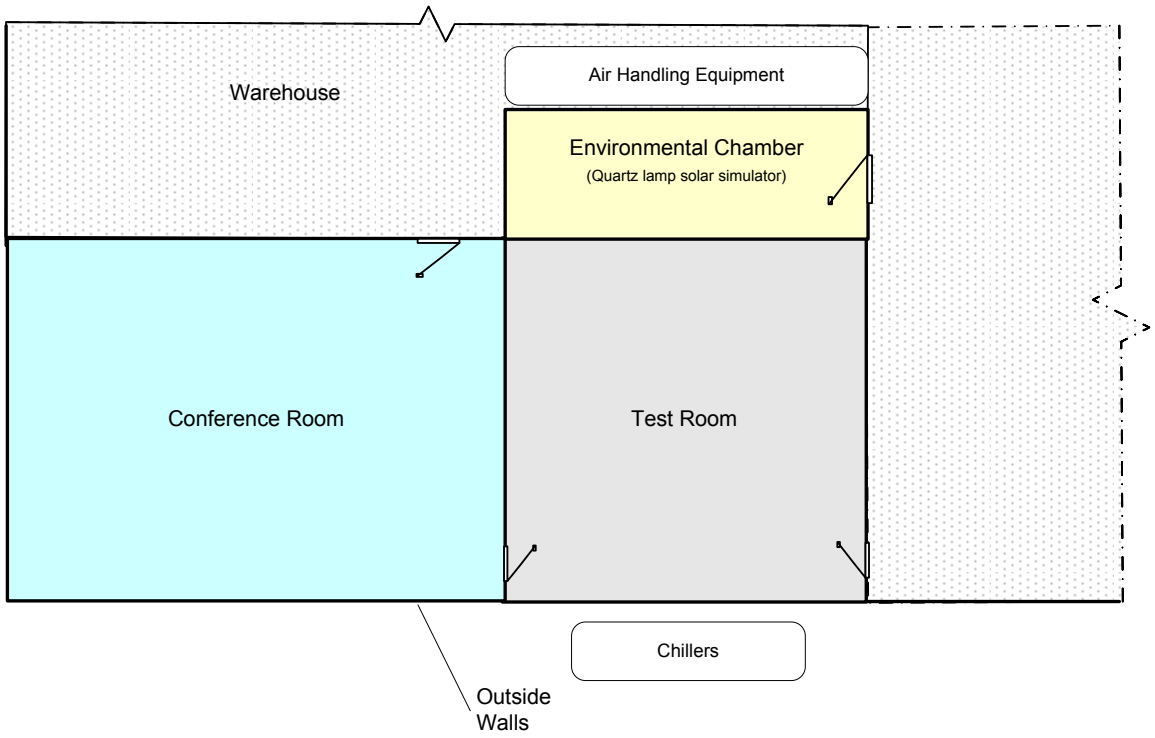

Figure 2: ADRF layout

The test chamber walls (except the West window wall) are all made from 12 inch thick staggered studs at 24 inches o.c. with R30 fiberglass batts installed in the airspace. Inside and outside surfaces are constructed of 5/8 inch sheet rock. A detailed list of test chamber size and thermal properties are shown in Table 1 and Table 2. The U-values are air-to-air values including film coefficients the components of which are used in the EnergyPlus chamber model and simplified heat balances reported in sections below.

Table 1: Test chamber thermal properties

Areas for UF plenum		
	[ft²]	[m²]
North:	26	2.41
South:	26	2.41
East:	26	2.41
West:	26	2.41
Top:	676	62.68
Bottom	676	62.68
Areas for RA plenum		
North:	75	6.95
South:	75	6.95
East:	75	6.95
West:	75	6.95
Top:	676	62.68
Bottom	668	61.94
Areas for test room		
North wall:	209.5	19.42
North door:	24.5	2.27

South wall:	64	5.93
South door:	21	1.95
South window:	80	7.42
East wall:	234	21.70
West wall:	46	4.27
West window, overall	188	17.43
West window, glass	173	16.0
Ceiling:	668	61.94
Floor:	676	62.68

Table 2: Test chamber U-values

Overall U-values		
Surfaces:	[Btu*h^{-1}*ft^{-2}*°F^{-1}]	[W(m²K)]
Walls:	0.028	0.16
Insulated Window:	0.035	0.20
Uninsulated Window:	0.500	2.84
South Wall:	0.029	0.16
Ceiling:	0.444	2.52
Floor:	0.334	1.89
UF plenum bottom	0.040	0.23
RA plenum top	0.035	0.20
Doors:		
Door @ North wall:	0.321	1.82
Door @ South wall:	0.350	1.99
Sum of UA		
	[Btu*h^{-1}*°F^{-1}]	[W °K^{-1}]
RA plenum walls	8.5	4.5
RA plenum roof	23.7	12.5
Room walls:	127.8	67.3
Room floor:	225.5	118.7
SA plenum walls:	3.0	1.6
SA plenum top:	225.5	118.7
SA plenum bottom:	26.9	14.2

The environmental chamber (EC) is attached to the west side of the test room and is separated from it by a curtain wall with double glazed clear glass window. The purpose of this chamber is to allow a wide range of outdoor temperatures to be simulated. The EC also contains an array of lamps which are used to simulate solar radiation. Details of this source are provided in sections below and in the Appendix E In the case of the room air stratification testing as it is discussed and analyzed in this paper, only the impact of solar radiation under summer cooling conditions was investigated.

The conference room is, like the test room, equipped with an underfloor air distribution system which works independently from the one in the test room and uses York MIT variable area diffusers. The data acquisition system is located here along with the interface to the York ISN

monitoring and control system. For marketing purposes, a viewing window is provided in the wall separating the conference room and the test room. This is an aluminum framed double clear glass window with an area 13.8 m² (149 ft²) of and U-value of 2.8 W/(m²K) (0.5 Btu/(hft²°F)). However, this window – except a small one-by-one-foot area - was insulated with an insulating panels during all tests which decreased its thermal conductivity to 0.16 W/(m²K) (0.031 Btu/(hft²°F)). The wall and window have approximately the same thermal conductivity so the average for the wall is nearly the same as this value.

3.1.2 TEST CHAMBER

Figure 3 shows a plan view of the test chamber and Figure 4 is a cross sectional view showing the three primary elements: Occupied space, underfloor plenum and return air plenum. Details of each of these are described in the following sections.

3.1.2.1 Occupied space/test room

As shown in Figure 3 and Figure 4 the test room is a 7.9 m (26 ft) square with an area of 63 m² (676 ft²) and a height of 2.7 m (9 ft) where all room air stratification experiments were conducted. Temperature sensors, manikins, personal computers, desk lamps and other equipment were placed in this room to simulate typical office arrangements. Interior spaces were simulated by placing foam insulating panels on the West window wall and over the windows on the South conference room wall. The West panels were removed when perimeter spaces were simulated.

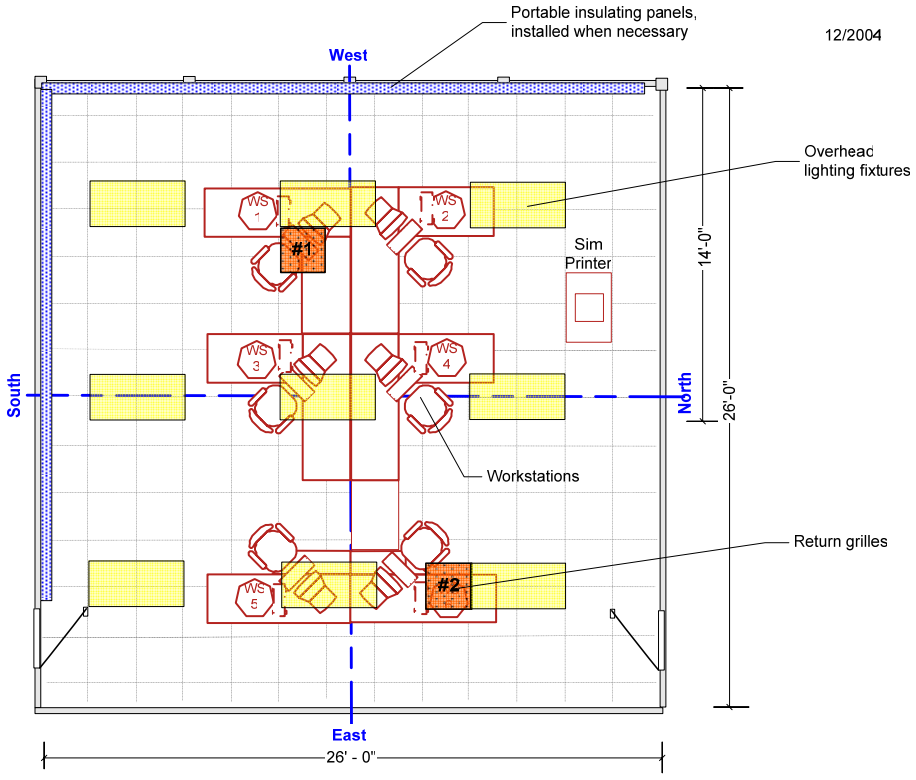

Figure 3: Test chamber layout

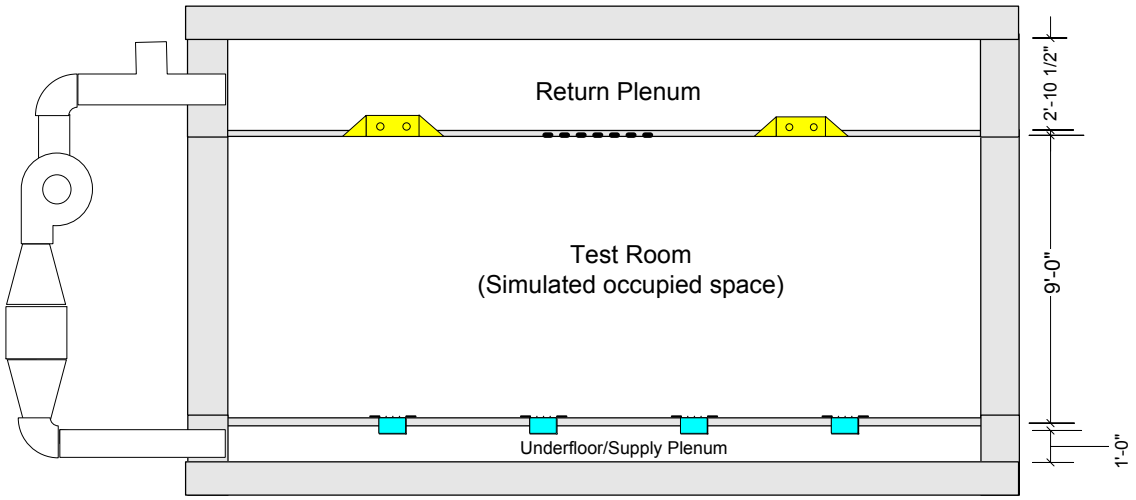

Figure 4: Test chamber cross-section

3.1.2.2 West window

As shown in Table 1 the double clear glass window between the EC and the test room has a total area of 17.5 m² (188 ft²) and a net glass area of 16 m (173 ft²) with the same thermal conductivity as the conference room window of 2.8 W/(m²K) (0.50 Btu/(hft²°F)) when it is not insulated (including typical summer film coefficients). This window is a made from 0.635 cm (.25 inch) thick clear glass lites separated by a 1.27 cm (0.50 inch) air space all mounted in 5.08 cm (2.0 inch) wide aluminum frame in five sections; it is a Vistawall Architectural Products Series 3000-S assembly. During interior zone tests this window is covered with foam insulating panels, in which case the conductivity is 0.16 W/(m²K) (0.031 Btu/(hft²°F)). Therefore, the average thermal wall conductivity of the entire West wall under interior zone testing conditions is 0.20 W/(m²K) (0.036 Btu/(h ft² °F)). We used Window5 [Mitchell, et. al. 2001] to calculate the thermal and optical properties for both a solar source and for an assumed spectrum for the solar simulator lamps. For PPG Double Clear glass the SHGC was 0.70 and 0.66, respectively. The dimensions and a picture of the window setup are shown in Figure 5 and Figure 6.

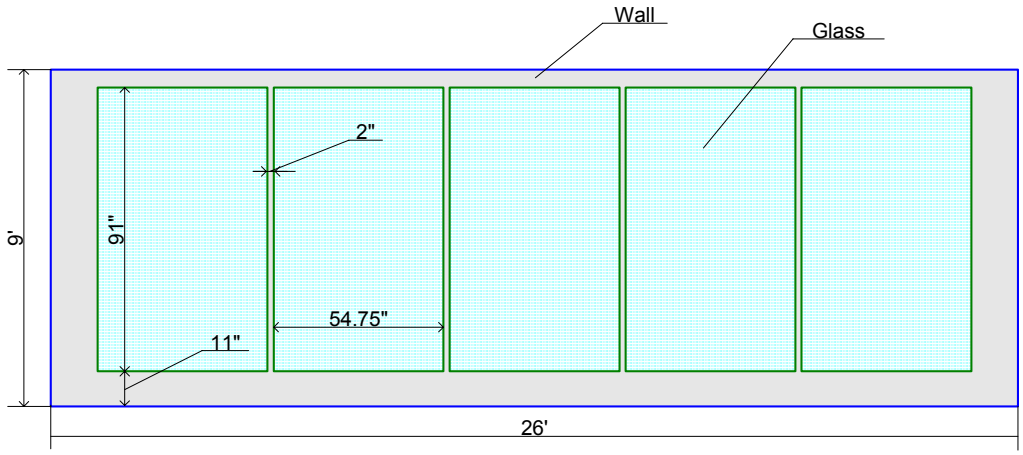

Figure 5: Double glazed window (5 sections) on the west wall of the test room

Figure 6: West wall windows, blinds open

As shown in Figure 6 this window was also were equipped with Venetian blinds to determine the impact of operating with blinds closed vs. open. The blinds are made from white 2.54 cm (1 inch) wide horizontal slats, Levolor Riveria (or equivalent).

3.1.2.3 Underfloor plenum

The underfloor (UF) or supply air plenum is a 30 cm (1 ft) high open service distribution space formed by a raised floor system on the top and an insulated slab on the bottom as illustrated in Figure 4. The raised floor system is constructed of 26 square Tate Con Core 1000 access floor panels [Tate 2005] each of which is 0.61 m (2 ft) as shown in Figure 7. Positile [Tate 2005] carpet tiles are installed on the floor panels. On the east and west wall one panel is split into two half-panels.

Figure 7: Floor panel as used in UFAD systems

Furthermore, the joints between the floor panels were taped with duct tape throughout all tests to prevent leakage. Holes are cut in a number of the panels to accept Krantz swirl diffusers or York MIT diffusers. Special slots were cut in the half panels at the window wall to accept bar grille diffusers for perimeter zone testing.

The bottom of the UF plenum consists of 1.9 cm (0.75 inch) thick plywood fastened to 2x8 joists 24 inch o.c. which are laid on top of the warehouse concrete slab floor. The space between the joists is filled with R30 fiberglass batt insulation.

Figure 8 is a photo of underfloor plenum in the York ADRF. The basket shown belongs to a Krantz swirl diffuser. Also shown (red wire) is a thermocouple mounted in the center of the basket to measure the temperature of the air as it passes through the diffuser into the room. A box housing a York MIT modulating diffuser is shown in the background.

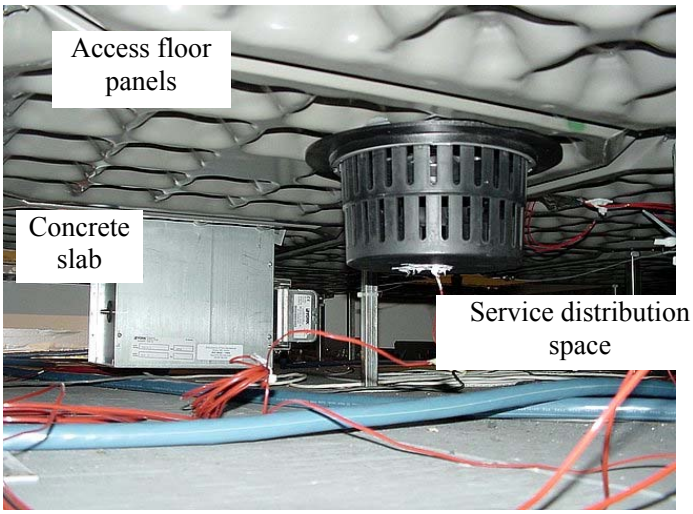

Figure 8: UF plenum in York ADRF showing a Krantz swirl and York MIT diffuser.

The UF plenum is used to distribute wiring for sensors. Figure 9 shows a view into the plenum with terminal strips for thermocouple wires. The large (blue) cables are thermocouple wire bundles that connect to the data acquisition system located in conference room; each cable holds two dozens of thermocouples.

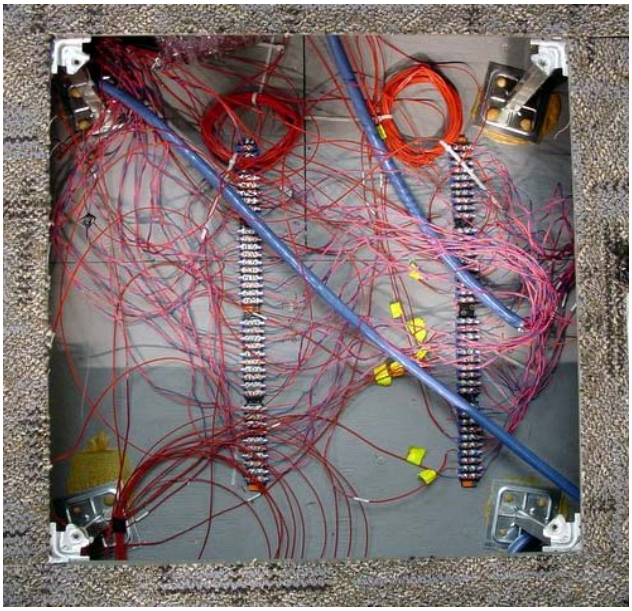

Figure 9: View into the UF plenum

Supply air distribution - The underfloor plenum is pressurized by air delivered by a central air handler into the chamber through an inlet in the South wall. This inlet also contains a modulating

damper for controlling the underfloor pressure. Depending on airflow, supply air temperature and location of diffusers, the range of variation in diffuser supply air temperatures is between 3°C and about 5.5°C (5-10°F). In an attempt to reduce this variation, a Y-fitting and flexible ductwork was installed to form nozzles for directing the air to minimize the variation. (See Figure 10)

Modular Fan Terminal (MFT) - Also installed in the UF plenum is a York modular fan terminal (MFT) heating system typically used in perimeter spaces. This sub-system, shown in Figure 10, consists of an MFT unit and intake and discharge ductwork that is connected to York MIT diffusers. This system was not used during testing. Figure 11 shows a detail of the MFT.

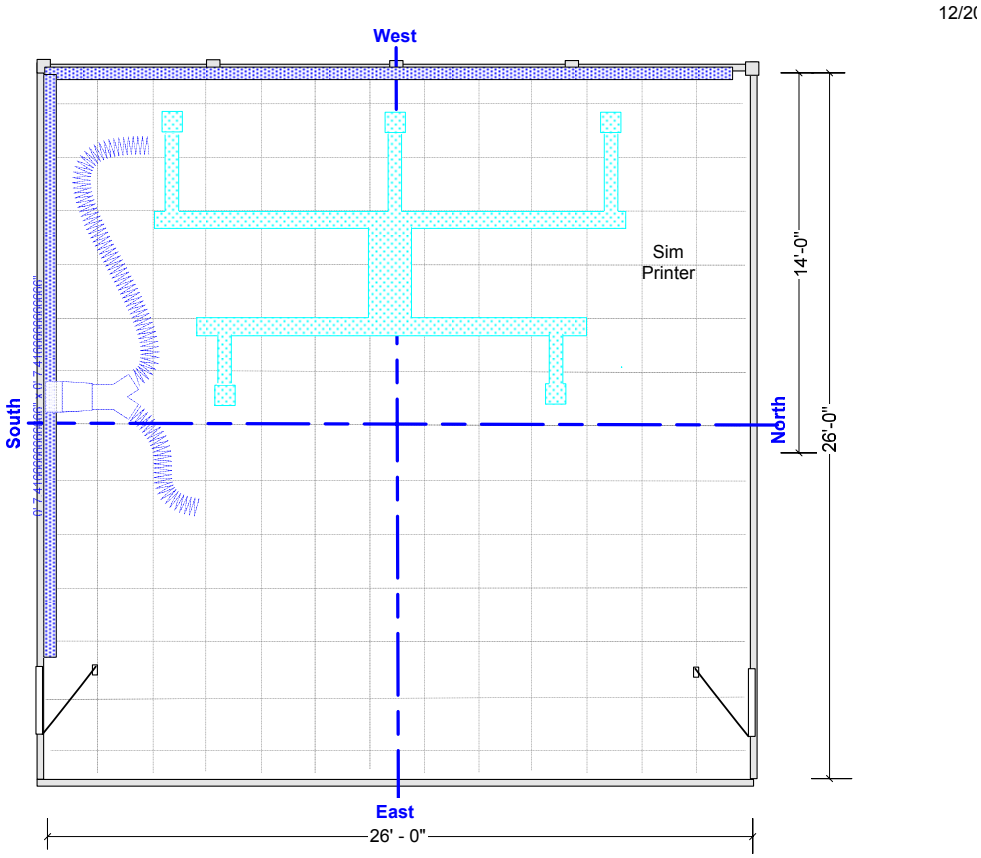

Figure 10: Underfloor plenum showing supply air distribution ducting and MFT system

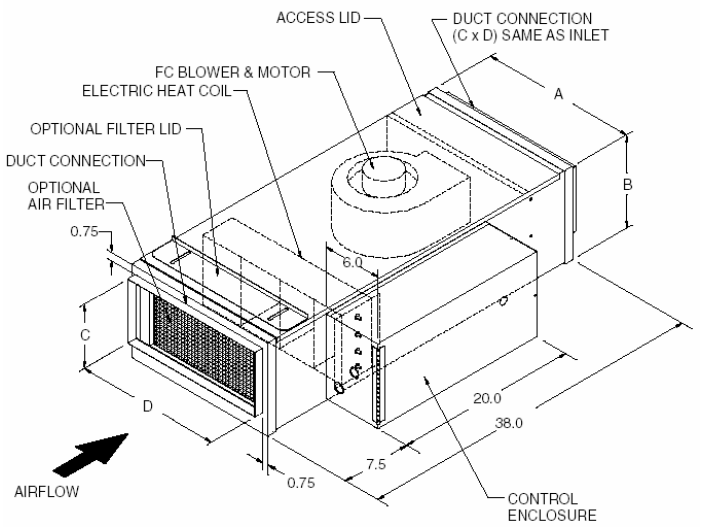

Figure 11: Modular Fan Terminal (MFT)

3.1.2.4 Return air plenum

The return air plenum is formed from the suspended acoustical ceiling and an insulated return plenum roof. The roof is formed from two sheets of 19.6 mm (0.5 inch) thick sheetrock and is insulated with 3.5 to 4.7 cm (9-12 inches) of blown-in fiberglass insulation. Above the insulation is an approximately 1.2 m (4 ft) dead airspace. Two 0.6 m (2 ft) square return air grilles conduct air from the test room into the return plenum.

Ceiling panels are standard acoustical ceiling panels installed in a typical T-bar ceiling frame system. Recessed florescent lighting fixtures are installed in the T-bar ceiling as shown in Figure 3.

3.1.3 TEST EQUIPMENT

In this section we describe the equipment used to create thermal loads in the test room and the diffusers used to provide cooling air flow. The test room was configured around an open plan arrangement with a total of 6 workstations (WS).

3.1.3.1 Thermal loads

Manikins

Each workstation consisted of a manikin, a personal computer and a desk lamp. To simulate human occupants, we installed specially constructed manikins. The manikins had heat tape wrapped around their body parts which had a resistance of – depending on their voltage and the tape itself – 23.4 Ohm per foot (7.1 Ohm per meter) or 11.7 Ohm per foot (3.6 Ohm per meter). Figure 12 shows a sample of a manikin's head with heat tape. When head, neck, torso, arms, hands and legs were assembled they formed the complete manikin as it is shown from the back in Figure 13. There, a small red light at the back of the neck is provided to indicate when the manikin is powered up.

Figure 12: Manikin with heat tape on the head

Figure 13: Assembled manikin sitting on chair from the back

Table 3 shows how the manikin's input power was distributed at each body part, very closely simulating the distribution of a real human while generating a total of 75 watts. We equipped each manikin with light clothing similar to typical office attire so the manikin simulates a seated person performing light office work.

Table 3: Power distribution for manikin's body parts

Body part	Input Power [W]
Upper torso	25
Head and neck	15
Upper arms	7
Lower arms	5
Hands	1
Upper legs	12
Lower legs	10
Total	75

Personal computers (PC)

As mentioned earlier, each workstation was assigned a personal computer. Different computer and monitor manufacturers were used so that the average power drawn from each PC was approximately 100 watts or 9.4 W/m² (3.07 Btu/(hft²)) as shown in Table 4.

Table 4: Power consumption of personal computers

Workstation ID	CPU (Tower)		Monitor		CPU & Monitor
	Manufacturer	Power [W]	Manufacturer	Power [W]	Power [W]
1	CyberServ	40	Gateway	60	100
2	CyberServ	30	KDS	75	105
3	Not known	40	Compudyne	60	100
4	Gateway	30	Gateway	65	95
5	Gateway	35	Gateway	65	100
6	UBM	25	Micron	65	90
Total [W]		200		390	590
Average [W]		33.3		65.0	98.3
Average [W/m²]		3.183		6.207	9.390
Average [W/ft2]		0.296		0.577	0.873

Printer

To simulate an office printer, we built a cardboard box with a light bulb inside. The simulated printer was powered through a current transformer which maintained the power at approximately 130 W, typical of average continuous consumption for a small office desktop printer.

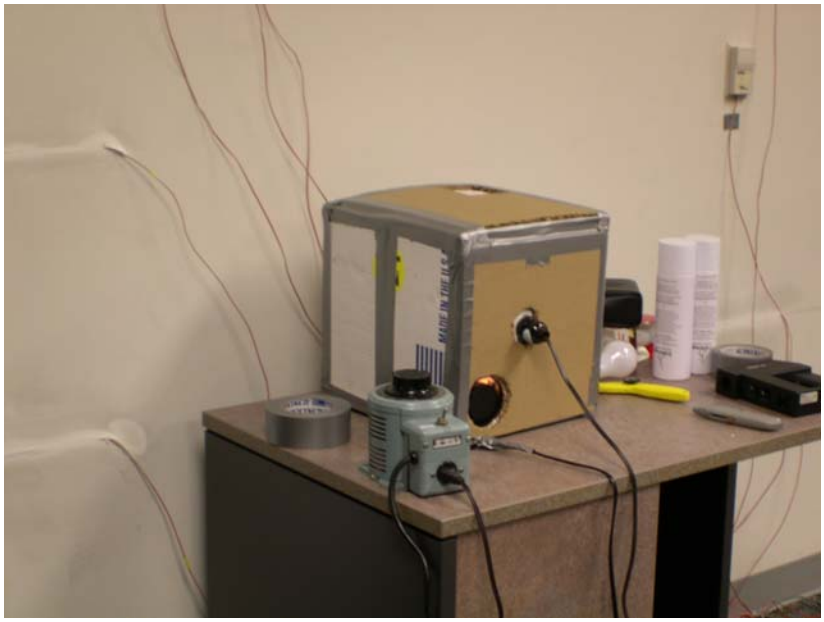

Figure 14: Simulated printer

Desk lamp

Each workstation was equipped with a desk lamp using a 60W light bulb, which was turned on whenever the manikin and the PC were turned on.

The complete workstation is shown in Figure 15. It shows the manikin, the personal computer and the desk lamp. In the background, the cardboard box with the transformer simulating the printer is visible.

Figure 15: Typical laboratory workstation

Overhead lights

Overhead lighting is provided by non-ventilated recessed florescent fixtures. A total of nine 5.08 cm x 10.2 cm (2 ft x 4 ft) Lithonia Paramax model number 2PM3N [Lithonia Lighting 2005] high-performance deep-cell parabolic troffer luminaires, with three T8 lamps each were used. Determining the fractions of lighting to space and return plenum was based on three independent studies; calorimeter testing, EnergyPlus sensitivity studies, and new data from experiments conducted at Oklahoma State University (OSU) [Fisher 2005]. The results will be reported in a future report.

Solar simulator array

The purpose of the solar array is to simulate solar gain to the test room under perimeter zone testing. The solar simulator lamps are mounted in the environmental chamber, which can be controlled from the conference room.

The solar array consists of 15 high intensity halogen quartz lamps (Chromalox QR25B430) [Chromalox 2003] which are rated at 2500 W each. These lamps operate at 2205°C (4000°F) so a significant portion (~28%) of the spectral distribution is in the infrared spectrum above 2.5 microns wavelength, the cutoff wavelength for transmission through clear glass. For perimeter testing, the number of lamps was switched between 5 and 10 lamps (1 or 2 banks of lamps, respectively) to simulate two different solar load conditions. Figure 16 and Figure 17 show pictures of the quartz lamps and how the solar array was installed in the environmental chamber (EC).

Figure 16: Quartz halogen lamps

Figure 17: Solar Array in EC

Figure 18 illustrates the distances between the lamp array and the window. We positioned and tilted the array to a 30° angle with the centerline of the array passing approximately through the center of the window to simulate the solar altitude for a west facing window in summer.

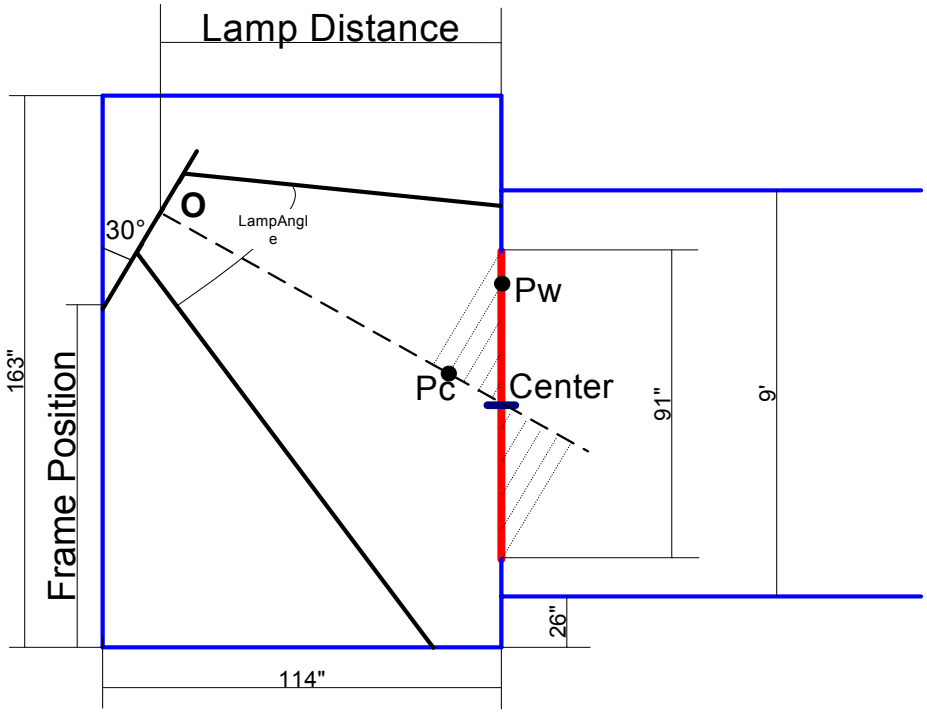

Figure 18: Cross-section of EC with lamp array

We conducted an extensive analysis, calibration, and adjustment of the solar array (by repositioning the lamps to even the radiant flux distribution) to determine as accurately as possible the total solar gain and the impact of a source with a significant infrared component. To accommodate a special feature installed in EnergyPlus[2] we measured the incident radiation on the test room inside wall and floor surfaces. Appendix E contains a chapter that summarizes all solar measurements and analyses. Based on the solar measurements and calculations we estimate the total full load (two banks of lamps) and part load (one bank of lamps) solar gain through the double clear glass window to be 68.1 W/m^2 (6.3 W/ft^2) and 40 W/m^2 (3.7 W/ft^2), respectively. The full load value is equivalent to a west facing low-e window with SHGC of 0.27 in Kansas City at peak load in summer.

Total loads

Table 5 shows an internal load component breakdown based on the three major configurations tested. We approximated these values based on individual calibration values for each component and an estimated light to return fraction of ~26% for overhead lights. During a test total workstation equipment (computers and task lights), overhead lights, and manikin power were each measured with a power meter. These results vary slighting from the final values used in various analyses since the light to return fraction was found to be about 15%.

Table 6 is a corresponding unit load summary that shows overall loads for interior and perimeter zone testing; not all of these configurations were tested.

Table 5: Typical total internal gains (IG)

Room load components, W	INT_8-2	INT_8-8	INT_8-9 adj

[2] This is an alternative way to calculate the solar gain without having to modify the complex Eplus solar gain calculations for an infrared source. This method entails measuring the distribution, the total window transmitted radiation and the window surface temperatures. (See Appendix E for details)

Number of workstations	6		4		2	
	Load, W	% of IG	Load, W	% of IG	Load, W	% of IG
Printer	130	6%	130	8%	130	11%
CPU Power	198	9%	132	8%	66	5%
Monitor power	***390***	***18%***	***260***	***15%***	***130***	***11%***
Manikin power	***450***	***21%***	***300***	***18%***	***150***	***12%***
Task light	***360***	***17%***	***240***	***14%***	***120***	***10%***
OH lights (Est. room fraction ~0.85)	680	30%	680	38%	680	52%
Total IG [W]	**2208**		**1742**		**1276**	

Table 6: Unit load summary (based on test chamber floor area)

Number of workstations	6		4		2	
	W/m^2	(W/ft^2)	W/m^2	(W/ft^2)	W/m^2	(W/ft^2)
Internal gain/Total interior load	34.6	3.2	27.2	2.5	19.7	1.8
Solar gain, 2 banks	68.1	6.3	68.1	6.3	68.1	6.3
Solar gain, 1 bank	40	3.7	40	3.7	40	3.7
Total perimeter load, 2 banks solar	102.7	9.5	95.3	8.8	87.8	8.1
Total perimeter load, 1 bank solar	74.6	6.9	67.2	6.2	59.7	5.5

3.1.3.2 Diffuser Types

To understand the impact of diffuser type on RAS performance we used a total of four types of diffusers. We studied different configurations depending on which type of zone we were investigating, interior or perimeter, as shown in Table 7. The following sections describe each of these diffusers.

Table 7: Diffuser configurations used during testing

Diffuser type	Interior zone	Perimeter zone	
		@ window	Interior
Krantz standard swirl	X		X
Krantz HD swirl	X	X	
York MIT	X	X	
Titus linear bar grille		X	
None		X	

Swirl diffusers

Standard swirl (SW) - This diffuser is Krantz's[3] standard 20.3 cm (8 inch) offering (Krantz DN 200; Price model RFTD) [Krantz (a) 2005] nominally rated for 136 m^3/h (80 cfm) at. 12.5 Pa (0.05 iwc). These diffusers were provided with distributor baskets (DB) with internal dampers. Figure 19 illustrates a typical discharge pattern. We chose these diffusers because we judged them to be fairly representative of swirl diffusers typically used on many projects in the US in terms of size, airflow, pressure drop and throw characteristics. Throw height as used throughout this report is defined in the same way as it is for traditional overhead system diffusers, i.e., the vertical height at which the average velocity is 0.2 m/s (50 fpm). We had the capacity to use a total of 16 of these diffusers in the ADRF.

[3] Krantz products are supplied by Price Industries, Winnipeg

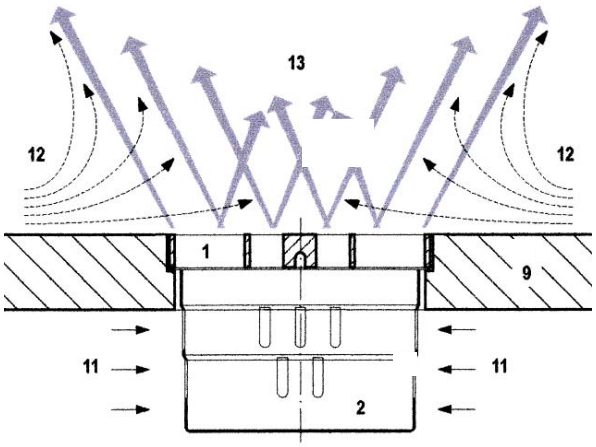

Figure 19: Discharge profile – standard swirl diffuser

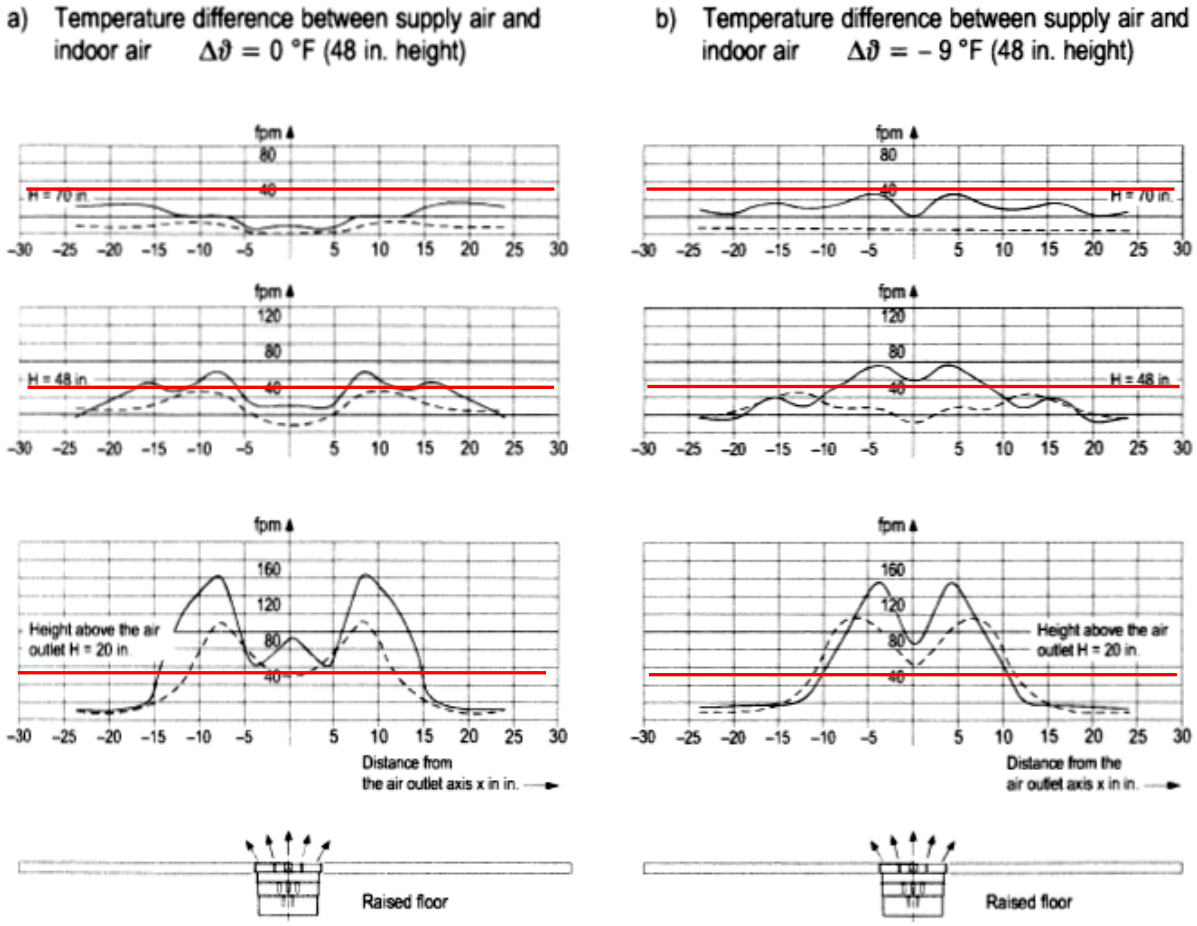

Figure 20: Velocity profile data for Krantz RFTD swirl diffuser

Figure 20 shows jet velocity data for Krantz diffusers. The figure shows two graphs for different test conditions; isothermal conditions (room and diffuser temperature the same at 1.2 m (4 ft)) on the left with and a temperature difference of 5°C (9°F) at 1.2 m (4 ft) on the right. The dashed line refers to an air outlet volume flow rate of 154 m³/h (88 cfm), whereas the continuous line represents an air flow rate of 120 m³/h (70.5 cfm). The graphs show air velocity profiles measured at three different heights: 0.5 meters (20 inches) 1.2 meters (48 inches) and 1.8 meters (70 inches). The y-axis in these charts represents the air velocity and the x-axis is the distance

from the center of the diffuser in inches. The red lines in Figure 20 indicate a velocity of 0.2 m/s (50 feet per minute). This is the velocity below which there would be minimal discomfort at a room temperature of 22°C (72°F).

These charts indicate that the clear-zone (the zone around the diffuser where the velocity is likely to exceed 50 fpm) of the diffuser is about 0.51 – 0.76 m (20-30 inches) diameter around the diffuser. Figure 22 illustrates the temperature decay of supply air at 18.8°C (66°F) due to mixing with 24°C (75°F) warm room air (at 4 ft). The different curves in the graph are measured thermoclines at different distances from the diffuser center. This data was provided by Krantz for the RFTD diffuser operating at 150 m³/h (88 cfm) supply air flow.

Figure 20 also indicates the diffuser throw height. Figure 21 shows a smoke visualization tests that illustrates the throw height.

Figure 21: Swirl diffuser throw

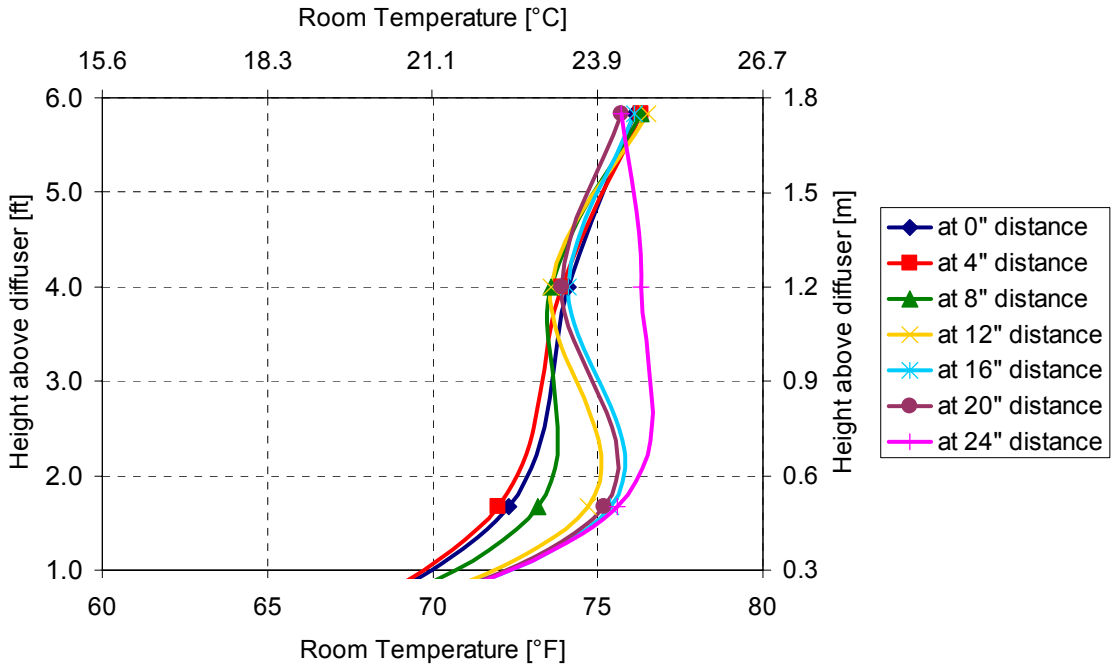

Figure 22: Temperature distribution for swirl diffusers at 88 cfm (150 m³/h)

Horizontal discharge (HD) swirl diffusers - Related to standard swirl diffusers, but different in throw characteristics are horizontal discharge swirl diffusers, which we have labeled HD swirls diffusers herein (although some references and figures refer to these as DV diffusers, to highlight the fact that mimic the performance of a displacement ventilation (DV) system. We have also used the designation 'UL' to indicate ultra low diffuser throw). The configuration of the diffuser is the same, but the discharge is virtually horizontal thus providing room distribution patterns similar displacement ventilation. We used a Krantz series Q-B-DN200 [Krantz (b) 2005] which is a Price model ARFTD nominally rated for 110.5 m³/h (65 cfm) at 18.75 Pa (0.075 iwc). These diffuser plates fit directly into a standard Krantz swirl mounting rings; we could deploy up to 14 of these HD diffuser plates.

Figure 23 shows how air passes through the specially designed radial slots of the HD diffuser. These deflect the low-turbulent air jet and cause it to only slide along the floor instead of being mixed with ambient air as it is the case for standard swirl diffusers.

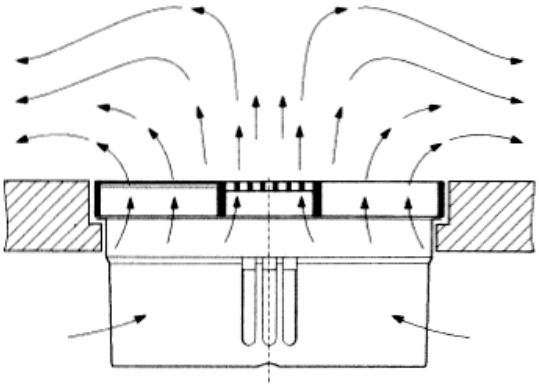

Figure 23: Discharge profile - HD diffuser

A comparison of Figure 21 and Figure 24 below shows clear differences in the throw characteristics between these two types of diffusers.

Figure 24: HD diffuser throw

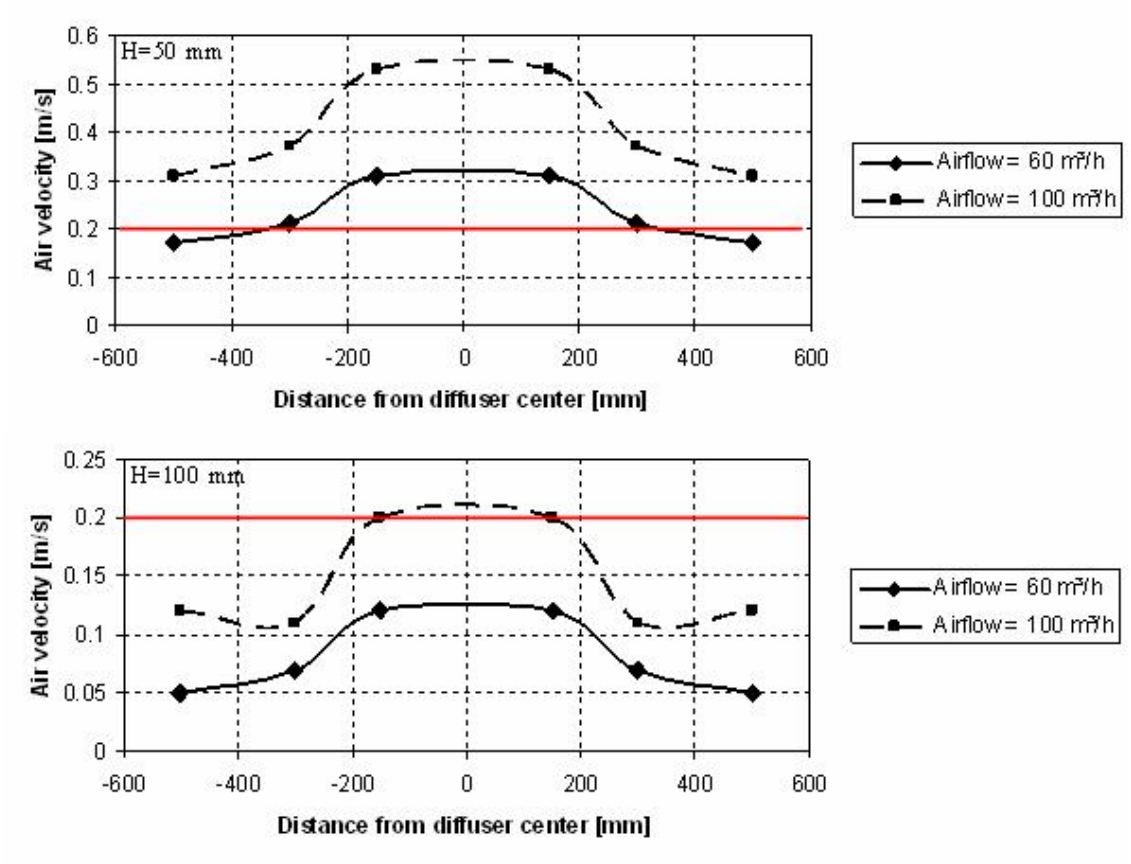

Figure 25: Velocity profile data for Krantz HD swirl diffusers

At the height of 50 mm (2 in) the clear-zone radius for airflow of 100 m³/h (60 cfm) is larger than 0.5 m (20 inch). Occupants seated close to the diffusers might feel discomfort due to cold feet and draft due to high air velocities.

The throw height of a HD swirl diffuser does not vary as much as it does for swirl diffusers. An increase in total airflow of the diffuser will not raise the throw height, but will enlarge the radius of the diffuser's clear zone.

The manufacturer does not provide information about temperature decay but temperature profiles of HD swirl diffusers under various load and diffuser configurations will be discussed in Section 4.

Variable area (VA) diffusers

VA diffusers are unique UFAD diffusers only supplied by York International. It is a variable volume diffuser where the airflow is modulated by a sliding metal plate. The York Modular Integrated Terminal (MIT) diffuser comes in various model configurations to provide a wide variety of options for heating and cooling operation (see York product literature for further information [York 2005]) but all are nominally rated for 255 m³/h (150 cfm) at 12.5 Pa (0.05 iwc). The grilles can be configured in various ways to provide discharge patterns from straight up (vertical) to various types of "spread" options. We used up to 10 of these in cooling operation mostly in a four-way spread configuration except for perimeter zones where they were configured to discharge the air toward the room, away from the window. Figure 26 shows a fully assembled MIT as it was used in the lab. The actuator with the two hub adapters are shown in the front,

which regulate the position of the damper subassembly. An exploded view of an MIT diffuser is shown in Figure 27.

Figure 26: Assembled York MIT diffuser with damper

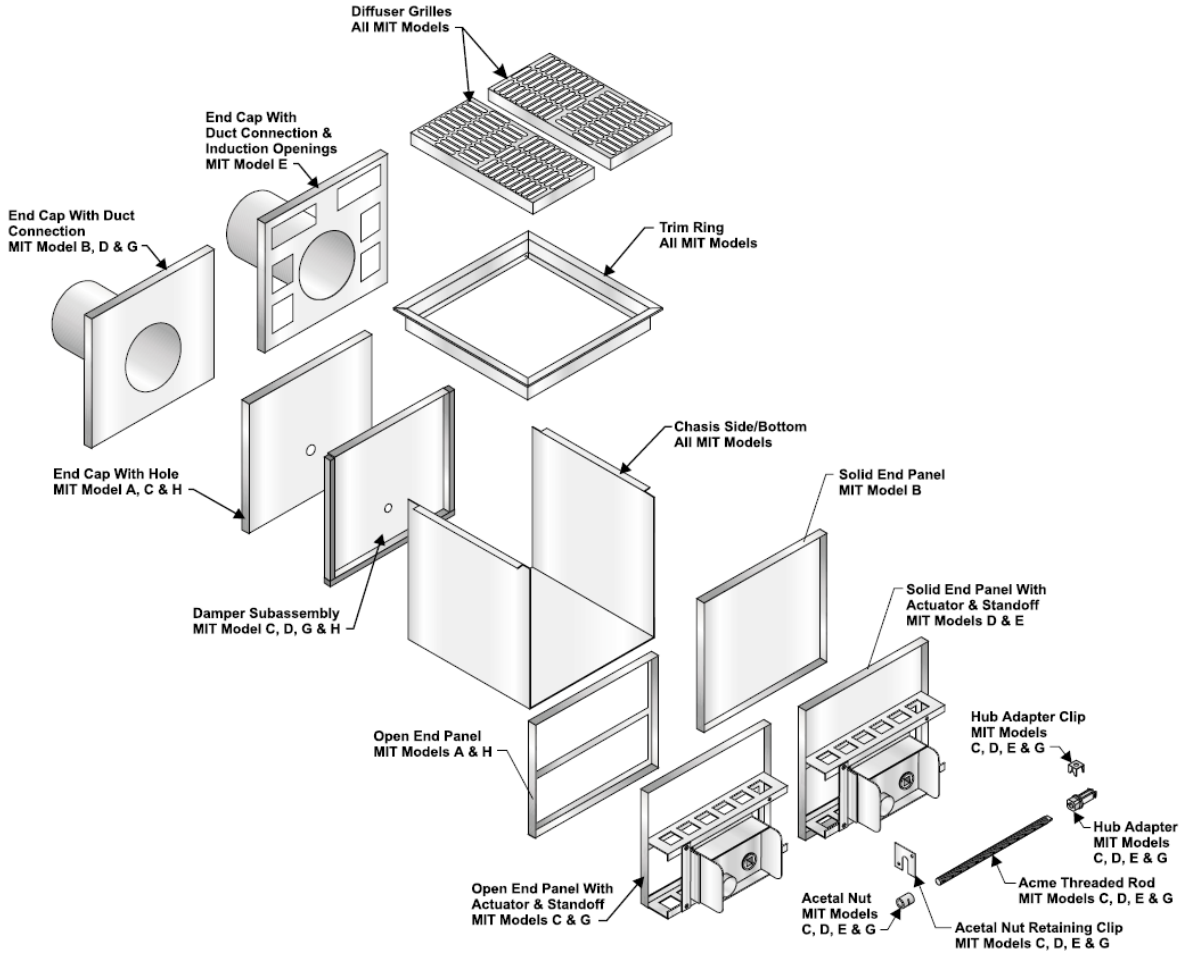

Figure 27: Exploded view of a York MIT variable area diffuser

It should be noted that for perimeter testing because half panels were used near the window, the MIT diffusers were located about 0.43 m (1.4 ft) from the wall. Normally these diffusers are mounted much closer, about 0.18 m (7 inches).

Linear Bar Grille Floor Diffusers

Linear bar grille diffusers are typically used to provide heating and cooling to perimeter zones in UFAD systems. They are usually installed a few inches from the perimeter wall and are connected to a fan coil unit by flexible ductwork as shown in Figure 28.

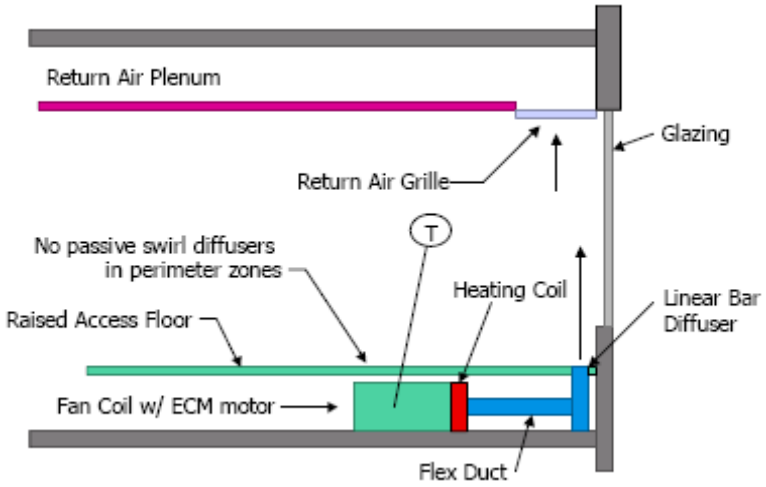

Figure 28: Typical perimeter zone configuration for VAV cooling with linear bar grilles

For our laboratory testing, we installed 10 nominal 8.9 cm (3.5 inch) wide by 45.7 cm (18 inch) long Titus CT-481 (Model number CT-481-5-xx-A with optional directional vanes) as shown in Figure 29. [Titus 2006] The bar core element is made up of 3.2 mm (0.125 inch) bars positioned on 6.4 mm (0.25 inch) centers with core element overall dimensions of 7 cm (2.75 inches) wide by 44.6 cm (17.6 inches) long. The bars have a 15° deflection angle (facing into the room) which causes the air to be blown into the room at a slight angle, instead of straight up.

Figure 29: Linear bar grille with adjustable vanes

We used linear bar grilles equipped with optional adjustable vanes as shown in the picture above on the right. They were used to change the direction of air flow to either the right or the left. An adjustable damper assembly was attached to the bottom of the diffuser via a string which could be used to change the amount of air going through the bar grille as shown in Figure 30. This

configuration allowed us to manually adjust the airflow to achieve the correct split between interior and perimeter airflow for a given operating condition.

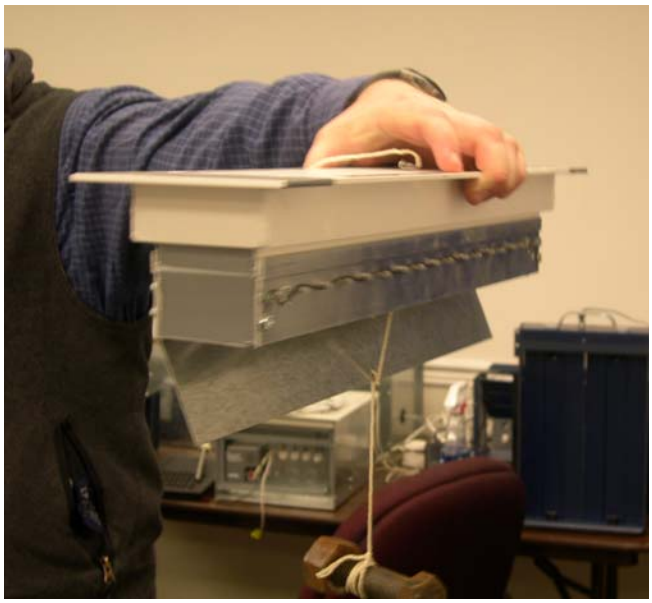

Figure 30: Linear bar grille adjustable damper mechanism

Depending on the underfloor plenum pressure, the diffuser design airflow can vary from 106 m³/h per meter of length for 2.7 Pa (19 cfm per foot for 0.011 iwc) to 524 m³/h per meter for 67.5 Pa (94 cfm per foot for 0.271 iwc).

We operated at approximately 12.5 Pa (0.05 iwc) under full load conditions, at which the design airflow for the linear diffuser is approximately 223 m³/h per meter (40 cfm per foot) but the actual airflow was adjusted using the bottom damper mechanism.

Diffuser performance characteristics for VAV operation

The diffusers described above have distinctly different operating characteristics. Ignoring for a moment differences in induction characteristics and discharge angles these diffusers perform generally as follows: Standard swirl diffusers have a constant discharge area thus the airflow and velocity decrease as plenum pressure decreases. This in turn causes the throw to decrease and since the throw is proportional to the momentum, the throw will vary with the square of the airflow. On the other hand, HD swirl swirls have a constant discharge area with flow varying as plenum pressure varies but the throw is nearly constant due to the limited vertical discharge. VA diffusers are normally operated at a constant plenum pressure but since the discharge area changes the velocity tends to remain constant and the momentum changes in direct proportion to the airflow. Consequently the throw varies less than for swirl diffusers.[4] Linear bar grilles operated in VAV mode are controlled by varying the pressure usually by a variable speed fan. However, when these are supplied without guide vanes, as is normally done, their airflow pattern is virtually vertical. The discharge area is constant so the throw varies as the square of the airflow, if too few diffusers are used, very high throws can occur. However, since the length of these diffusers can be readily increased, low throws are achievable at the expense of a greater number of diffusers. Table 8 summarizes these operating characteristics.

[4] MIT diffusers can be operated with a lower plenum pressure that will lower the throw, which in this case should decrease as the square of the velocity.

Table 8: Summary of diffuser operating charcteristics

	Discharge area	Vertical throw	Nominal design airflow and pressure, cfm (iwc)
Swirl, Standard	Fixed	Variable	80 (0.05)
Swirl, DV	Fixed	Nearly constant	65 (0.075)
Variable area	Variable	~ Constant	150 (0.05)
Linear	Fixed	Variable	200-250 (0.0125) [4ft long, 4-5" wide]

3.1.4 ADRF CONTROL STRATEGIES

3.1.4.1 System control

The control functions for the facility (other than unit controls built into the chiller) consist of standard York ISN [York ISN 2005] and Flexsys system (York's UFAD product line) control products [custom programmed and configured (using native algorithms and programming procedures) to support the ADRF. These are divided between two basic controls subsystems; the main supply air handling unit (AHU) with ISN controls and York Flexsys system unit controls called Flexfloor units. Additional controls are provided for the environmental chamber air handler, and for a low temperature refrigeration unit used to operate the EC for heating conditions (not used for our testing). These controls are completely independent from the data acquisition system sensors except for the room control thermostat and the underfloor pressure measurement (both the Flexfloor and DAQ monitored this sensor). Figure 31 shows a schematic of the air handling system for the ADRF. As shown in the diagram, the supply AHU supplies both the test chamber and the conference room but only the flow to the test chamber is measured.

The control system was interfaced through a front-end computer running York's Facility Manager (FM) software. [York ISN] From this interface we could change operating parameters, monitor control settings, and system response. Since the ISN and Flexfloor units are networked together we could operate and monitor all system components from the interface. Although his system had a data monitoring capability it operated so poorly that we abandoned it. For programming of sequences and tuning the controls we relied on York's programming tool called ICE. We encountered considerably difficulty in getting the controls configured and tuned properly for our lab setups, we were never satisfied with the quality of the control and in some cases the test results were compromise as a result. In the following sections we describe the individual control loops in so far as how they were supposed to operate.

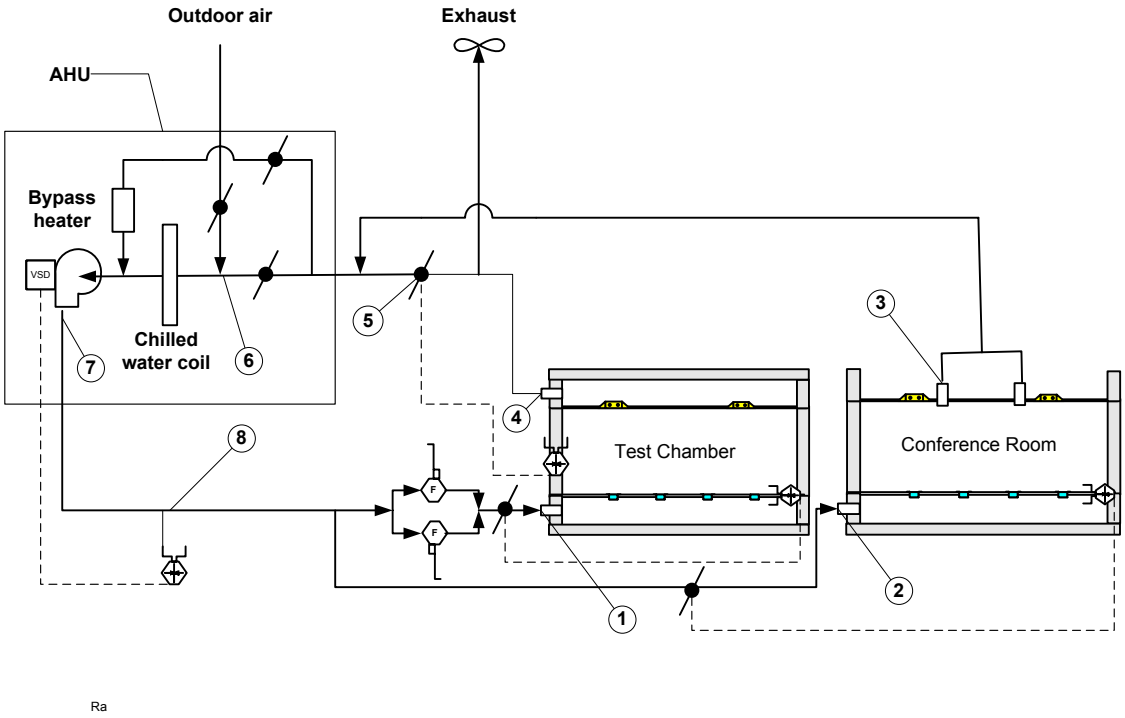

Figure 31: ADRF System schematic

Air handler and chilled water system

The supply air AHU controls airflow based on a duct static pressure control loop (see point #8 in Figure 31) via a variable speed drive (VSD). Discharge temperature is controlled by a chilled water coil. The control valve is oversized so under certain conditions we found it difficult to control SAT reliably at temperatures we desired. In addition, the chiller was oversized for low loads which resulting in cycling. We installed a reheater on the EC AHU to false load the chiller, which improved the overall control. Since the bypass heater was installed in the bypass, we found that it operated erratically at low airflow rates which complicated the control of the SAT. Low SATs we found were a particular problem until we installed the EC reheater and reconfigured the chiller for low temperature operation.

Return/Exhaust system

As shown in Figure 31, the return systems are different between the test chamber and the conference room; the later has a ducted return system which results in the conference room operating always at neutral pressure (i.e., the ceiling is open to the warehouse). These features resulted in some control and operational difficulties. For example, to maintain zero pressure in the test chamber under all test conditions (i.e., the return/exhaust system is important to control in- and exfiltration to ensure that the system extraction rates are as accurate as possible) we installed automatic control of exhaust damper #5. We manipulated the airflow to the conference room by changing the room set point or manually controlling its supply damper to place the system in a condition where the exhaust damper could achieve control of room pressure. Under high flow conditions (e.g., perimeter load testing) we manually turned on the exhaust fan in addition to manually controlling the conference room airflow. Using these procedures we were able to achieve very precise control of the test room pressure.

Environmental chamber

The environmental chamber is provided with a constant volume air handler with a chilled water coil and is configured as a closed recirculation system. This unit controls the EC room temperature to set point. Typically we used operating points of 35°C (95°F) for summer/solar conditions, and 24°C (75°F) for interior load tests. We installed a reheater in the return duct to false load chiller when we were operating at low load conditions such as for the interior tests. During perimeter tests there is sufficient load to load the chiller so stable operation is achieved.

3.1.4.2 Conference room

Room temperature and supply plenum pressure are controlled from standard Flexfloor units independent of the test chamber. A York MFT unit provides heating when necessary. As noted above sometimes we had to override these controls to manually control the airflow to the room and thus the return volume to support test chamber return/exhaust control. Normally we attempted to maintain the conference room at temperatures near the test chamber operating points of 22 – 24°C (72 – 76°F).

3.1.4.3 Test chamber

Underfloor plenum

Plenum pressure is controlled in two primary ways: (1) constant pressure mode for Flexsys system operation or when swirl diffusers are operated in CAV mode; and (2) pressure reset mode when swirl diffusers are used for VAV operation. In the latter mode, the plenum pressure is reset based on deviation from room temperature control set point.

Room control, interior zone tests

To support a variety of operating conditions we programmed the following controls sequences for room temperature control. We used one central temperature sensor located just east of the room center line for controlling room temperature. This signal can be switched between input to the central AHU controller (for swirl diffuser control) or the Flexfloor unit.

Open Loop - Occasionally for certain types of tests (e.g., idealized plum tests) we operated the test chamber in open loop meaning we set the airflow at a given setting by manually operating the supply plenum damper or setting the plenum pressure to a given value thus allowing the room temperature to float.

CAV – We attempted to use constant volume control (referred to internally as temperature reset control) for swirl diffuser tests and calibration tests. However, we were never able to tune this loop well enough to achieve satisfactory operation under this mode and eventually abandoned using it.

VAV, swirl diffusers – As mentioned above room temperature for swirl diffuser operation is controlled by two cascaded loops (referred to internally as pressure reset control), one that resets supply plenum pressure set point from room temperature deviation, and the other a supply air (SA) plenum damper control loop that controls damper position to achieve the plenum pressure setting.

VAV, VA diffusers – This is the standard York operating mode where dampers are modulated from the room temperature signal and the plenum pressure is controlled to a constant value by the SA damper control loop.

Room control, perimeter zone tests

For perimeter zone tests we used similar strategies as for interior tests, i.e., the control thermostat was placed in the same location, but the control was semi-automatic as described in the following.

VAV, swirl/linear diffusers – For these tests we maintained a constant underfloor pressure via the SA damper control loop (to provide correct volume for internal loads) and manually adjusted the linear bar grilled dampers to achieve room temperature control. (See Results section for a more complete description)

VAV, VA diffusers – For these tests we used the same standard York control system as we used for interior tests except in this case additional diffusers were installed near the west window.

3.1.5 INSTRUMENTATION AND DATA ACQUISITION

3.1.5.1 Data Acquisition (DAQ) System

The data acquisition system consists of the components shown in Figure 32. The heart of the system is an Agilent data logger, Model HP34970A. [Agilent 2005] This data logger has a 3-slot card cage with a maximum capacity of 120 channels of analog input and a standard RS-232 and GPIB interface that allows connection to a PC. The scan rate for this equipment is 250 channels per second. The data logger interfaces to the York/ADRF DAQ computer which runs specially created visual basic (VB) software. This software allowed us to monitor trends and data channels in real time. The software also contained the sensor calibration tables which processed sensor channel data streams form the Agilent data logger.[5] This computer also served as an on-site archive for all test logs. The DAQ PC was accessed over the local intranet to CBE laptop PCs. With these laptops we downloaded the test log files (they could also be viewed in real time) for processing by our Matlab data processing software (see below). The DAQ channel schedule is included in Appendix C.

[5] One limitation of the HP34970A is that only linear calibration curves can be used. However, any calibration curve, e.g. polynomial, can be implemented the DAQ monitoring program. Please refer to the Agilent website [Agilent 2005] for more information about this product.

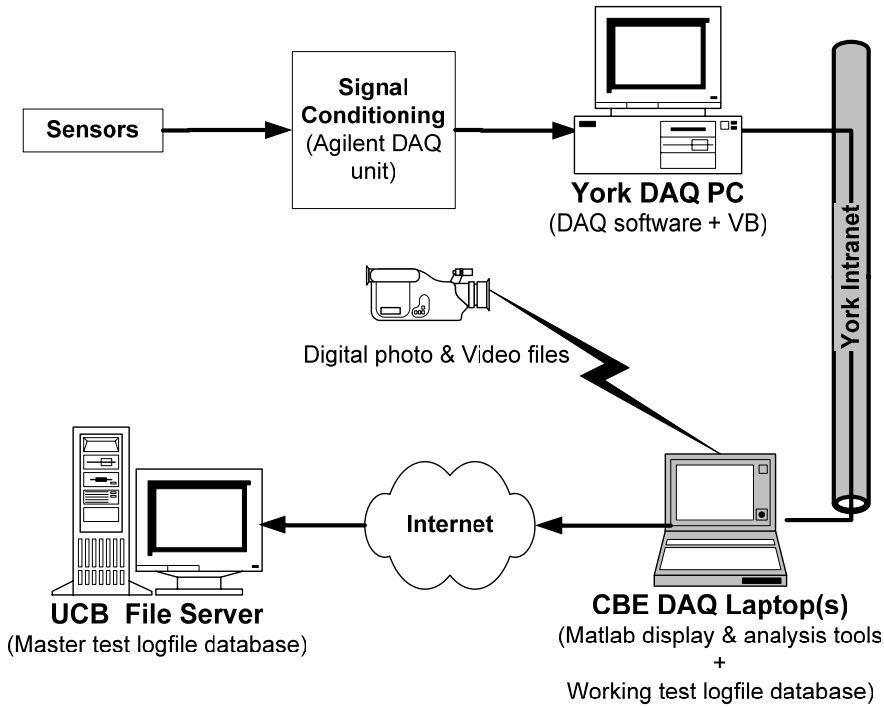

Figure 32: Data acquisition system schematic

3.1.5.2 Instrumentation

Temperature Sensors

In Table 9 we summarize the temperature measurement points for the ADRF. Except for floor and window surface temperatures (where we used infrared temperature (IRT) sensors), for all other temperature measurements we used Type T thermocouples (TC). These thermocouples are made from 26 ga wire and were fabricated up on site. Junctions were welded and TC assemblies (including DAQ system) were calibrated in York's sensor laboratory using a secondary standard reference with accuracy of 0.01°C (0.018F) from Automated Systems Lab, Model F250 precision thermometer. These TC have a time constant of about 10-20 sec in still air. We created multi-junction sensors as indicated below by wiring sensor beads in parallel to form a spatially averaging sensor. Surface mounted sensors we installed with conductive epoxy, except wall sensor which we embedded slightly below the surface under a coating of spackle.

Table 9: Test chamber temperature sensor summary

	Temperature Measurement	Sensors	Comments
Supply	Chilled water	2	one in return, one in supply
	Air handler	2	One sensor per AHU
	Supply	1	duct
	Supply plenum	18	sensors spread in supply air plenum (12 "supply air plenum", 6 "MIT")
	Diffuser supply air temperature	0	derived from supply plenum air temperature, # of sensors depends on # of diffusers
	Slab	1	TC located within slab of underfloor plenum
	Floor panel on UF plenum side	4	one sensor per corner
	Plywood	1	deck
Chamber	Floor surface on room side	2	2 IRT sensors, one in south west, other one in north east corner
	Trees	68	3 trees with 16 TC each, 4 trees with 5 TC each
	Stat	3	controls
	Spare sensors	2	various locations, changed with test (there are actually 5, but only 2 in use)
	Ceiling room side	2	one NW, one SE
	Plume	2	one in, one out; for plume temperature measurments only (not sure if ever used)
	Window surface	2	IRT sensors on different heights of the window
	Air above window	2	one on north side, one on south side
	North Wall	10	2 at 27" and 88" AFF on west side, 6 at different heights in the middle and 2 at door at 27" and 88" AFF
	East wall surface	2	one on wall at 27" and one at 88"
	South wall surface	2	one at 27" and one at 88" panel AFF
Return	Ceiling plenum side	4	one sensor per corner
	Return	7	one per return air grill, one in return duct and one sensor per corner
	Roof	2	one air, one insulation
	Attic	1	
Outside	Outside	1	Outside air temperature
	Plant	2	one plant air, surface temperature of plant wall
	Brick wall east side	2	air temperature between brick wall and sheetrock test chamber wall
	Conference room	1	one for air temperature
	Environmental chamber	1	one for air temperature
	Total Number of Temperature Sensors	147	

Test chamber sensors - A layout of the TCs for the test chamber is shown in Figure 33. To measure differences in vertical temperature distribution, a number of thermocouples were installed on a string at different heights to form a so-called "thermocouple tree." This string was clamped between the ceiling and the floor. Figure 34 shows part of this tree with three thermocouples. For perimeter tests we installed shields on the trees to mitigate the effects of radiation biases. These were constructed of aluminum foil covered insulation board as shown in Figure 35.

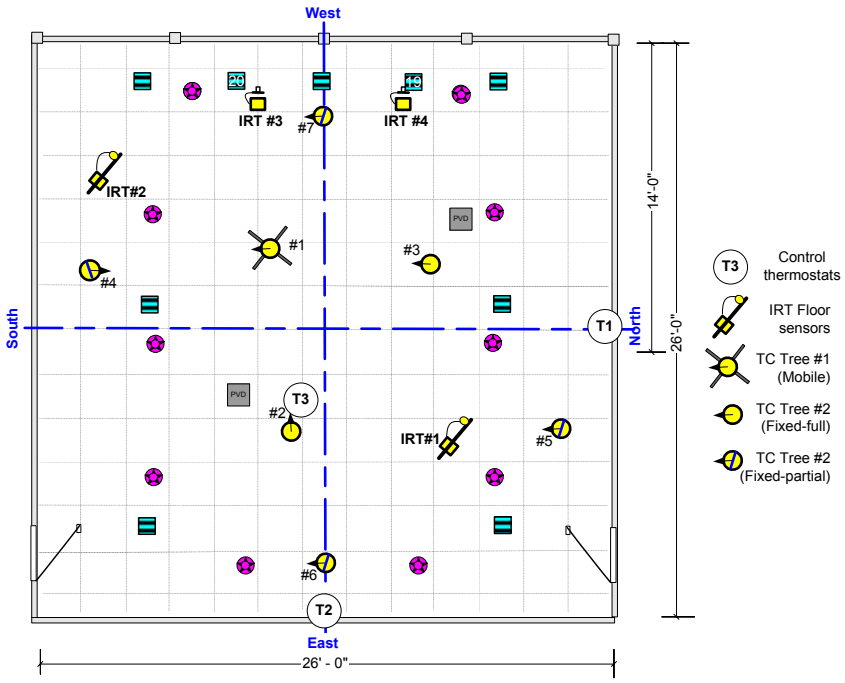

Figure 33: Test room sensor layout

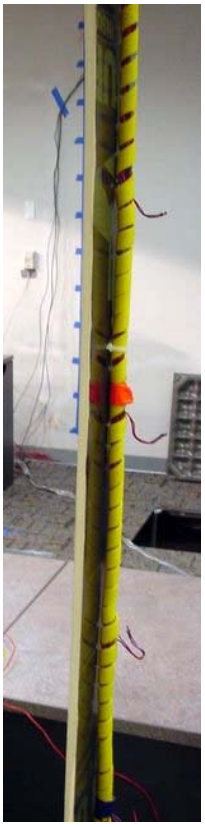

Figure 34: Stratification measurement tree

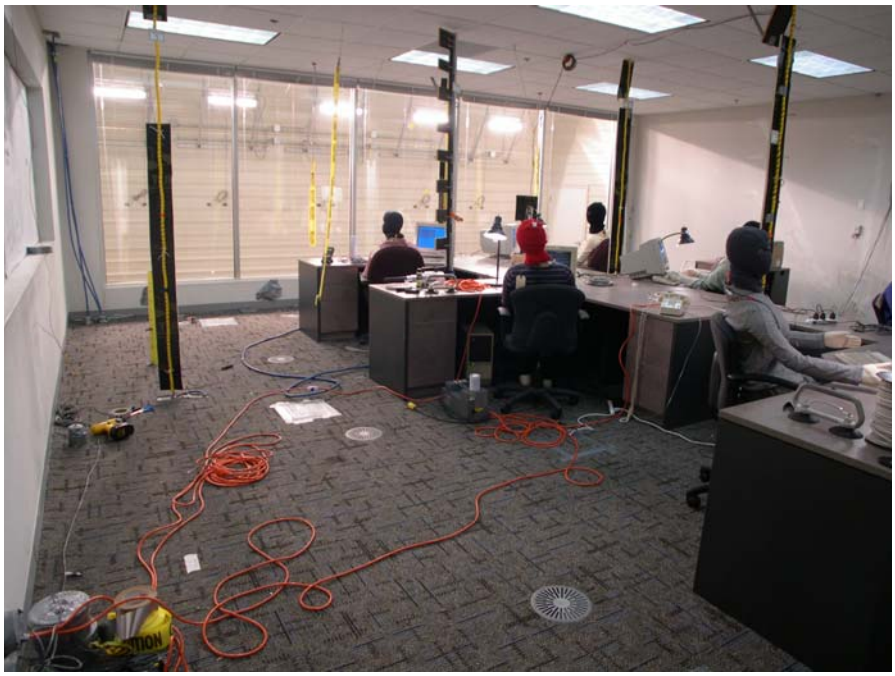

Figure 35: Test room view showing thermocouple trees with shielding

There were a total of 7 thermocouple trees in the test room. One of these trees was on a movable stand. Tree number 1, number 2 and number 3 were equipped with 16 thermocouples. At the top and bottom, 2 TCs were mounted at 5.5 cm (2 in) and 10.2 cm (4 in) from the floor and ceiling, respectively. The remaining TCs, were arranged to be approximately 24 cm (9.6 inch) apart. The positions of the fixed trees are shown in Figure 33 indicated by the yellow circles with a diagonal line, but also in other diagrams of the laboratory layout in this report.

For the top of the raised floor and window surface temperatures we used two each Raytek MID infrared temperature sensors. [Raytek 2005] These are two-piece infrared temperature measurement system with miniature sensing head separated from the electronics. These sensors are powered by 12 to 24VDC with maximum current of 100mA; accuracy is 1% of reading. The standard RS-232 allows communication for remote setup and/or monitoring. The floor IRTs were setup for an emissivity of 0.95 while the window sensors were set for 0.87.

UF plenum sensors - Figure 36 through Figure 38 show the locations and photos of supply plenum sensors. Sensors were installed in the diffusers and were used both for plenum average temperatures and diffuser average supply temperature calculations (See data reduction section). Variable area diffusers had temperature sensors mounted inside them as well.

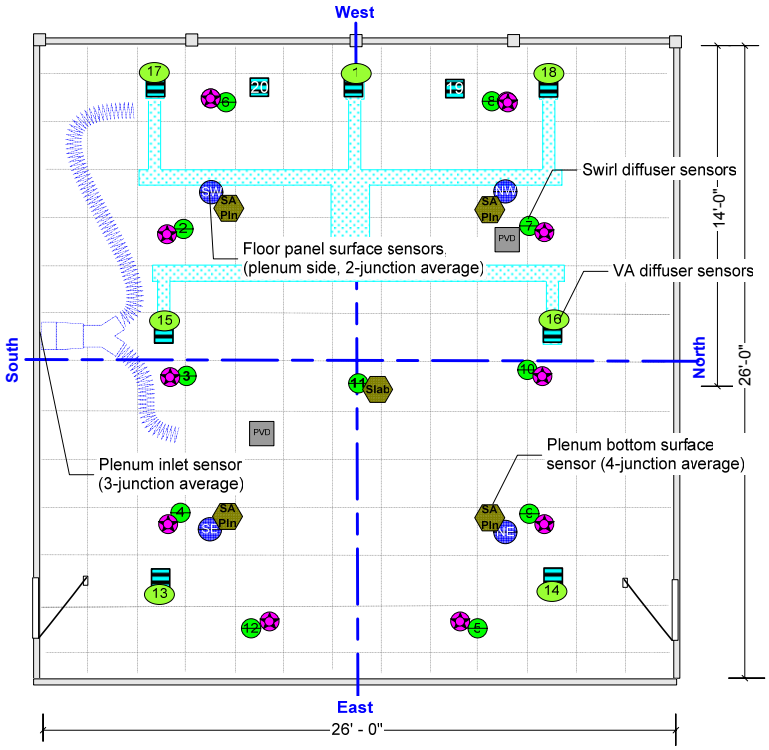

Figure 36: Temperature sensors in UF plenum

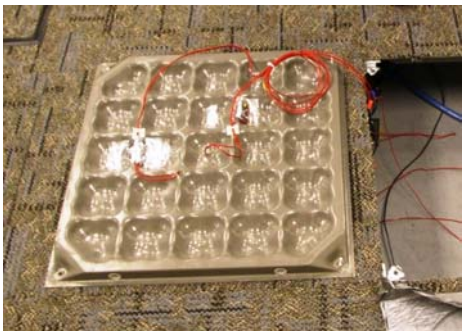

Figure 37: Raised floor panel underside surface temperature sensors (2-junction average)

Figure 38: Supply plenum inlet control damper and sensors (3-junction average)

Return plenum sensors - Figure 39 shows locations of all sensors in the return plenum. As indicated, each return grille was equipped with a 5-junction thermocouple to provide an averaged reading. Likewise, a 3-junction averaging sensor was provided at the return duct exit from the plenum. We used four thermocouples, one in each quadrant of the return air plenum, to measure the temperature of the return air plenum itself. One sensor measured the inside surface temperature of the top of the return air plenum. Sensors were embedded into the acoustical tile ceiling on the RA plenum side for all four locations shown, and on the room side for Southwest (SW) and Northeast (NE) locations as shown in Figure 41 and Figure 42.

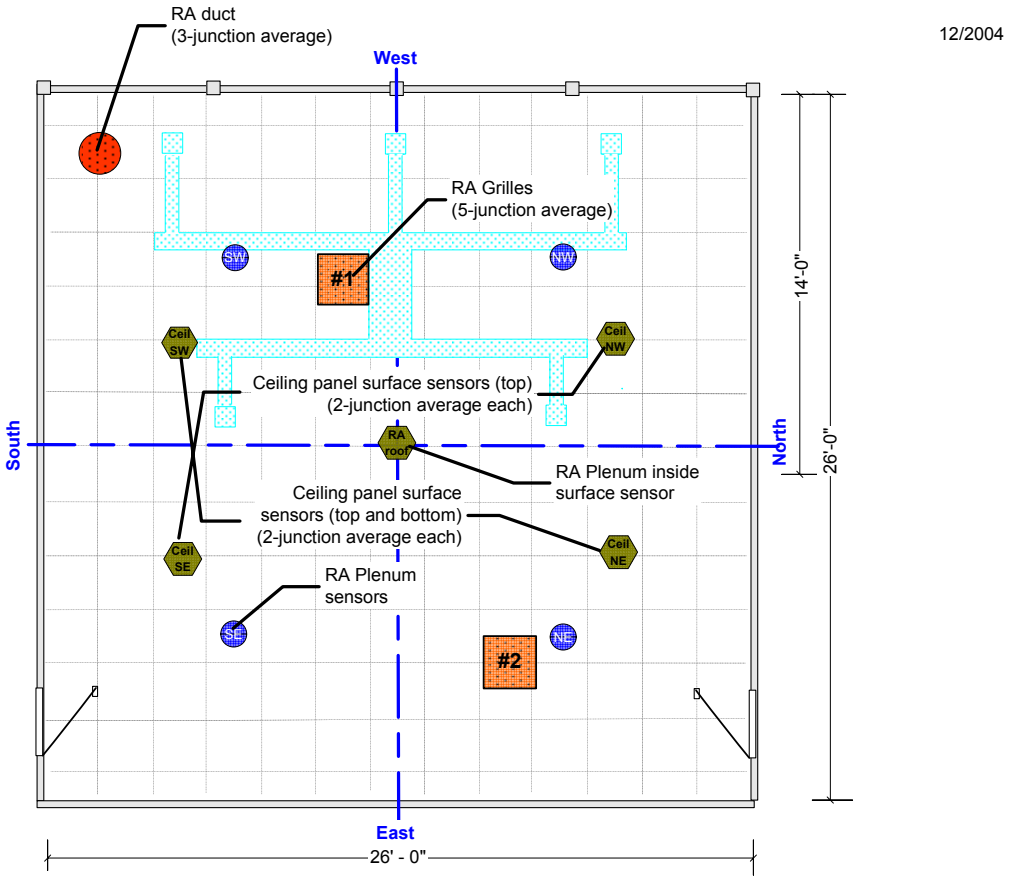

Figure 39: Return air plenum sensors

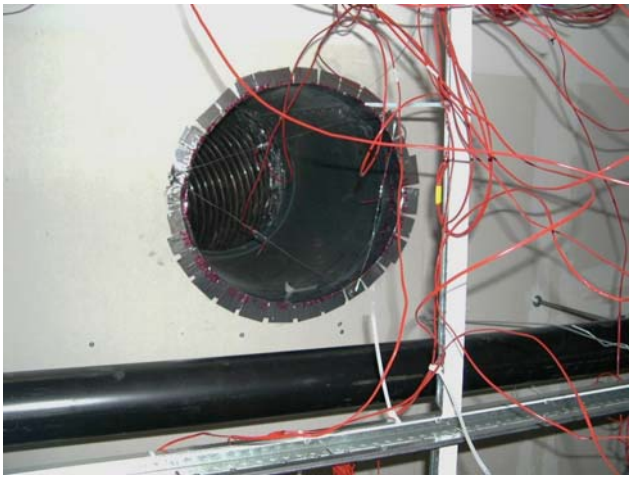

Figure 40: Return plenum outlet duct and sensors

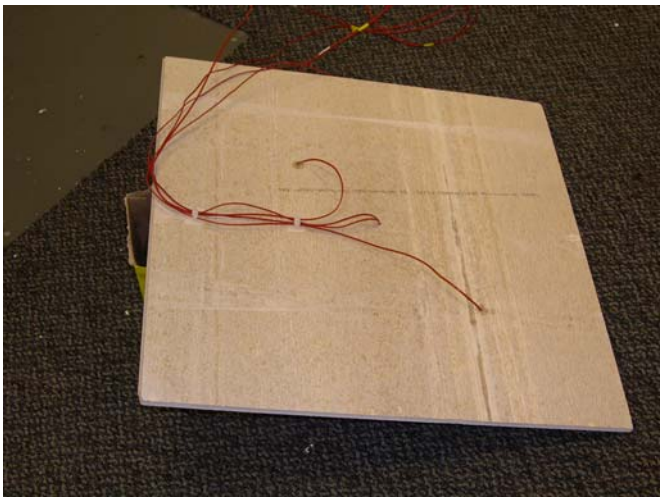

Figure 41: Ceiling panel surface sensors, RA plenum side

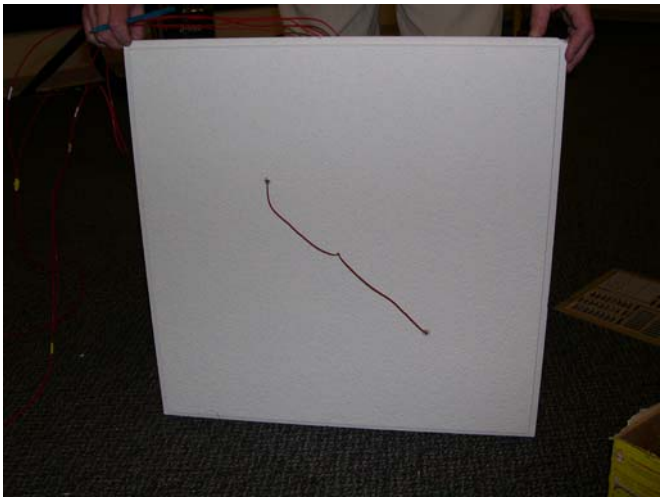

Figure 42: Ceiling panel surface sensors, room side

Flow Meter

The supply air duct before entering the test chamber plenum was divided into two ducts, each with its own flow meter. One of the ducts contained a 15.2 cm (6 inch) diameter flow meter and the other one a 20.3 cm (8 inch) flow meter. We split these so that each meter would operate in its optimum flow range to provide measurement accuracy for this critical parameter. For low flows – typically below 236 liters per second (500 cfm) we used the 6 inch flow meter, whereas up to 700 liters per second (1500 cfm) we used the 8 inch flow meter. Airflows above this range were measured with both flow meters by adding their values. The flow meters were made by Thermo Electron Corporation, Brandt SmartFlow pressure transmitter Model MST24000003S/4S100 with 6" and 8" pitot static flow tubes. Please refer to Brant literature for more details. [Brandt MST 2005] The vendor claims that these flow meters are calibrated at the factory to accuracy 0.15% of span for ranges of 40% to 100% of maximum span. We could not corroborate that these specific instruments were in fact individually calibrated and the documentation was unclear as to the total system accuracy specifications. However, since we calibrated these we assume the accuracy is no better than that of our calibration device of 3% of reading (see future reports for details of calibration and instruments and measurement uncertainty).

We encountered several problems with the flow meters. Initially we assumed that the factory calibration was accurate, but as testing progressed it became obvious that we needed to calibrate the meters. During the calibration we discovered that the pressure sensing tubes had leaks and the zeros drifted. Once calibrated the flow measurements for Sessions 6, 7 and 8 appear to yield reasonable results. However, there are still a number of inconsistencies in the data from previous sessions even though we attempted to back calculate corrected coefficients that we hope to resolve during future work.

Pressure Transducers

To measure underfloor pressure differential we used a Setra Model 264 pressure transducer, Model R25 WD 11 A1 F and for the test room-to-plant differential, Model 2641 R25 WB 11 A1 F bidirectional transducer. Both of these had a range of 0.001 Pa (0.25 iwc) with an accuracy of 0.25% of full scale. [Setra 2006]

Power monitoring

We measured internal gains input from four circuits each equipped with an Ohio Semitronics (OSI) power transducers, Model GW5-019C. [Ohio 2003]. These transducers have a rated accuracy of 0.2% of reading.

Solar instruments

We used two instruments to measure the radiation flux from the simulated solar lamp array. An Epply E6 thermopile [Epply (a) 2006] with and without filters was used to investigate the radiative power of the array over its whole spectrum and to compare with measurements by an Epply precision spectrum pyranometer Model PSP. [Epply (b) 2006] The thermopile has an aperture angle of 65° and an estimated accuracy of 2% in the range of 0.3 to 3 microns. When the thermopile is used without a filter window it can measure wavelengths to about 18 microns. With a quartz crystal widow it has a cutoff similar to the PSP of about 2.8 microns. The PSP has a calibration accuracy of 1% of reading. We had the PSP and the E6 calibrated by Epply before taking final measurements.

3.2 DATA MANAGEMENT, REDUCTION AND DISPLAY

3.2.1 MATLAB TOOLS AND PROCEDURES

As shown in Figure 32 the data management software resides on the CBE laptop(s). We developed this software especially for this project using Matlab, a robust mathematics and visualization software suite. Figure 43 shows a more detailed diagram of how the data was managed during testing. The Matlab testing and analysis tools are graphical user interface (GUI) based tools that perform two basic functions: (1) display of data for monitoring purposes (UI Tool), (2) input of test conditions, data averaging, and creation of formatted output files (HeaderMaker Tool). These are described in more detail below.

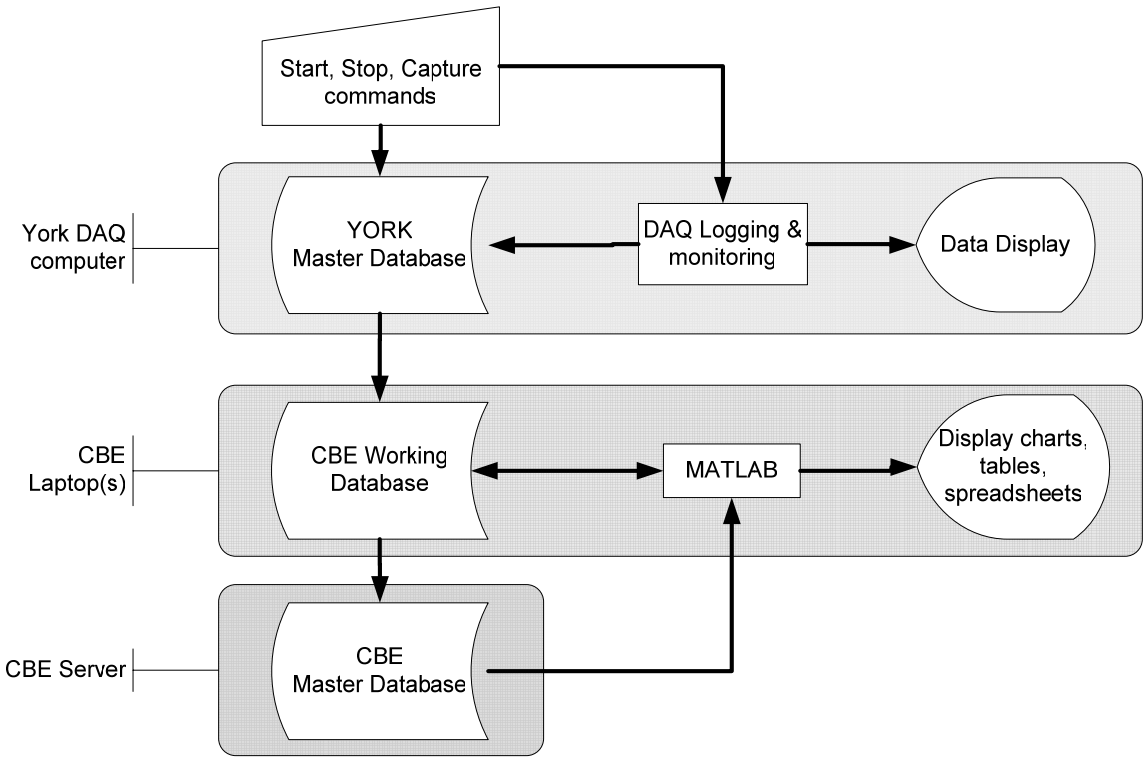

Figure 43: Data management and display

3.2.1.1 UI Tool

Data monitoring

This tool creates trend displays of monitored data for all data channels. These trend displays can be configured to simultaneously show selected data points together as shown in Figure 44. This figure shows a chart with measured data over a period of time for test PER 8-11. The x-axis represents time; the y-axis shows the actual values of the channels chosen (temperatures, airflow).

This tool also contains a RAS profile monitoring display where RAS trees can be displayed as shown by Figure 45; animation allows these displays to be viewed as they change over the course of a test. For these profiles, the room temperature is plotted on the x-axis, and the room height is plotted on the y-axis; the vertical temperature distribution of each of the seven thermocouple trees are shown together but can also be individually shown. During testing we used the UI Tool to monitor progress, investigate problems, and identify steady state conditions. This tool operates on text based log files downloaded from the DAQ computer. This file contains data from all sensor channels. Matlab's internal tool set also allows for zooming, and insertion of comments, etc.

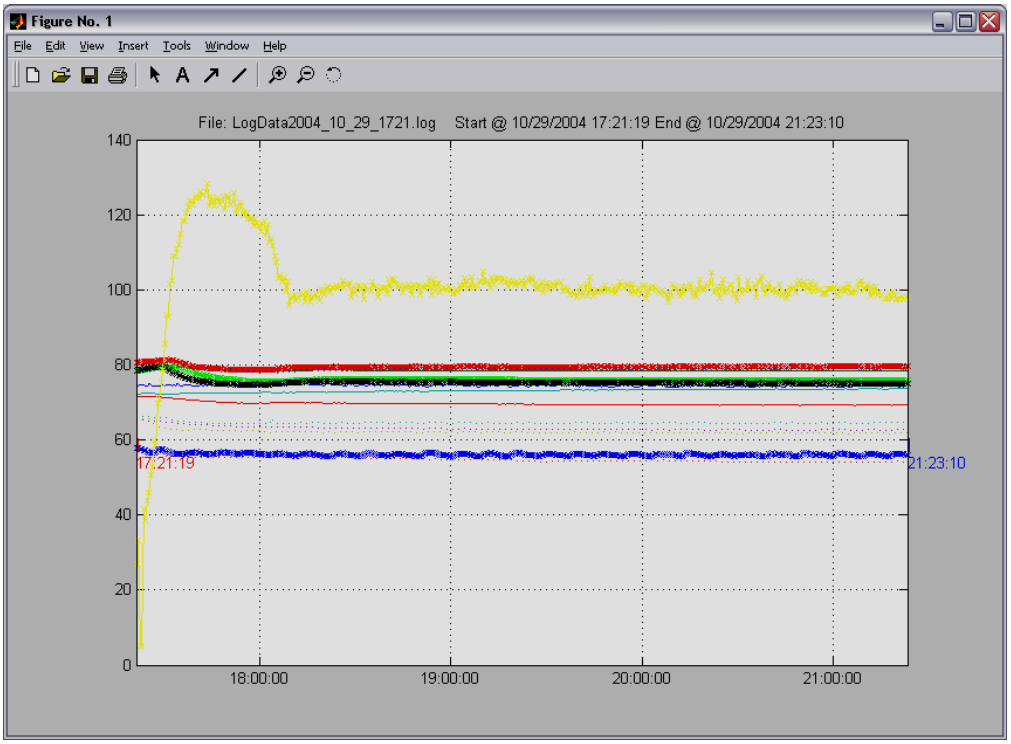

Figure 44: Typical trend display

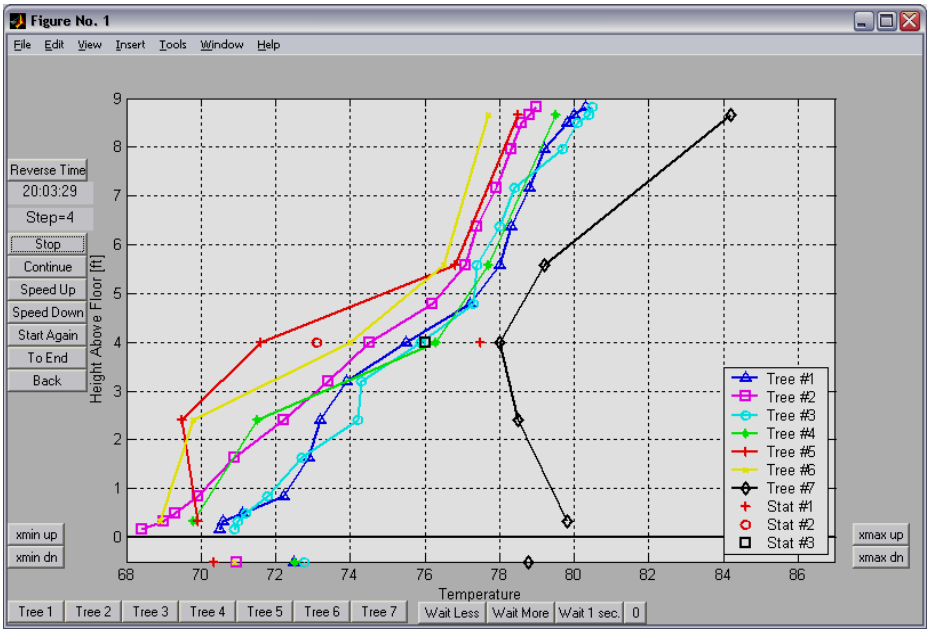

Figure 45: Profile animation plot for PER 8-11

Real time data statistics

Built-in to the UI Tool is a legend that allowed us to track certain data statistics to assist with monitoring and adjusting using averaged data and to help identify when steady state was achieved. Figure 46 show an example of this display. The legend contains the average value, standard deviation, and rate of change of each parameter shown over the period selected by the

time marks shown (in this example the steady state period was chosen from 18:21 to 21:22). The time period is user selectable by placing stop and start tick marks.

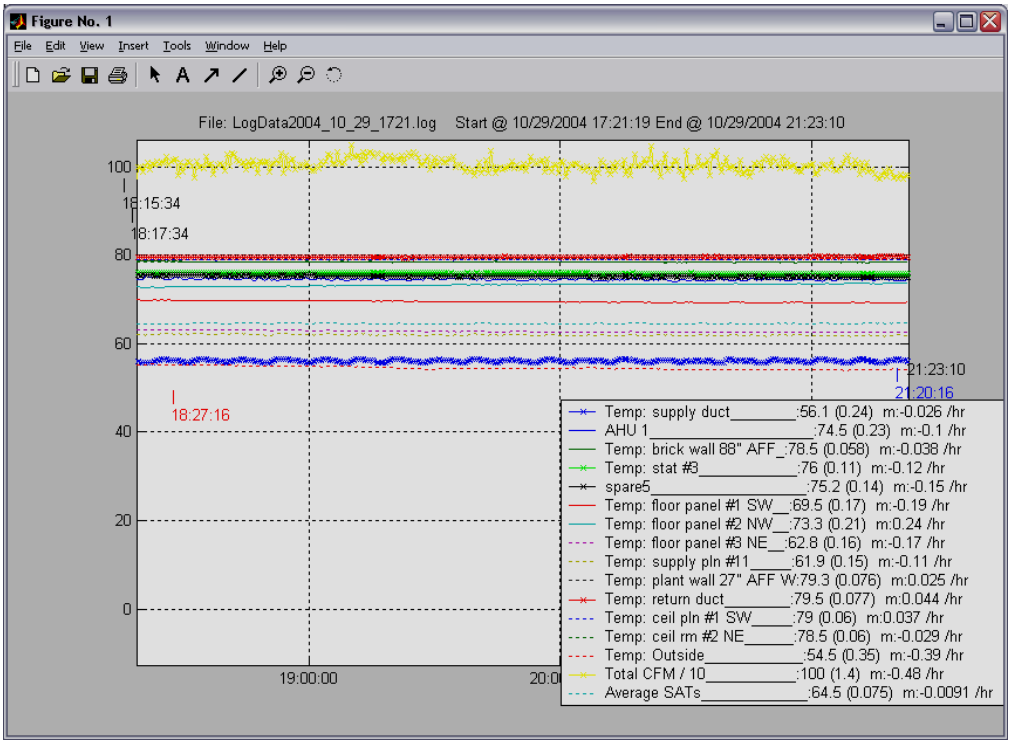

Figure 46: Steady state period for PER 8-11

3.2.1.2 HeaderMaker Tool

We developed this tool to process data from a completed test to assist with analysis and archiving in a database. This tool consists of a main GUI that has a section for test setup parameters to be entered, a data file management section, direct access to the UI tools, and a notes section. When a test is completed, its text log file is imported, setup parameters and notes are entered, a steady state period is selected using the UI Tool (see above), and when complete the imported data is processed and an output file is created with a header that consists of the setup data. The processing includes averaging for all data points over the steady state period, application of calibration coefficients, and calculation of metrics and uncertainties for selected parameters. A section of this output file is dedicated to reproducing an exact replica of the raw sensor channel data but averaged over the steady state period. An example of the HeaderMakerGUI is shown in Figure 47.

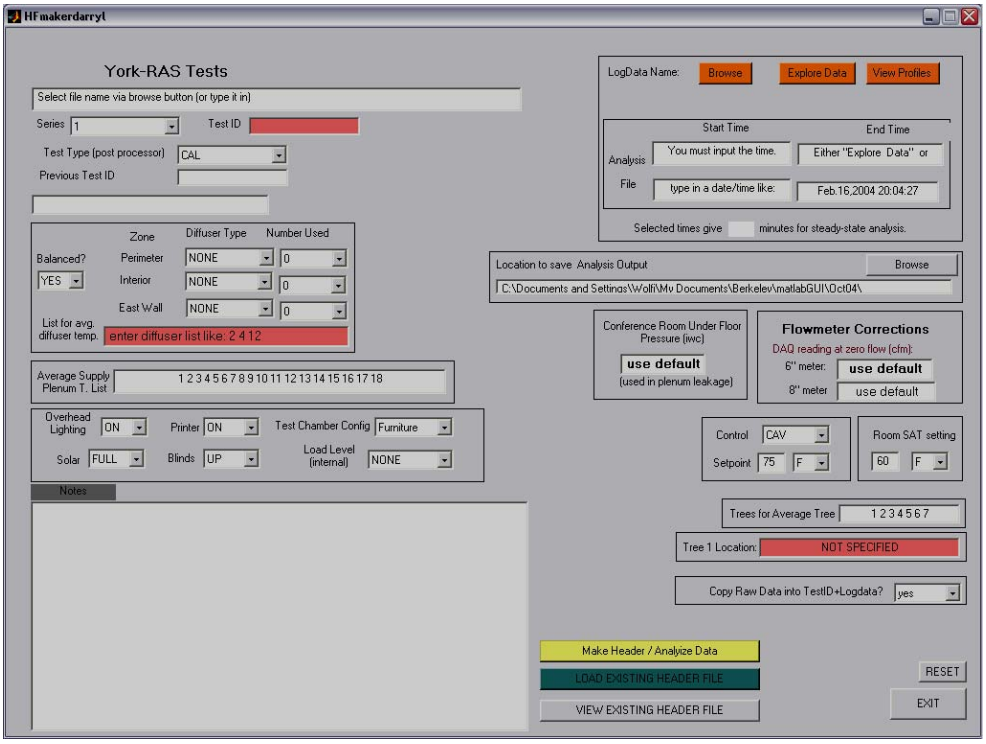

Figure 47: Matlab HeaderMaker graphical user interface

Test setup data fields are available for the following parameters:

- Test type
- Test identification
- Diffuser type
- Number of diffusers
- Which diffusers to use to calculate the average supply air temperature into the test room
- Which diffusers to use to calculate the average plenum temperature
- Status of overhead lighting (on/off)
- Status of the printer (on/off)
- Test chamber configuration
- Status of solar load (off/1 bank/2 banks/3 banks)
- Blinds (closed/open)
- Internal load, i.e. the number of workstations (2/4/6 WS)
- Trees to use for calculation of the average tree
- Position of the mobile tree in the test lab
- Control strategy (CAV/VAV/open loop)
- Room setpoint
- Room supply air temperature setting

- Start and end time for data analysis
- Conference room underfloor pressure
- Flow meter correction

3.2.2 DATABASE

The database consists of an MS Excel spread sheet, containing information about each test that was conducted at the York ADRF. Each column in this file is a copy of a HeaderMaker output file for a given test. (See the database in Appendix F for more details.)

3.3 EXPERIMENTS

3.3.1 TESTING OVERVIEW

In this section we will describe the testing objectives, how we setup and conducted tests and how the how the actual testing compared to the original test plan. We have included more details of the testing in the Appendix D and in the following documents:

- Original and revised test plan
- Test summary spreadsheet showing all major tests accomplished. In this summer we focus only on the tests are of potential utility in our analyses.
- Room setups where we show the configuration of the major test equipment and RAS measuring trees.
- Thermocouple tree setups and profiles. These figures show the test configuration and the relationship between the RAS measurement trees and the diffuser layouts. Included are the measured steady state RAS profiles for all seven trees as well as the trees selected for averaging.

3.3.1.1 Introduction

The full scale testing component of this project is aimed at providing fundamental information based on realistic simulations of actual office configurations and loads to inform the room air stratification EnergyPlus model development work and to add to the body of knowledge about how UFAD systems behave in actual practice.

Part of the testing effort was devoted to addressing a number of outstanding questions about how the performance of UFAD systems is influenced by various design, installation, and operating factors frequently encountered in practice. This effort is important to understanding how much variation to expect in performance in real systems and to identify which factors are important enough to be incorporated in the models and in system design and operating procedures and is worthy of more detailed testing in the future. Testing to support this goal was exploratory in the sense that many tests for many variations were performed as opposed to many tests for a few conditions. We view this effort as preliminary to more focused and replicated tests for the most important conditions identified by the exploratory tests.

These more detailed and focused tests were originally conceived to be part of the full scale test plan, i.e., to conduct detailed enough tests over a broad range of conditions so empirical models could be derived. This goal was not achieved due to the time and resources required to develop the laboratory and because some of the significant problems with controlling the chamber were never fully resolved. In addition, one set of tests, for which we devoted significant effort, resulted in a dead-end; the centralized ideal plume tests (see discussion below).

One of the major objectives of this testing, however, was to conduct accurate enough tests that heat balances for the chamber could be closed thus providing a database of results suitable for validating the UFAD models incorporated in EnergyPlus. This is an iterative process since some variables could not be measured (due to resource constraints) and therefore had to be estimated and/or tested in EnergyPlus as we developed the final models and validating them (e.g., wall conduction). Also, the test chamber was not perfectly insulated as would occur if a facility with guarded walls was used. Thus there were variations from test to test and, more importantly, from test session to test session where some of the parameters differed significantly. In this regard, EnergyPlus serves as our "heat balance engine" because it has the most advanced heat balance computations available. These issues are discussed in more detail in the EnergyPlus validation final report.

The testing covered three major categories of the original plan:

- Shakedown and calibration
- Idealized plume tests
- Room air stratification testing
- Sensitivity testing

A summary of the accomplishments in these areas as compared to the original plan are shown in Table 10.

3.3.1.2 Test Plan Summary

Table 10 is a summary of final accomplishments based on the plan as revised on 7/9/04 relative to the original test plan. Modifications based on actual accomplishments are shown in italics.

Table 10: Testing summary and accomplishments

Test Category	Original scope	Revised plan & accomplishments
Shakedown & calibrations		
Lighting calorimeter	Create calorimeter to develop accurate lighting fixture heat gain to return air model	Continue analysis to corroborate with full-scale tests, and OSU light fixture testing summer of 2004. *(Deferred to future work)*
Full scale lighting	Full scale tests to validate calorimeter model	Tests complete, *analysis incomplete* (see above)
Chamber heat loss calibrations (walls, floor, ceiling)	Calibrate chamber surface heat transfer characteristics to allow heat balance to be calculated during full scale tests	Most tests completed, may require replication runs due to instrumentation problems. *(Some calibration tests not used due to unknown problems.)*
Diffuser clear zone	Establish clear zone for each diffuser type to insure proper placement of RAS measurement trees	Priority 2. Conduct minimum number of tests to verify clear zone for MIT and linear bar grille diffusers to ensure RAS trees are not adversely impacted. *(Measurement trees were fixed and diffuser locations limited; filtered results when trees appeared impacted by diffuser flow.)*
Quartz lamp array calibrations	75 point test of quartz lamp solar simulator to determine incident radiation	Priority 1 • Review procedures and methods with the aim of reducing effort while preserving ability to perform heat balances for perimeter cases. • Install IRT window surface temperature sensors. • Revise procedures to measure transmitted energy at window and radiation incident on interior surfaces consistent with new capabilities installed in EnergyPlus. *(Testing complete, analysis progressing and to be completed in future phase of work)*

Miscellaneous	Floor leak testing, instrumentation checkout and calibration, controls verification testing; post processing software development, comparison metrics development	Priority 1. • Complete flow meter calibration • Periodic floor leak testing has been integrated into testing procedure. • Continue development of comparison metrics and modify post-processing software as appropriate. *(Suspected flow meter errors resulted in inconclusive results for sessions prior to S6)*.
Plume tests		
Simulated, idealized plumes	Simulate ideal plumes used in UCSD salt tank testing, but in full scale	Priority 2. Complete comparison analysis with analytical model. *(Conclusions deferred due to uncertain results for S5)*
Window plumes	Detailed investigations of window thermal plumes with anemometer, thermocouples, and smoke visualization to inform UCSD model development for different diffusers, and blinds open or closed.	Priority 1. Conduct smoke tests for three diffuser types and no diffusers with blinds open and closed. *(Completed)*
RAS performance		
VAV/CAV control	Investigate RAS performance when subjected to common UFAD control strategies for three configurations (interior, perimeter office, and perimeter open plan) using three diffuser types and load conditions.	Priority 1. • This will be the heart of the revised testing plan where testing will be confined to "bracketing" typical operating conditions (e.g., 72°F and 76°F room set points) to determine range of impacts of office configuration, diffuser type and throw, and load. • *Test using VAV control mode only (due to problems instituting stable control in the chamber for CAV mode.)* • *Test for interior office and perimeter open plan only* • *Test for 4 diffuser types (incl. DV) and two internal load conditions, 2 and 6 workstations.* • *Confine perimeter testing to two solar load conditions using 6 workstations only and four diffuser types.*
DV tests	Study RAS performance under simulated DV conditions for interior and perimeter zones and compare using Eplus DV version	*Included as additional diffuser type in RAS testing.*

Detailed testing for empirical models		
Empirical model	Create full matrix of open loop tests for interior, perimeter private office, perimeter open plan with variations of diffuser type, throw, load, and room airflow to allow regression models to be created.	Canceled
Sensitivity tests		
Floor leakage	Determine impact of leakage on RAS performance by testing with and without sealed floors and varying plenum pressure; compare to other tests which are all conduced with sealed floors.	Priority 2. Conduct at least two tests to determine impact on RAS due to leakage. *(Completed)*
Partitions	Determine impact of cubicle partitions on room horizontal and vertical temperature uniformity	Canceled
Load components	Test each of 4 load components (OH lights, workstations, people, and solar) one at a time to determine impact on RAS.	Priority 3. Test one load component at a time. *(Canceled)*
Return location	Determine impact on RAS performance in perimeter zones due to location of the diffuser near the wall vs. inside the room	Priority 3. Conduct one test, time permitting *(Completed)*
UFAD vs. OH	Conduct direct side-by-side comparison tests with overhead vs. UFAD chamber configurations.	Canceled

3.3.1.3 Test sessions and timeline

Activities in the ADRF were conducted in sessions in which our CBE research team would spend 1-3 weeks on site at the ADRF. York personnel provided support during that time primarily with assistance during setup and changes to the test facility, and maintenance and problem solving and repairs to facility equipment. York also was primarily responsible for procurement and installation of all testing instrumentation as specified by CBE and for resolving modifications and repairs during the time between sessions.

An overview of test session activities is shown in Table 11is a summary of the primary activities that occurred during each session. Figure 48 is an annotated timeline for the entire testing effort.

Table 11: Test session overview

Session	Start date	Activities
S0	1/10/2003	Initial lab visit and solar characterization
S1	6/20/2003	Lighting calorimeter testing
S2	8/1/2003	Lab shakedown, controls debugging, complete lighting calorimeter testing, start installation of single plume generator
S3	9/92003	Initial calibration tests, single ideal plume tests
S4	1/7/2004	Shakedown, controls tuning, calibration tests, preliminary heaters based ideal plume tests.
S5	2/6/2004	Complete heater based ideal plume tests, shakedown workstations loads, preliminary interior RAS tests
S6	5/13/2004	Interior RAS tests, flow meter calibration, initial perimeter tests
S7	7/13/2004	Setup for perimeter tests, install TC tree shields, preliminary perimeter tests, detailed solar calibration
S8	10/26/2006	Final interior, perimeter and sensitivity tests

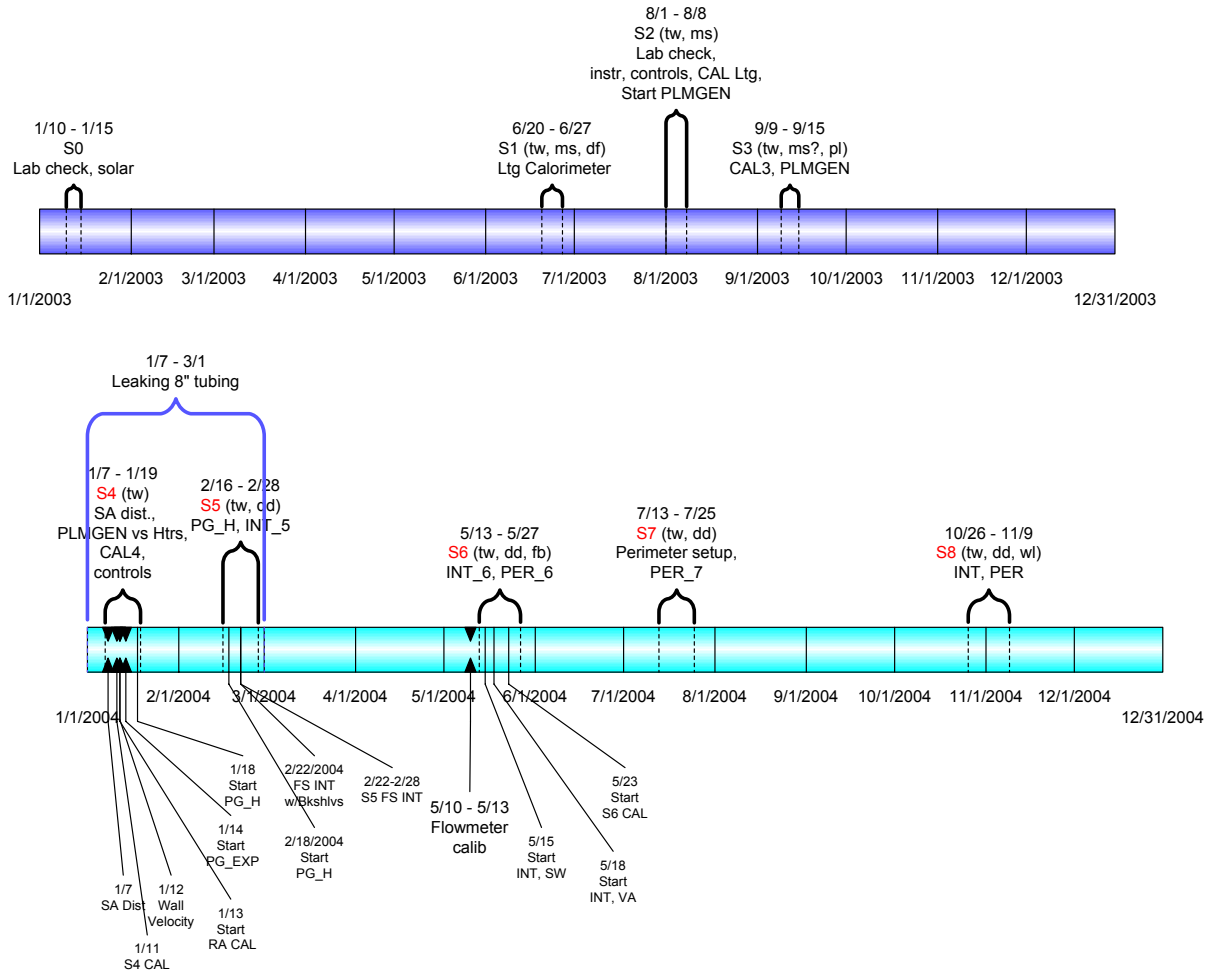

Figure 48: Testing timeline

3.3.2 TEST TYPES

Throughout the testing period we conducted types of tests that resulted in different setups (a fifth setup was used to conduct calorimeter tests of the overhead light fixtures but is not reported herein). These were tests for:

- Chamber calibration
- Ideal plume (called plume generator (PG) tests)
- Interior zone
- Perimeter zone

In the following sections we describe the purpose of these test types and how these experiments were conducted.

3.3.2.1 Calibration Tests

Supply plenum

To determine the heat flux through the floor we used data from our stratified tests. Although we tried to conduct a specific calibration test for this case, it was inconclusive. The methods and results we will discuss in detail in a future Eplus validation report; in general we used Eplus to perform a heat balance on the supply plenum (assuming a mixed condition) with a known heat extraction and surface temperatures. However, these results depend on assumptions about how the furniture covers and insulates the floor.

Chamber

We conducted chamber calibration tests to help determine the actual surface conductivities for the test room so a comprehensive heat balance can be made under stratified conditions that would allow us to better understand thermal distribution in UFAD systems. This extends to the supply and return plenums, for these we need to know the surfaces conductances to better understand the heat fluxes occurring across the major interacting surfaces, i.e., the floor and ceiling, respectively.

For these tests we created mixed conditions (using large mixing fans) in the chamber so that we could run our heat balance engine, EnergyPlus, to determine the conductance's from known heat gains and measured heat extraction rates. Since the walls are virtually identical for the two plenums and the test room walls, we conducted a "system level" test where we measured the overall extraction for given heat gains in the chamber so the only unknown in this case are the gains/losses from the exterior walls (and return plenum roof and underfloor slab). We were careful not to blow air directly on the walls and therefore increase the heat transfer coefficient.

Return plenum/overhead lighting

We built a special test calorimeter to IES specifications [IES 1991] to try and test lighting fixture heat gain to the return plenum to remove another known from the heat balance of the return plenum. In these tests we varied the airflow and "return plenum" temperature over typical actual operating ranges and measured the extraction rate from the calorimeter. Using calculated values of calorimeter wall fluxes we determined the percentage of lighting power input that appears as heat gain to the return, assuming it is all convective gain. The results from these tests will be presented in a future report.

Solar simulator

To help calibrate the solar array we conducted calibration tests with only the solar array providing heat gain to the test room. Using EnergyPlus with measured extraction and known conductances for other surfaces we can determine the heat input required to provide a heat balance.

We also measured the transmitted radiation with a pyranometer and calculated the forward fraction (see Appendix E) to determine the solar input. In addition we measure the radiation incident on all the walls and floor with a pyranometer (for use in a modified version of Eplus). By comparing all these methods we should be able to calibrate the solar gain term for one and two bank solar array configurations. These methods and results will be presented in future reports.

Calibration tests were conducted under constant air volume (CAV) control at various temperature settings while holding room airflow and diffuser throw at high values to promote mixing.

3.3.2.2 Plume Generator Tests

So we could better understand physical principles of underfloor air distribution systems and compare to UCSDs bench scale testing results, we conducted a series of idealized plume (labeled "plume generator") tests. We began these tests by constructing an ideal plume generator that created one large plume in the center of the room. However, it became obvious early in this testing that the profile shapes were not characteristic of typical UFAD systems, therefore we abandoned this path of inquiry.

Alternatively, we conducted a second set of experiments using small portable heaters to generate plumes. While these heaters had fans to force the air through the heating element, a plume was created several feet away from the heaters. The profiles for this case were more classically shaped. We conducted a number of these tests in open loop control mode; i.e., uncontrolled at a given entering airflow and supply temperature. Unfortunately, we are still uncertain about the room airflow measurements for these cases.

3.3.2.3 Fully Configured Tests

In this series, we conducted tests where the test chamber was fully configured to simulate a typical office environment as shown in Figure 49 for both interior and perimeter office arrangements. Perimeter conditions were realized using the simulated solar array which we describe elsewhere. We tested over a broad range of operating conditions including room airflow, room control temperature, diffuser type, number of diffusers, and at various load situations. These tests were all conducted using a VAV control strategy as is common practice in real buildings. (We intended to use a CAV strategy but the controls could never be tuned properly.)

These tests determine how much design and operating conditions influence room air stratification, cooling load and energy use.

We conducted additional tests to determine sensitivity of RAS to secondary effects such as floor leakage and ceiling radiation.

Interior Tests

To test simulated interior zones we covering the window on the west wall of the test chamber with insulating panels to minimize the heat conduction through the window and make the west wall equally well insulated as the other walls. The solar array for interior testing was turned off which as illustrated in Figure 49 through the gray-colored solar array attached to the west wall of the lab. We tested many different configurations to study the impact of various design and operating parameters on stratification. Since this was exploratory testing, we were focused on

testing the upper and lower bounds of the parameters (i.e., 'bracketing" the operational range) that affect stratification as shown in Table 10.

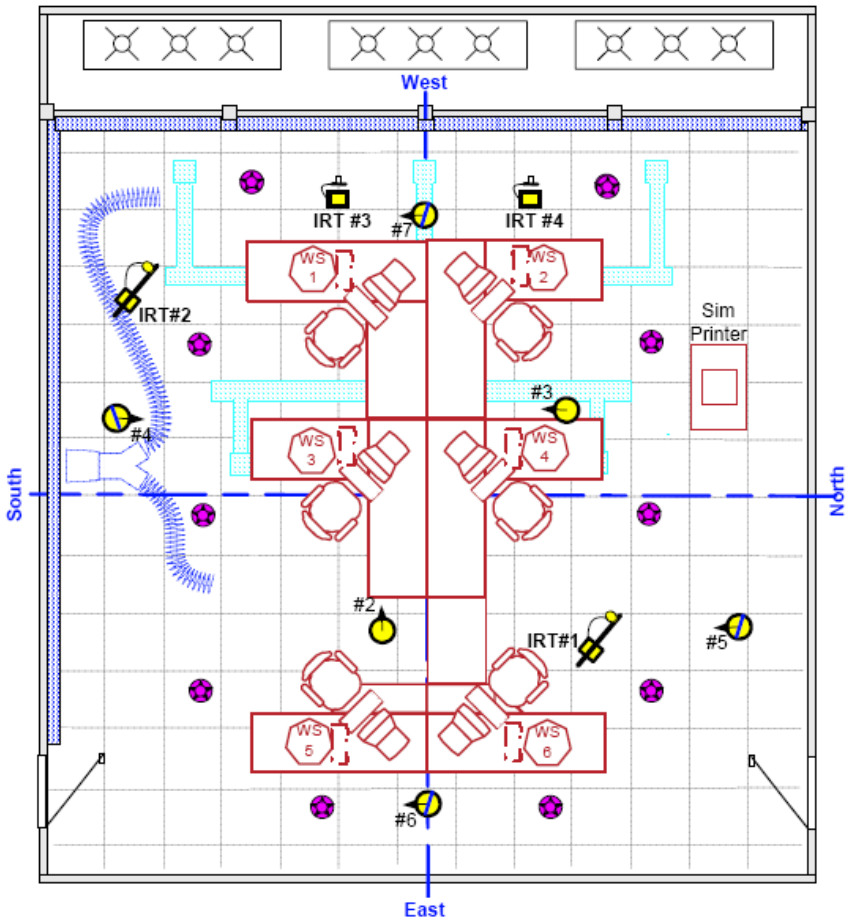

Figure 49: Typical layout for interior testing

Perimeter Tests

For perimeter zone testing we removed the insulation which was covering the window for interior tests and activated the solar array in the environmental chamber. This is shown in Figure 50 with the solar array now colored in orange to illustrate that the array is in use. Since we conducted these tests with the interior zone equipment at their full load condition and adjusted the interior airflow accordingly, we thus simulated an open plan perimeter zone configuration. We adjusted the airflow through the diffusers at the window to account for the additional load from the solar gain. Due to lack of time, we limited our testing to one setpoint, two solar load conditions with blinds open or close, and several different diffuser configurations.

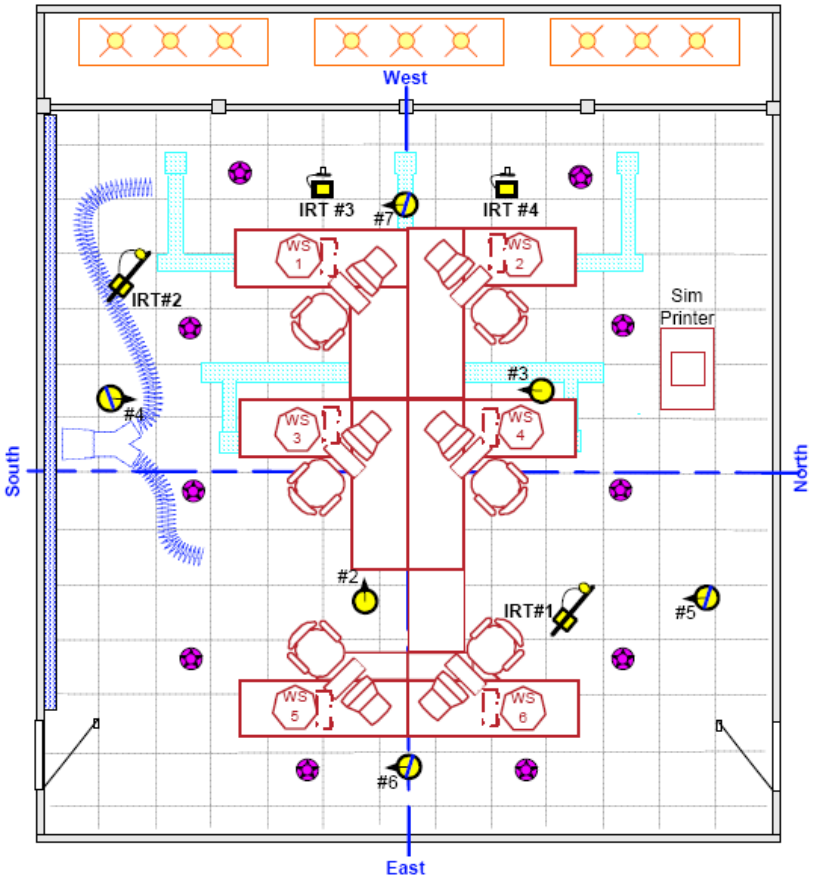

Figure 50: Typical layout for perimeter testing (shown for test with no diffusers at window)

3.3.3 CONDUCTING TESTS

Since each test took several hours to ensure steady state conditions, during a test session we conducted tests back to back tests 24 hours per day. To start a test, we configured the chamber for the particular configuration required and started the data logger. Except over night, we continuously monitored test progress by downloading the entire sensor suite of data periodically using our Matlab processor. Using this tool we track progress and made adjustments in operating parameters as necessary through the Facility Manager front-end. When a test was concluded we stopped the data logger momentarily to create a new log file. Sometimes we conducted smoke tests to better understand the room air distribution and plume and diffuser flow interaction; we took videos of the smoke tests to capture these operating details.

At the end of a test we used the Matlab HeaderMaker tool to enter all the pertinent test information in the fields provided in the graphical user interface (GUI). We then processed the log file which concatenates the test information to the processed data into an output file (.out file) in text format. These output files constitute the test record, although we augmented it with notes in lab notebooks. These processed files what appear in the test database.

3.3.3.1 Steady state

While data was still being acquired, it was necessary to examine how transitions occurred and how much longer a test needed to be continued before it was considered to be in steady state. We monitored steady state by observing the data trends and their real time statistics of standard deviation and rate of change. To be considered in steady state, several critical temperatures (e.g., average room air, wall, ceiling and floor surface) had to be below rates of change of 0.03-0.06°C

(0.05-0.1°F) per hour and the airflow had to not have excessive step changes (not always achievable due to control problems). In addition to the trends we reviewed animated RAS profiles to be sure they were not changing shape near the end of the test.

3.3.3.2 RAS trees and average profile

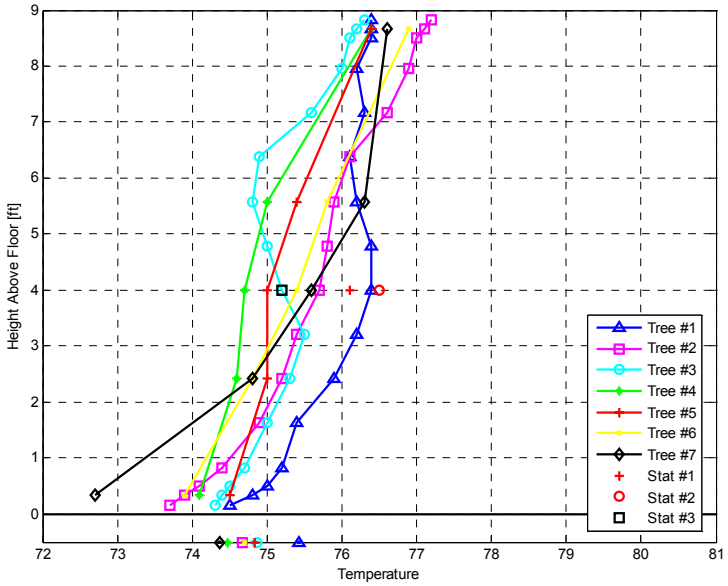

Figure 51: Typical steady state RAS profiles showing influence of diffuser flow at perimeter trees

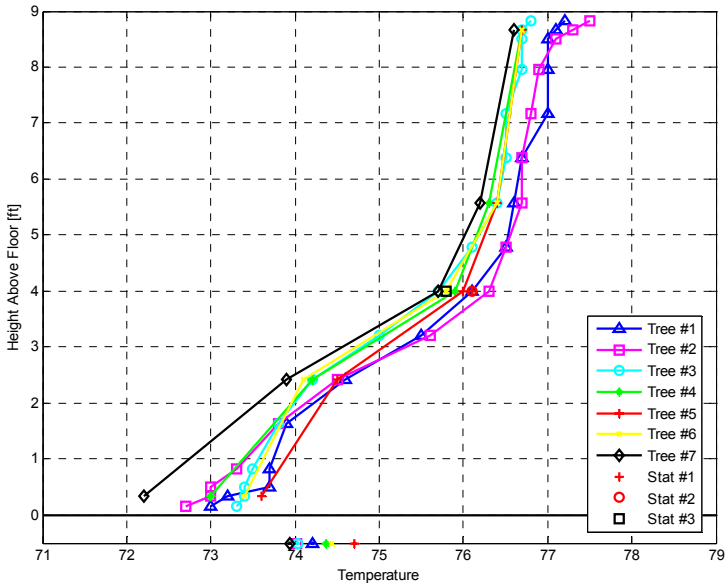

Figure 52: Typical profiles for a test where trees are not impacted by diffuser flows

Figure 51 and Figure 52 show charts of RAS profiles for all seven profile measurement trees each for a different test. In Figure 51 we can clearly see that some trees are influence by diffuser airflow due to the odd shape at the top and the difference between these and the trees in the middle of the room. In this case we select only trees #1 and #2 as being representative of room

average room conditions outside of the clear zone of diffusers. In Figure 52 all the trees are very close together so they could all be selected for the average, although this average is unlikely to be much different than that for of the center trees. For each test we reviewed these profiles to determine which trees to select for the averaging.

4 SIGNIFICANT FINDINGS – IMPACT OF DESIGN AND OPERATING PARAMETERS ON ROOM AIR STRATIFICATION

In this section we report on the results from interior and perimeter zone testing where we explored the impact on room air stratification of different design and operating conditions. These included diffuser type, number of diffusers (varying throw height), and variation in load, and floor leakage. Other tests were conducted to study the impact of ceiling to floor radiation and supply air temperature; these results will be included in future reports. The results shown here represent our major findings based on an in-depth analysis of the experimental data. However, other results are still pending completion of the work outlined in Section 6.

4.1 STRATIFICATION PROFILES AND PERFOMANCE

4.1.1 THERMAL STRATIFICATION

Although we have reserved the discussion about how these experimental results relate to the evolving theory of UFAD stratification as developed by our colleagues at UCSD to a future report, their work to date is helpful in providing an overview of the fundamental principles. UCSDs [Liu and Linden 2005 and 2006] work embodies a long history of research on displacement ventilation and, more recently, UFAD by a number of other researchers.

In simple terms, the stratification performance of UFAD systems under cooling operation is based on the interaction between warm thermal plumes that emanate from heat loads in the space and cool "fountains" or turbulent velocity airflows from the diffusers. The interaction of the thermal plumes and fountains tends to divide the room thermal environment into two vertical layers, a warmer upper layer and a cooler lower layer. This demarcation is most likely a horizontal region or band rather than an abrupt line. The diffuser flow is governed by the interplay of momentum and buoyancy forces which are influenced by diffuser design parameters and the operating environment. This results in a throw height below which mixing is induced. If the throw is high enough, this fountain flow also interacts to some degree with the upper region which causes warm air to be induced into the lower region. All of these processes plus heat loads in the lower region that do not generate thermal plumes combine to determine the temperature in the lower part of the occupied zone.

4.1.2 TERMS AND NOMENCLATURE

To help understand the following test results, we first present a few facts and associated nomenclature about stratification.

Figure 53 is an illustration of a typical stratification profile. This figure identifies several parameters and illustrates some important concepts. In particular, note the large temperature change near the floor from SAT (the supply air temperature entering the room from the diffusers) and the temperature at the 4-in. height. This is caused by the rapid mixing from the diffusers near the floor. As the temperature increases vertically the shape can change due to a number of influences that will influence the performance; especially at the location of the controlling thermostat (labeled "Tstat" in the figure). Also shown is the temperature difference between ankle height at 4 inches and head height at 67 inches shown as (ΔT_{oz}). This region we define as the occupied zone (OZ). ASHRAE Standard 55 places limits on this difference of 3°C (5°F). However, Zhang [Zhang, et. al. 2005) has reported that this limit may be too conservative. The room temperature difference (ΔT_{room}), i.e., the difference between the SAT and the return air

temperature (RAT) is also illustrated. There are several other terms that we use in the following discussion that we define here.

- Stratification – When we use this term we are referring to the ΔT_{oz}, which defines the most important parameter, but also the entire room difference can also be used to characterize stratification.
- Performance – In general we use this term in a general way to denote the combination of factors such as stratification, airflow, and comfort conditions.
- Load condition – We use the term "condition" to emphasize that although we use number of workstations (WS) to characterize the load it is not the load of just the workstations that occurs; i.e., the load at 72°F with 2 WS is not the same as at 76F and 2 WS due to differences in conduction loads. Also, the overhead lights and conduction losses/gains will influence the load/heat gain to the space that is being conditioned. Considering these factors, the maximum load condition for these tests would occur at 72F and 6 WS with overhead lights on.
- Diffuser throw – As noted previously, technically we defined throw in the same way as for overhead diffusers, the vertical height at which the velocity of air being delivered by the floor diffusers has reduced to 0.2 m/s (50 fpm). However, we do not measure this in our tests and primarily use this term in a general sense to indicate how the diffuser flow interacts with the thermal plumes.
- Diffuser Design Ratio (DDR) – This refers to the ratio of the actual airflow to the nominal design airflow recommended by the manufacturer. We use it as an indicator of relative throw heights.
- Normalization – Unless otherwise noted, the charts shown in this report are presented with "normalized" data. We present the results this way so that we can compare tests more directly with one another by normalizing them to the same supply air temperature and room set point. In this process, we assumed that the room extraction rate was the same but since the overall room temperature differential changes somewhat; we adjusted the airflow (and the number of diffusers to maintain the same DDR). In some chart legends we show both the nominal and normalized number of diffusers (non-integer numbers) for reference purposes. This procedure is described in more detail in the Appendix B.
- Extraction rate – Extraction rate in its simplest terms is determined by applying the first law of thermodynamics to a steady flow system, namely, the room return to supply temperature difference multiplied by the room airflow. This represents the amount of heat removed from the space by the airflow and is equal to the *net* heat gain into the space. The net heat gain to the room is the internal gains from people, lights, equipment, and solar minus or plus heat transfer across room surfaces. One of the distinguishing features of UFAD (as compared to overhead systems) is that one of the largest components of heat transfer is through the raised floor. This makes the net heat gain to the room significantly less than for OH systems.
- Equivalent comfort - Since stratified conditions exist in the occupied zone, the concept of determining the airflow quantity required to maintain a uniform well-mixed occupied zone temperature (e.g., as controlled by a 4-ft high thermostat) is no longer valid. For purposes of allowing a comparison between cooling airflow quantities used by UFAD vs. OH systems, we have defined an *equivalent comfort condition* for a stratified room as follows (see Figure 53 for a schematic diagram identifying key features of a room air temperature profile):

1. The average occupied zone temperature ($T_{oz, avg}$), calculated as the average of the measured temperature profile from foot level (4 in.) to head level (67 in.), is equal to the desired setpoint temperature (as measured in a well-mixed OH system).
2. The occupied zone temperature difference (ΔT_{oz}), calculated as the head-foot temperature difference, does not exceed the maximum limit specified by ASHRAE Standard 55 of 5°F.

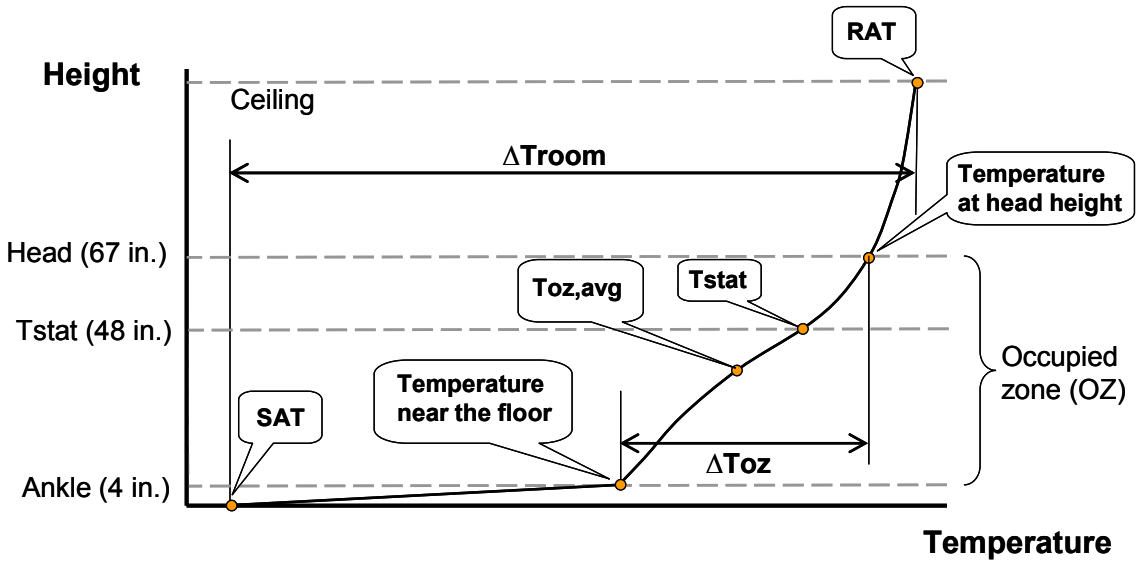

Figure 53: Stratification profile

4.2 INTERIOR ZONE TESTING

For this series of tests the ADRF was configured to simulate typical loads and configuration for an open plan interior office space. The only major departure from typical is the lack of partitions which we eliminated to allow us more freedom and clearance to work in.

Unless otherwise noted, the charts shown in this and subsequent sections are presented with "normalized" data to allow us to compare results at the same supply air temperature and room set point (See definitions in Section 4.1). In particular, we note that all test results shown are normalized to diffuser supply temperature of 18°C (65°F).

4.2.1 DIFFUSER TYPE

In Session 6, we investigated extremes of design and operation conditions for 3 diffuser types – Krantz standard swirl, Krantz HD swirl diffusers, and York MIT variable area (VA) diffusers. We attempted to "bracket" the operating conditions by changing the room setpoints from 22.2°C (72°F) to 24.4°C (76°F), internal loads from 2 to 6 workstations, and design conditions by changing the number of diffusers. One workstation adds a heat gain of about 240 W (820 Btu/h) to the cooling load of the room. By varying the number of diffusers while keeping the total room airflow constant, different throw heights could be achieved which allowed us to see the impact of throw height on room air stratification.

4.2.1.1 Standard Swirl and HD Swirl Diffusers (Krantz)

Table 12 shows tests that we used to compare swirl and HD swirl diffusers. It shows test IDs, as well as the number of diffusers, airflow, DDR and extraction rate. The laboratory layout for these tests can be found in the layouts shown in the Appendix A.

Different throw heights, same loads

In Figure 54 and Figure 55 we present typical results from this testing. The tests show how the profiles change based on DDR which is, to first order, an indicator of throw height. Figure 54 shows two cases each, a high throw (DDR>1) and a low throw (DDR<1) for 22.2°C (72°F) and 24.4°C (76°F) set points, respectively, all at a load condition of 2 WS. Two workstations is a heat gain of approximately 1360 W (4651 Btu/h) or 21.7 W/m² (6.9 Btu/(h-ft²), 2.0 W/ft^2)) including overhead lighting and the simulated printer. Figure 55 shows similar cases for a 6 WS load condition. These tests have a total heat gain of approximately 2350 W (8037 Btu/h) or 37.5 W/m² ((11.9 Btu/(h-ft²), 3.43 W/ft^2). In addition to the standard swirl results, we also show the results for HD swirl diffusers (tests INT_6-1 and INT_6-2). These diffusers result in significantly more stratification in the lower zone than the others. In some cases these diffusers lead to a greater room temperature difference (ΔT_{room}) than Krantz swirl diffusers for the same operating conditions. This will require further study to better understand why and when this occurs. The temperature differences range from about 5.5K to 8K (10°F to 14°F). The results shown in Figure 55 illustrate how variable the stratification performance can be for swirl diffuser depending on throw height. The cases shown for high throw with DDRs > 1, although not expected to occur in practice with well designed systems, do illustrate what can occur if the system is under designed or high throw diffusers are used.

Note in Table 12 that the extraction rates are less than the internal gains to the room. This results from the fact that heat is transferred from the room to the supply plenum thus reducing the cooling load for the room.

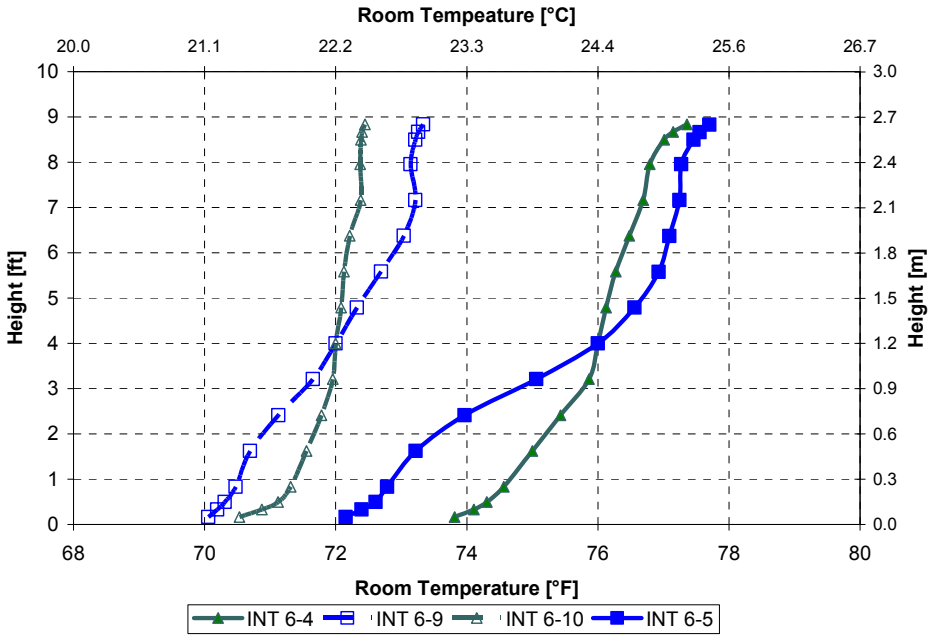

Figure 54: RAS profiles for swirl diffusers at 2 WS load conditions

Table 12: Data for tests with swirl diffusers under various operating conditions

Test ID	Test basics	Airflow		DDR	Extraction Rate	
		cfm/sf	m³/(sm²)	[-]	Btu/(hft²)	W/m²
INT 6-1	72°F, 7 HD, 6 WS	0.80	0.24	1.11	7.81	24.68
INT 6-2	76°F, 7 HD, 6 WS	0.51	0.16	0.96	7.57	23.85
INT_6-3	76°F, 2 SW, 6 WS	0.54	0.16	2.07	6.77	21.4
INT 6-4	76°F, 2 SW, 2 WS	0.24	0.07	1.27	3.10	9.81
INT 6-5	76°F, 6 SW, 2 WS	0.25	0.08	0.48	3.34	10.58
INT 6-6	76°F, 4 SW, 6 WS	0.54	0.16	1.19	6.72	21.21
INT 6-7	76°F, 4 SW, 6 WS	0.51	0.16	0.99	6.82	21.56
INT 6-8	72°F, 10 SW, 6 WS	0.84	0.26	0.59	7.81	24.70
INT 6-9	72°F, 6 SW, 2 WS	0.44	0.13	0.63	3.89	12.31
INT 6-10	72°F, 2 SW, 2 WS	0.47	0.14	1.70	3.68	11.62
INT 6-11	72°F, 4 SW, 6 WS	0.83	0.25	1.42	6.48	20.48

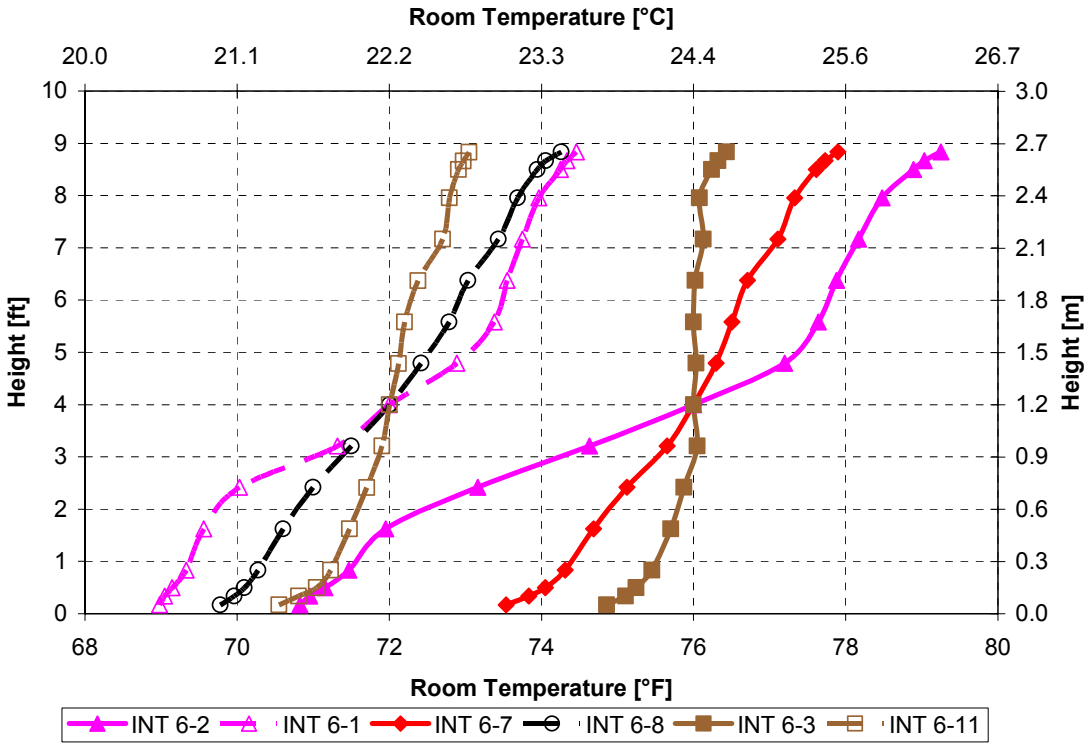

Figure 55: Swirl and HD swirl diffusers under fixed 6 WS load conditions

Similar throw heights, different loads

To determine how these results might depend on load, we compared tests with the same throw but different load conditions as shown in Figure 56. This chart shows three different pairs of profiles. Each pair has similar DDRs ranging from 1.7 to 1.2 and 0.6. However, the internal loads for each pair are different (2 WS versus 6 WS). Data and basic information about the runs is tabulated in Table 13. Their laboratory layout is shown in Appendix A. Although diffuser layout, the number of diffusers and the internal loads are different the vertical stratification profiles with similar

DDRs are very close to one another, especially below 2.1 m (7ft). This result indicates that the vertical temperature distribution strongly depends on diffuser throw height (as indicated by the DDR) and is independent of load for a given throw.

Note that for all of the tests shown in this section that the airflow requirements depend on setpoint and load and are independent of stratification when operated in VAV mode controlled by a thermostat at 4 ft. However, if we were to make this comparison at equivalent comfort conditions (see Section 4.1 for a more complete definition of equivalent comfort) for the more stratified cases by, for example, adjusting the setpoint to keep the occupied zone average temperature the same as the lower stratified cases, the airflow requirements would be lower.

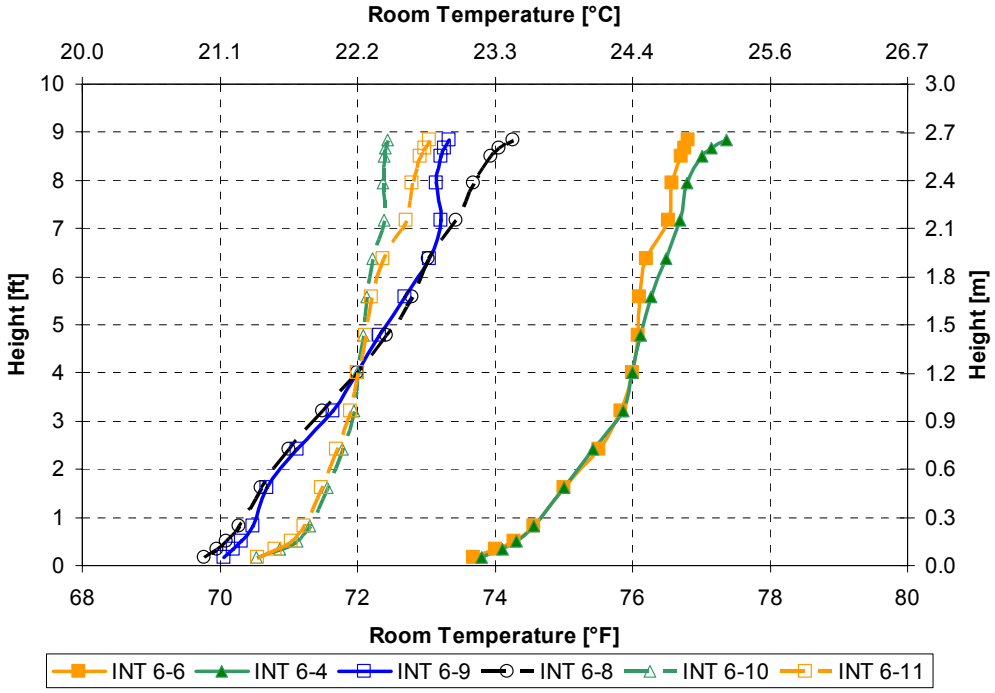

Figure 56: Krantz swirl diffuser tests with similar DDRs and different loads

Table 13: Data for swirl diffuser tests with similar DDRs and different loads

Test ID	Test description	Airflow		DDR	Extraction Rate	
		cfm/sf	m³/(sm²)	[-]	Btu/(hft²)	W/m²
INT 6-4	76°F, 2 SW, 2 WS	0.24	0.073	1.27	3.10	9.81
INT 6-6	76°F, 4 SW, 6 WS	0.54	0.163	1.19	6.72	21.21
INT 6-8	72°F, 10 SW, 6 WS	0.84	0.255	0.59	7.81	24.70
INT 6-9	72°F, 6 SW, 2 WS	0.44	0.134	0.63	3.89	12.31
INT 6-10	72°F, 2 SW, 2 WS	0.47	0.142	1.7	3.68	11.62
INT 6-11	72°F, 4 SW, 6 WS	0.83	0.252	1.42	6.48	20.48

Different throw heights and different loads

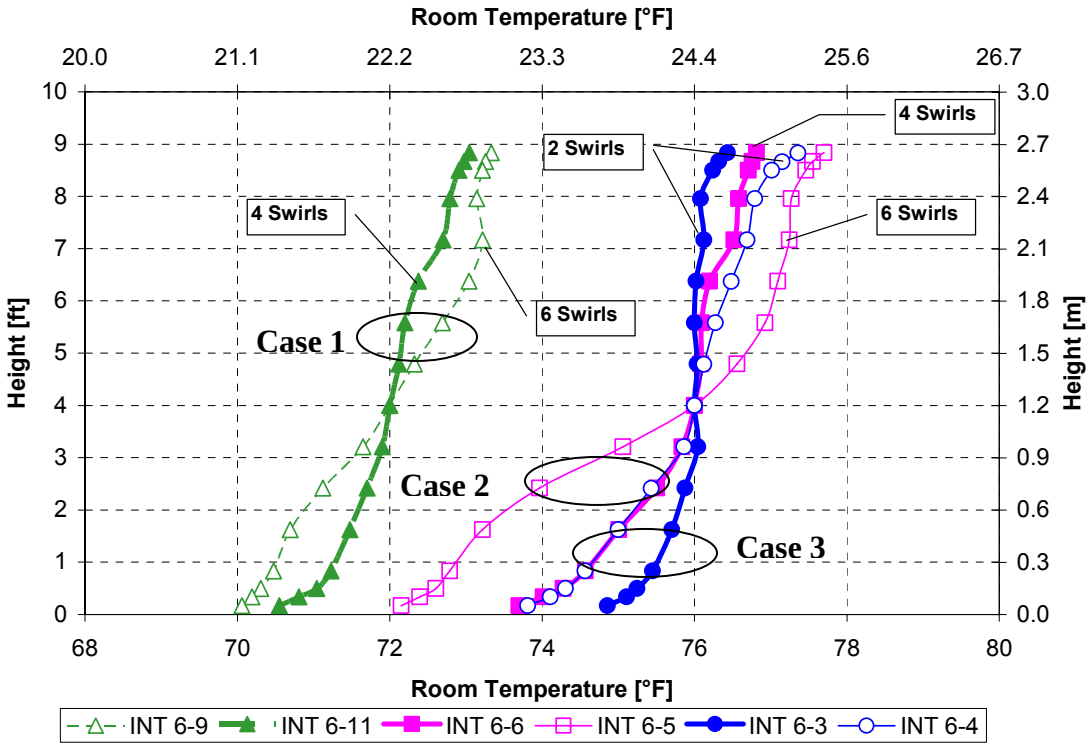

Figure 57: RAS profiles for swirl diffusers with changing DDR with load changes

The data compiled in Table 12 can also be used to investigate the impact of load changes on profile shape. We summarize these cases in Figure 57 where three sets of data are shown. Each set has the same color and data symbol and is identified by a case number. .Each set represents a case where the load is decreased from 6 WS (heavy lines, filled symbol) to 2 WS (thin line, open symbol). However, as the load decreases the number of diffusers is increased from 4 to 6, except for the blue lines (INT_6-3 and INT_6-4) where the number of diffusers is constant. For the same number of diffusers the DDR would decrease as the load is reduced due to the reduction in room airflow, which is shown for this latter case. Increasing the number of diffusers as load decreases exaggerates the change in stratification. In Cases 1 and 2 the differences are exaggerated due to the difference in number of diffusers which suggests that the difference would be negligible if the same number was used. In Case 3, which uses the same number of diffusers, the difference is exaggerated due to using a well-mixed case as the comparison. We conclude from this analysis that there are no significant differences in stratification as load is varied as occurs in real buildings. See Section 4.2.4 for further results on this topic.

4.2.1.2 Variable Area Diffusers (York MIT)

We conducted tests similar to the above swirl tests for York MIT variable area diffusers for room setpoints of 22.2°C (72°F) and 24.4°C (76°F). The number of diffusers was varied from 2 to 6. Internal loads were varied from 2 workstations to 6 workstations.

Appendix A shows the laboratory layout for the variable diffuser test series for 2, 4 or 6 diffusers under various load conditions, respectively. The vertical temperature distribution for VA diffusers and basic test data is shown in Figure 58 and Table 14.

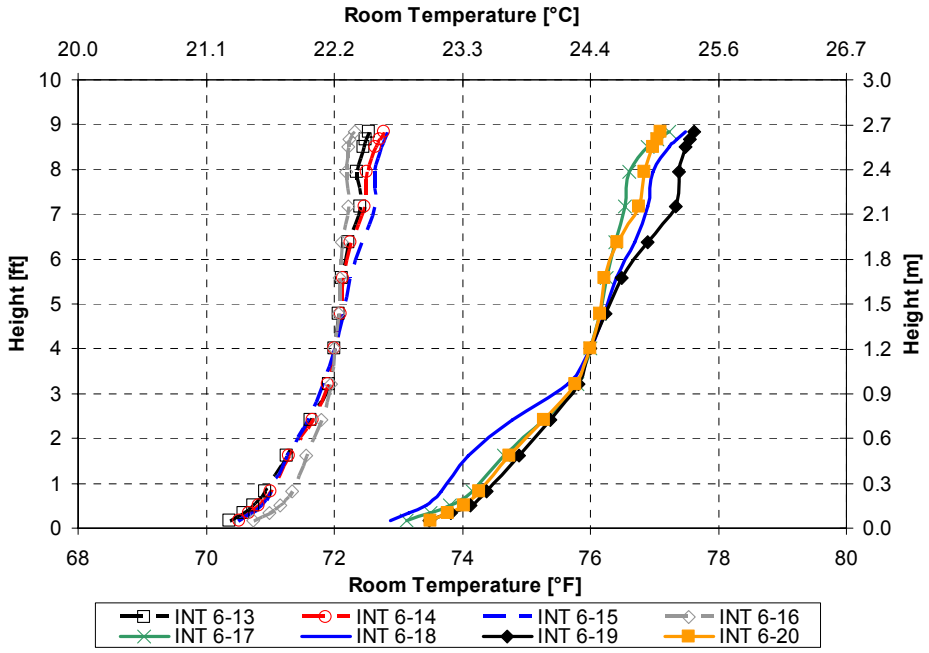

Figure 58: Room air stratification profiles for York VA diffusers under different load conditions

Table 14: Airflows and DDRs for variable area diffusers under extreme operating conditions

		Airflow		DDR	Extraction Rate	
Test ID	**Test description**	cfm/sf	m³/(sm²)	[-]	Btu/(hft²)	W/m²
INT 6-13	72°F, 6 VA, 6 WS	0.92	0.279	0.58	7.27	22.93
INT 6-14	72°F, 4 VA, 6 WS	0.93	0.282	0.92	7.03	22.18
INT 6-15	72°F, 4 VA, 2 WS	0.39	0.120	0.43	3.24	10.17
INT 6-16	72°F, 2 VA, 2 WS	0.53	0.162	1.14	4.06[6]	12.77
INT 6-17	76°F, 2 VA, 2 WS	0.22	0.067	0.62	2.76	8.73
INT 6-18	76°F, 4 VA, 2 WS	0.22	0.068	0.34	2.87	9.04
INT 6-19	76°F, 6 VA, 6 WS	0.51	0.154	0.44	6.89	21.77
INT 6-20	76°F, 4 VA, 6 WS	0.52	0.160	0.67	6.48	20.48

To maintain the same room temperature setpoint, the effective area of York MIT diffusers changes when airflow requirements vary due to changing loads in the room (refer to Section 3.1.3.2). As loads decrease the discharge area reduces due to the action of the modulating damper. The area change is roughly proportional to the airflow change so that the discharge velocity is essentially constant. (Although we show the DDR in Table 14, it is of little usefulness with these diffusers because it does not characterize their performance as it does for swirl diffusers.) This constant air velocity will maintain the throw height of the diffuser at the same level at all times for a wide range of operating conditions. As the results presented in Figure 58 show, this results in a consistent profile over a wide range of operating conditions (load, number of diffusers, and

[6] It is not clear why this test operated at significantly higher extraction rate and airflow than INT_6-15. The diffusers must have been full open allowing the DDR to exceed its rated airflow.

room setpoint). Note also that in these tests, like the swirl tests, the airflow requirements are driven by the load and room setpoints primarily.

4.2.1.3 All diffuser types

To compare the performance of the various diffuser types that we tested, we show three profiles at each room setpoint for a 6 WS load condition in Figure 59. We selected tests that represent as closely as possible a "design" condition at peak load (6 WS) with diffusers operating at their design airflow rates. Since there is no experiment with a 22.2°C (72°F) room setpoint and a DDR of approximately 1, INT 6-7 was shifted to this setpoint using the normalization method described in Appendix B. Likewise, INT_6-20 is not operating at the design airflow for VA diffusers as indicated by the DDR of 0.67. (Although as stated above, DDR does not represent throw for VA diffusers, in this case DDR does show how close to design flow the diffusers are operating.) However, since there is little difference in performance for VA diffusers based on their airflow rate, INT_6-20 can be used it to represent the VA diffusers performance in this comparison.

As shown in Figure 59 and Table 15, swirl and VA diffusers perform equally under typical design conditions.

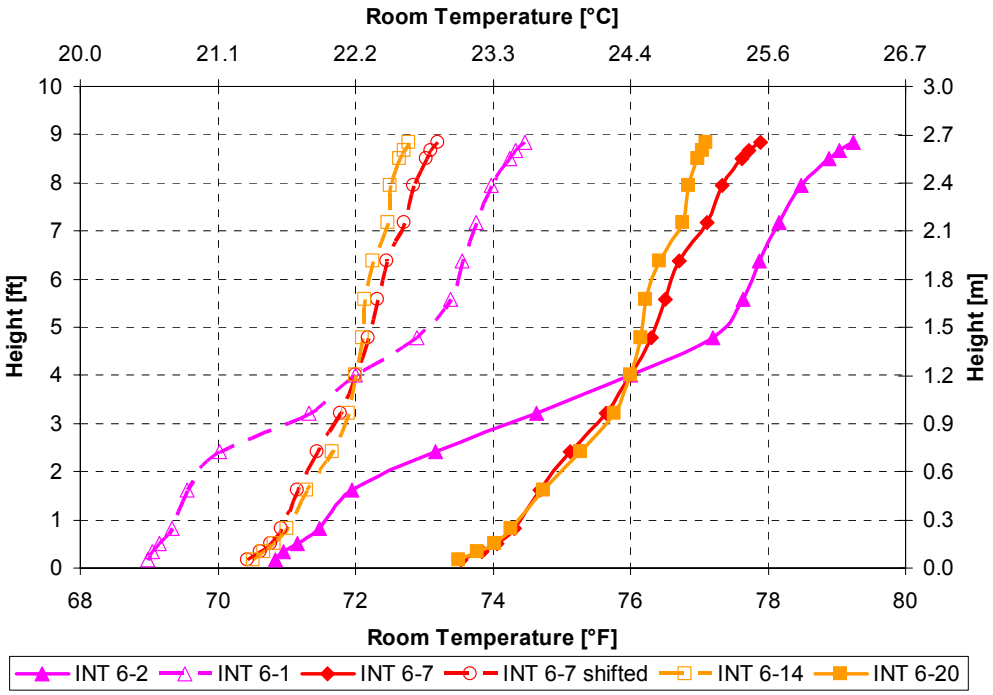

Figure 59: Comparison of VA, SW and HD diffusers under peak load conditions

Table 15: Data comparison of VA, SW and HD diffusers under peak load conditions

Test ID	Test description	Airflow		DDR	Extraction Rate	
		cfm/sf	m³/(sm²)	[-]	Btu/(hft²)	W/m²
INT 6-1	72°F, 7 HD, 6 WS	0.80	0.24	1.11	7.81	24.68
INT 6-2	76°F, 7 HD, 6 WS	0.51	0.16	0.96	7.58	23.85
INT 6-7	76°F, 4 SW, 6 WS	0.51	0.16	0.99	6.82	21.56
INT 6-7 shifted	72°F, 4 SW, 6 WS	0.80	0.24	0.99	*6.82*[7]	21.56
INT 6-14	72°F, 4 VA, 6 WS	0.93	0.28	0.92	7.03	22.18
INT 6-20	76°F, 4 VA, 6 WS	0.52	0.16	0.67	6.48	20.48

As is clearly shown in these results, the low throw characteristics of the HD swirl diffusers leads to stratification much larger than the other diffusers. Air leaving HD swirl diffusers is spread horizontally along the floor and does not induce mixing with room air as much as swirl diffusers do. This leads to cooler temperatures in the lower zone of the room, since the effect of mixing only occurs up to the height of about 25 cm (10 inch). However, the room extraction – driven by room temperature difference (since airflow is about the same for standard swirls and HD swirls) – is increased for HD swirl diffusers. Preliminary heat balances on the chamber (not shown here, see Section 6), indicates that less heat is transferred to the plenum, despite the fact that the warmer ceiling causes increased radiation transfer to the plenum. This result has yet to be fully explained.

We can conclude from these results that constant throw diffusers (VA) have consistent stratification over a wide range of airflow and operating conditions, whereas the stratification with constant outlet area diffusers (swirls) strongly depends on the amount of airflow (which directly impacts throw). Ultimately, this leads to great potential but also challenges for controlling room air stratification with swirl diffusers. Moreover, the performance (profile shape and airflow requirements for a given 4-ft room setpoint) at design conditions is virtually the same for VA and swirl diffusers when operated at their respective nominal design airflow rates.

4.2.2 NUMBER OF SWIRL DIFFUSERS

As shown in Figure 56, tests for swirl diffusers with similar throw height (represented by DDR) have the same vertical temperature distribution. As a next step, we investigate in more detail how the impact of diffuser throw height changes the vertical temperature distribution in the room. To do so, we conducted a series of tests in Session 8 with different numbers of Krantz swirl diffusers at constant load conditions of 6 WS.

Appendix A shows the laboratory layouts for this diffuser throw height study. The "base test" with 4 diffusers is INT 8-7. The following tests (INT 8-2, INT 8-3 and so on) increase the number of diffusers by 2 for each test to INT 8-6 with 14 diffusers (see Table 16).

We conducted all 6 tests at a room setpoint of 23.3°C (74°F). Adding diffusers test to test, at constant overall room airflow reduces the airflow per diffuser and thus its throw height. This is indicated by the DDR shown in Table 16 where the results are summarized. As we mentioned in previous sections, the diffuser design ratio (DDR) is a rough indicator of diffuser throw height, at

[7] In the normalization procedure, we assume the extraction rate is constant (therefore this shifted extraction rate is shown the same as for the base INT_6-7 case) to be able to calculate a new airflow. This works well in general when we normalize over small differences in supply temperature and room setpoint, but we know that when we extrapolate from a 76°F setpoint to a 72°F the extraction can no longer be assumed constant.

least for diffusers with a constant effective area. The results from this study are shown in Figure 60.

Table 16: Basic data for throw height study

Test ID	Test description	Room Airflow		Extraction Rate		DDR [-]
		cfm/ft²	l/(sm²)	Btu/(hft²)	W/m²	
INT 8-7	74°F, 4 SW, 6 WS	0.65	3.30	6.21	19.54	1.2
INT 8-2	74°F, 6 SW, 6 WS	0.62	3.14	6.45	20.36	0.81
INT 8-3	74°F, 8 SW, 6 WS	0.64	3.23	7.06	22.29	0.64
INT 8-4	74°F, 10 SW, 6 WS	0.59	2.98	6.65	20.98	0.48
INT 8-5	74°F, 12 SW, 6 WS	0.57	2.89	6.55	20.70	0.39
INT 8-6	74°F, 14 SW, 6 WS	0.60	3.05	6.89	21.70	0.36

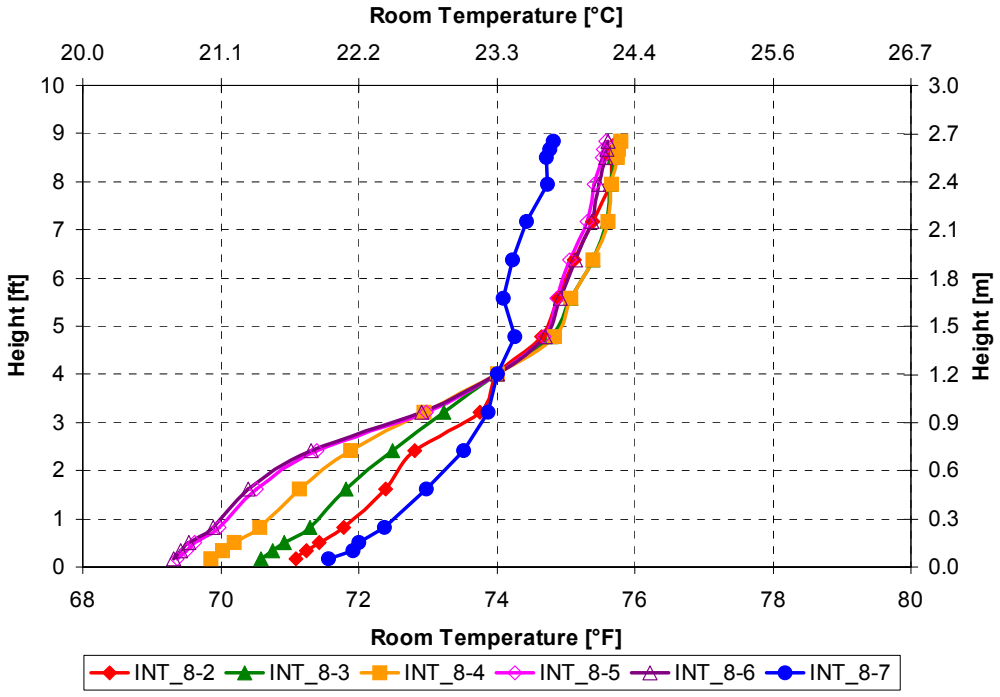

Figure 60: Results of diffuser throw height study

The change in DDR, due to constant airflow and increased number of diffusers, only changes the temperatures in the occupied zone, whereas the return air temperature remains the same throughout these tests. The baseline test INT 8-7 with 4 Krantz swirl diffusers is an exception where the return temperature is about 1°F lower than the other tests. We have not determined the cause of this but we have observed in the testing a general trend of decreasing return temperature and some distortion of the upper profile as the throw of the diffusers increases (i.e., for DDR > 1). This suggests that for these cases the mixing process envelops the entire room causing a more uniform temperature and/or diffuser airflow affecting the trees in the upper region whereas at lower throws the mixing process is confined to lower regions of the room; in the other cases shown it appears to be confined to the region below the thermostat. A more appropriate comparison test would be one that was conducted with a DDR = 1, but we did not test this configuration. Since the tests shown have all been normalized to a supply air temperature of 18.3°C (65°F) they all have the same temperature difference between supply and return air

temperature. These results also suggest that there is a limit of achievable lowest temperature in the occupied zone since, as shown in Figure 60, adding diffusers has a diminishing returns effect when the number exceeded 12 diffusers.

4.2.3 AIRFLOW REQUIREMENTS

Another factor that can be discerned from this testing is the impact on airflow requirements for different design and operating conditions. It is apparent from the results shown in Table 17 that for the constant diffuser supply temperature of 18°C (65°F) and a 4 ft. thermostat height, the airflow requirements are derived primarily from the load conditions, i.e., the combination of number of workstations and room setpoint. Airflow is not impacted by diffuser type or the magnitude of stratification; note the variations in ΔT_{oz}. However, the relative impact of the greater stratification of swirl diffusers relative to VAs is not represented by these results. It is better to compare at equivalent comfort conditions (i.e., equal average occupied zone temperature) where the potential for reduced airflow of swirls relative to VA diffusers can be shown more realistically. When we did one preliminary example of this sort of comparison using HD diffusers (we increased the setpoint for the swirl case to yield the same average occupied zone temperature), we found that the HD swirl airflow was close to 20% less than for VA diffusers operating at the same load condition. To increase stratification (relative to VA diffusers) requires that the number of swirl diffuser be increased enough to reduce their airflow below their design value. Then the setpoint must be increased relative to the VA setpoint to realize equal comfort. Therefore, some of this benefit will be offset by the cost incurred by having to increase the number of swirls over and above what their design nominal airflow would dictate. A more complete discussion of these effects is shown in [Benedek et. al. 2006] and Section 4.1.2.

Table 17: Airflow and ΔT_{oz} summary for swirl and VA diffusers at various operating conditions

Load condition	72°F Setpoint				74°F Setpoint				76°F Setpoint			
	SW		VA		SW		VA		SW		VA	
	Airflow cfm/ft^2	ΔT_{oz}, °F	Airflow cfm/ft^2	ΔT_{oz}, °F	Airflow cfm/ft^2	ΔT_{oz}, °F	Airflow cfm/ft^2	ΔT_{oz}, °F	Airflow cfm/ft^2	ΔT_{oz}, °F	Airflow cfm/ft^2	ΔT_{oz}, °F
6 WS	0.84	2.2 – 2.8	0.92	1.5 – 1.5	0.60	2.2 – 5.5	0.60	N/A	0.54	0.9 – 2.7	0.52	2.4 – 2.7
2 WS	0.44	1.3 – 2.5	0.45	1.1 – 1.5	0.30	1.7 – 6.6	0.34	N/A	0.24	2.2 – 4.5	0.22	2.8 – 3.3

4.2.4 LOAD VARIATION, SWIRL DIFFUSERS

To simulate how a real system operates, we conducted a series of tests where we kept the number of diffusers constant but varied the load by decreasing the number of workstations from 6 to 2 while maintaining a room setpoint of 23.3°C (74°F). For systems with swirl diffusers this should result in a decrease in DDR as the airflow is decreased under VAV control. However, it was not clear how the RAS profile would change since the load and DDR are both decreasing. The results are summarized in Table 18 and Figure 61 (normalized to a diffuser supply temperature of 18.3°C (65°F) and to the room setpoint of 23.3°C (74°F)). The laboratory layouts can be found in Appendix A.

We have some concern about the results for test INT_8-9 because we discovered during our analysis that a heater in the supply plenum was operating during the test, thus potentially skewing the results. Therefore, we include test INT_6-5 for comparison purposes since it was conducted at the same conditions as INT_8-9 except at a room setpoint of 24.4°C (76°F). By normalizing this test to 23.3°C (74°F) setpoint we have a more direct comparison as shown in Figure 61 where it shows that the 2 WS load condition has virtually the same profile as the other loads.

These results and those shown in Section 4.2.1.1 for cases of different throw and different loads indicate that very little change in RAS profile occurs as loads decrease under VAV control.

Table 18: Basic data for load variation study

Test ID	Test basics	Room Airflow		Extraction Rate		DDR
		cfm/ft²	l/(sm²)	Btu/(hft²)	W/m²	[-]
INT 8-2	74°F, 6 SW, 6 WS	0.62	3.14	6.45	20.36	0.81
INT 8-8	74°F, 6 SW, 4 WS	0.49	2.49	4.61	14.51	0.65
INT 8-9	74°F, 6 SW, 2 WS	0.36	1.82	3.31	10.40	0.49
INT_6-5	74°F, 6 WS, 2 WS	0.31	1.56	3.09	10.54	0.48

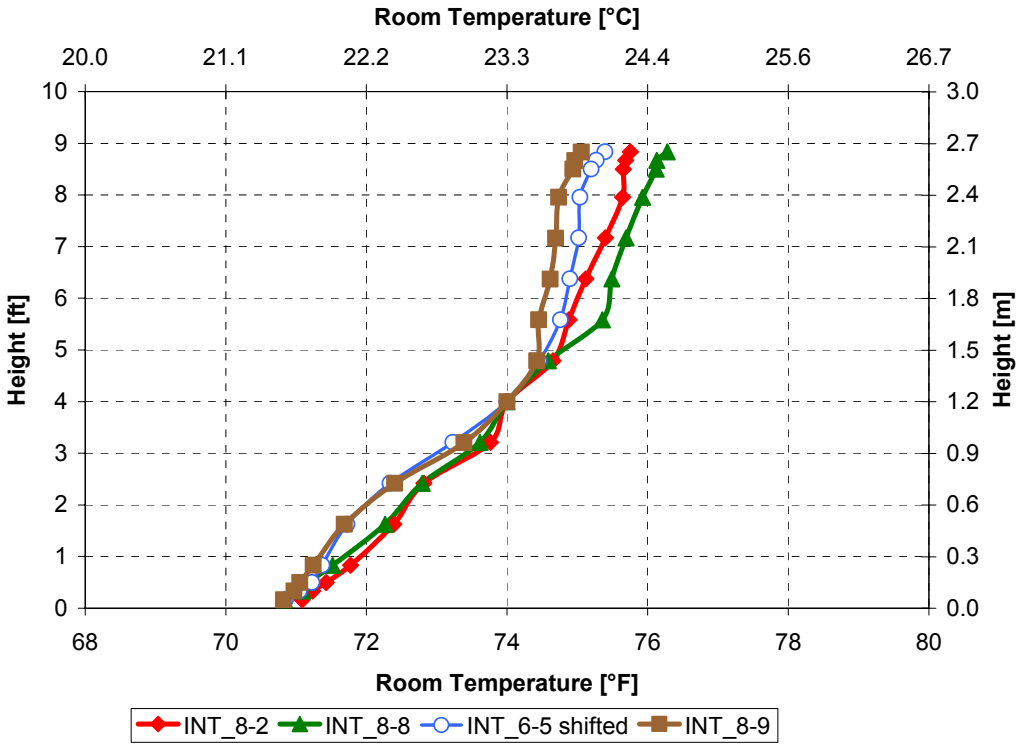

Figure 61: Results of load variation study

4.2.5 FLOOR LEAKAGE

Supply plenum leakage is one of the most important issues facing the UFAD industry. In general, there are two types of leakage, Category 1 leakage where the supply air leaks outside the plenum and Category 2 where air leaks into the space. Category 2 leakage enters the room from the gaps between the floor panels and PVD boxes and for VA diffusers, gaps in the damper assembly when it is closed. For more detailed information about leakage refer to our papers on design and commissioning practices [Bauman et al. 2006, Webster and Bauman 2006]

Figure 62 shows two different sets of leakage rate curves. One set, for comparison purposes) is for manufacturers data that we extrapolated from single point measurements at 12.5 Pa (0.05 iwc) using a power exponent of 2. These are typical rates for Tate floors (manufacturer) with various combinations of carpeting. This data is based on laboratory testing of relatively small areas for a floor without penetrations; actually leakage in real buildings can be substantially greater due to penetrations, construction practices, edge conditions, and field conditions that could change the

tolerances between tiles. The other set is represented by two tests where we measured the leakage for the York ADRF laboratory.

The term "carpet tiles offset" means that carpet tiles are overlapping the gaps between the floor panels. In this case, the carpet tiles provide a seal at the floor panel gaps. In practice, the carpet tiles are usually installed this way.

When carpet tiles have exactly the same size as the floor panels, they can be aligned with the panels. The curves labeled "aligned carpet tiles" indicate such an installation. The only advantage of this installation is that only one carpet tile needs to be removed to open the underfloor plenum, whereas in the case of overlapped tiles a minimum of 4-6 of them have to be removed.

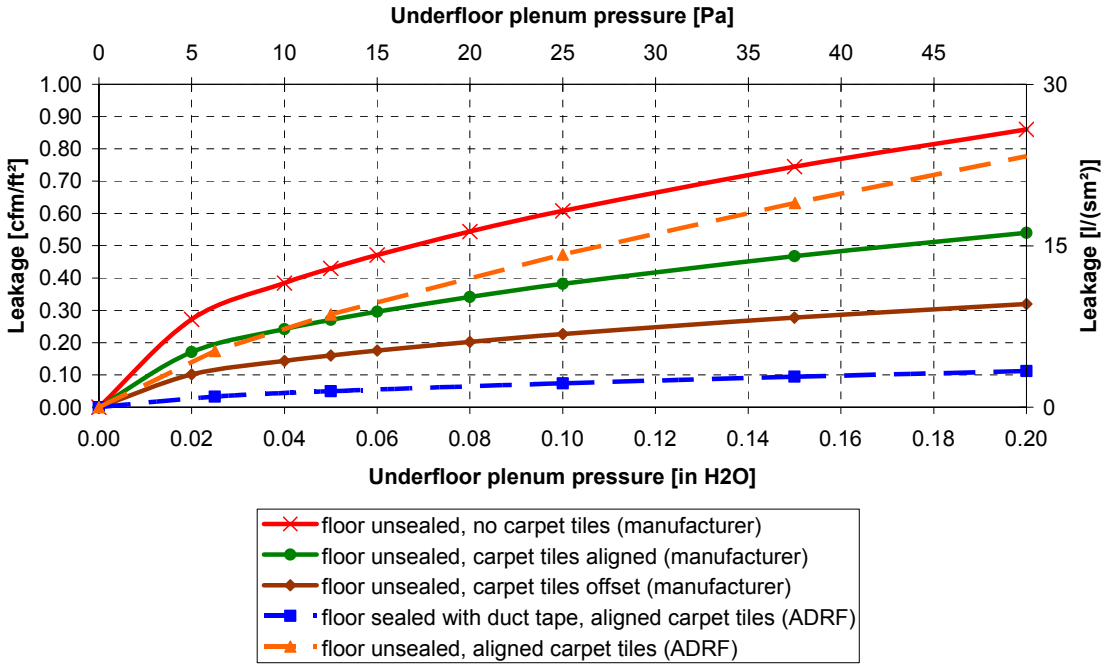

Figure 62: Leakage rates obtained at the York ADRF and from manufacturers

As mentioned previously, all of our testing was conducted with the floor joints taped with duct tape and edges sealed with caulking and duct tape. At the typical underfloor plenum pressure of 12.5 Pa [0.05" H_2O], the leakage rate is very small. For leakage testing, the duct tape, which sealed the laboratory floor panels, was removed on a portion of the floor so that higher leakage rates could be obtained. At the typical underfloor plenum pressure of 12.5 Pa [0.05" H_2O], leakage rates similar to a typical unsealed floor with aligned carpet tiles were measured; see orange curve in Figure 62. These rates are greater than we would expect in a real installation even allowing for sources other than the floor. We believe a good target is 0.1 cfm/ft^2 for floor leakage at 0.05 iwc which is about 17% of a typical interior zone airflow rate of 0.6 cfm/ft^2. Our leakage test rate is almost three times as high at 0.3 cfm/ft^2, but we intentionally made it high to ensure we had a measurable effect.

We conducted a total of four leakage tests; two with swirls and two with VA diffusers. In each set of two tests, one was made at 6 WS and the other at 2 WS to show the impact of leakage at high and low load conditions. The laboratory layouts can be found in Appendix A.

Data for all leakage tests are shown in Table 19 and Figure 63 is a leakage rate summary chart for all tests.

Table 19: Leakage test results for all leakage tests

Test ID:	Test description	Plenum pressure	Leakage into lab		Total to Room		Total to Diffusers		leakage	DDR
		iwc	cfm/sf	l/(sm²)	cfm/sf	l/(sm²)	cfm/sf	l/(sm²)	%	[-]
Swirl Diffusers										
INT 8-7	74°F, 4 SW, 6 WS	0.082	0.047	0.24	0.62	3.13	0.57	2.89	7.5	1.2
INT 8-15	74°F, 4 SW, 6 WS	0.039	0.253	1.29	0.60	3.03	0.34	1.74	42.2	0.72
INT_8-2	*74°F, 6 SW, 6 WS*	*0.040*	*0.029*	*0.15*	*0.57*	*2.91*	*0.54*	*2.76*	*5.1*	*0.81*
INT 8-16	74°F, 4 SW, 2 WS	0.015	0.128	0.65	0.33	1.67	0.20	1.02	38.8	0.42
INT 8-9	*74°F, 6 SW, 2 WS*	*0.016*	*0.015*	*0.08*	*0.36*	*1.83*	*0.35*	*1.75*	*4.2*	*0.49*
VA Diffusers										
INT 6-14	74°F, 4 VA, 6 WS	0.050	0.027	0.138	0.69	3.520	0.67	3.383	3.9	NA
INT 8-17	74°F, 2 VA, 2 WS	0.051	0.30	1.543	0.34	1.920	0.08	0.377	88.2	NA
INT 8-18	74°F, 2 VA, 6 WS	0.051	0.30	1.542	0.59	3.010	0.29	1.468	51.3	NA

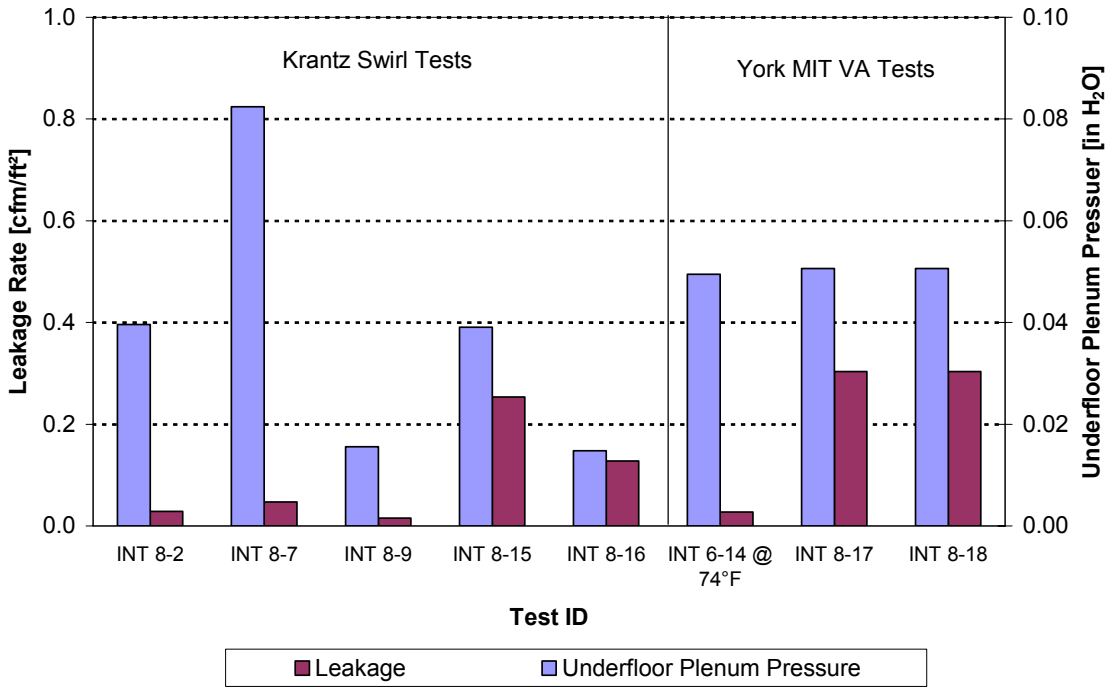

Figure 63: Leakage rates for Krantz swirl and York MIT VA diffusers (IP units)

4.2.5.1 Krantz Swirl Diffusers

Figure 64 shows the results for swirl diffusers at 6 WS load conditions and 23.3°C (74°F) room set point. Test data for all swirl tests is shown in Table 19. The first leakage test was set up with 6 workstations and 4 Krantz swirl diffusers at the same room setpoint (INT 8-15). The reference test with the same test parameters but without leakage is INT 8-7, colored blue. As noted previously, INT_8-7 is not an ideal test to use for comparison because it is a high diffuser throw

case. In hindsight, both the reference test and the leakage test should have been conducted with 5 diffusers. Shown also for comparison purposes is INT_8-2 which is a 6 WS with a number of diffusers that yields a DDR somewhat comparable, although still greater than that for INT_8-15. A test with the same DDR would most likely result in stratification virtually the same as INT_8-15. Table 19 shows that the total airflow entering the room is equal for both runs whereas the amount of air going through the diffusers if leakage is present is only 58% of the total room airflow. The other 42% enters the room through the gaps between the floor panels. Note also that the plenum pressure is reduced by 50% for leakage of this magnitude. This indicates that floor leakage can indirectly reduce Category 1 leakage.

These results show that the effect of floor leakage is to increase the stratification in the lower zone. We might conjecture that this is due to a displacement ventilation-like effect resulting from the leakage air entering the room with little, or no, momentum. However, the comparison test INT_8-2 shows that almost the equivalent stratification can be achieved by increasing the number of diffusers to increase stratification. This suggests that the increased stratification for the leakage test is more of a function of the decreased throw height (due to reduced airflow) of the diffusers rather than the leakage itself.

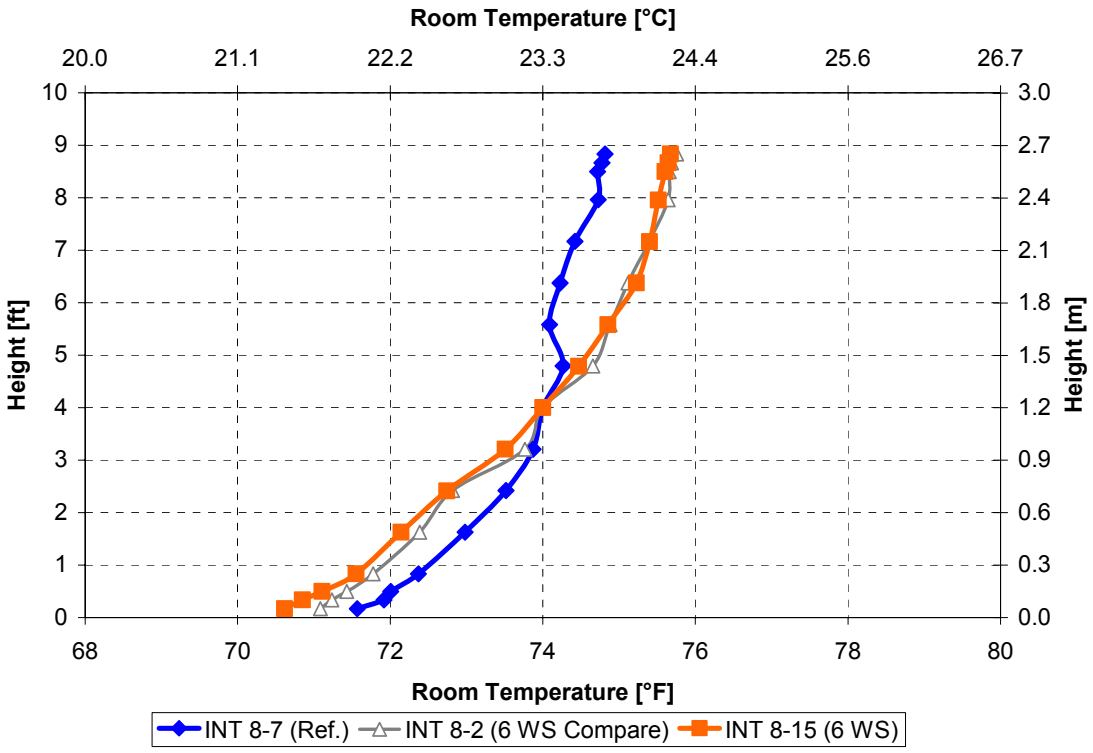

Figure 64: Results for leakage study for Krantz swirl diffusers under high load conditions (6 WS)

The next leakage test (INT 8-16) was performed with lower internal loads (2 WS) and at the same setpoint. Figure 65 shows that more stratification is created when the load is reduced. The leakage for INT_8-16 is 39% of room airflow which is roughly the same as INT_8-15.

Using INT_8-7 for the reference is not valid for making a direct comparison to INT_8-16 because it is not a 2 WS test. A non-leakage 2 WS test would have a lower airflow and thus more stratification than INT_8-7, but we did not test a 4 SW, 2 WS configuration without leakage. INT_8-9 is a 2 WS test comparable to INT_8-16 in terms of DDR. It shows a result similar to the 6 WS case but with somewhat less stratification suggesting that the leakage flow may have an effect over and above just the decrease in diffuser flow.

Comparing INT_8-15 and INT_8-16 does allow us to observe what happens when there is leakage and the load is reduced; i.e., the stratification increases. This is somewhat counter to the conclusions from our load variation study discussed in Section 4.2.4. And it is unlikely that this result is influenced by the leakage alone since the percentage of leakage is constant as load is decreased. (This constant percentage results from the fact that as a system with swirl diffusers is throttled, the leakage and airflow decrease roughly proportionally since they are both governed by the same Bernoulli effects.) We currently have not good explanation for this effect.

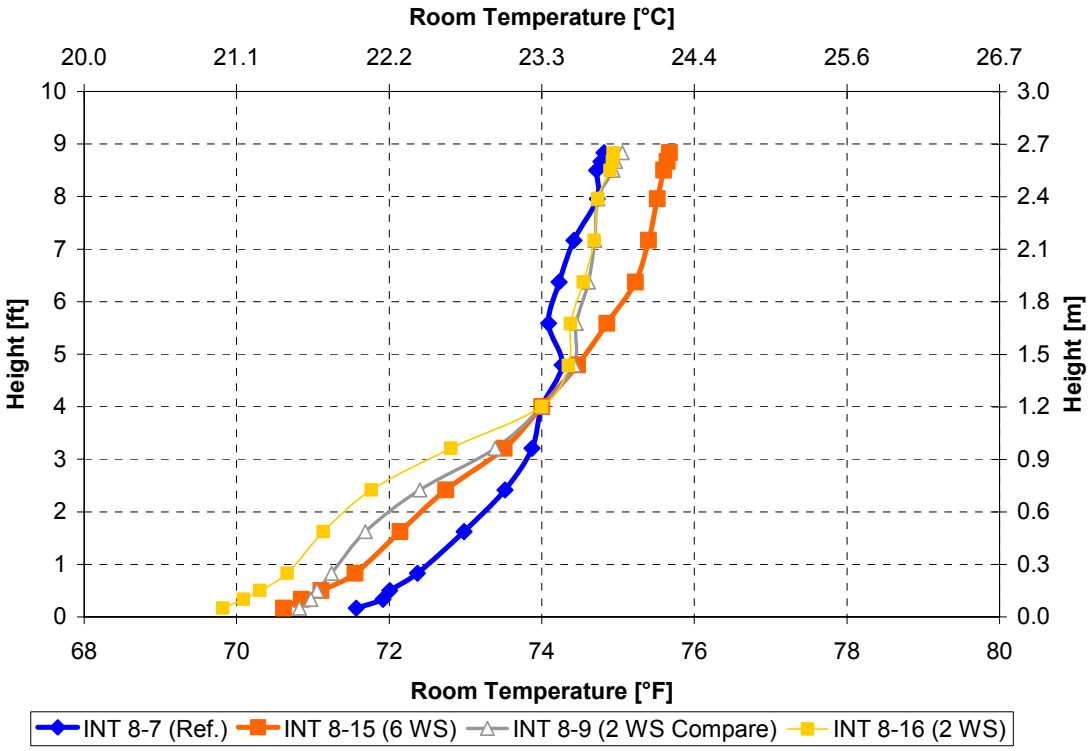

Figure 65: Results for leakage study for Krantz swirl diffusers under low load conditions

4.2.5.2 York Variable Area Diffusers (MIT)

Like the leakage experiments with Krantz swirl diffusers, we conducted two tests with VA diffusers at the same low (2 WS) and high (6 WS) load conditions and room setpoint of 23.3°C (74°F). The results are illustrated in Figure 66. The temperature profile of INT 6-14 has been normalized to a set point of 23.3°C (74°F) so that it can be compared to the high load leakage test as we did for the swirl diffuser cases.

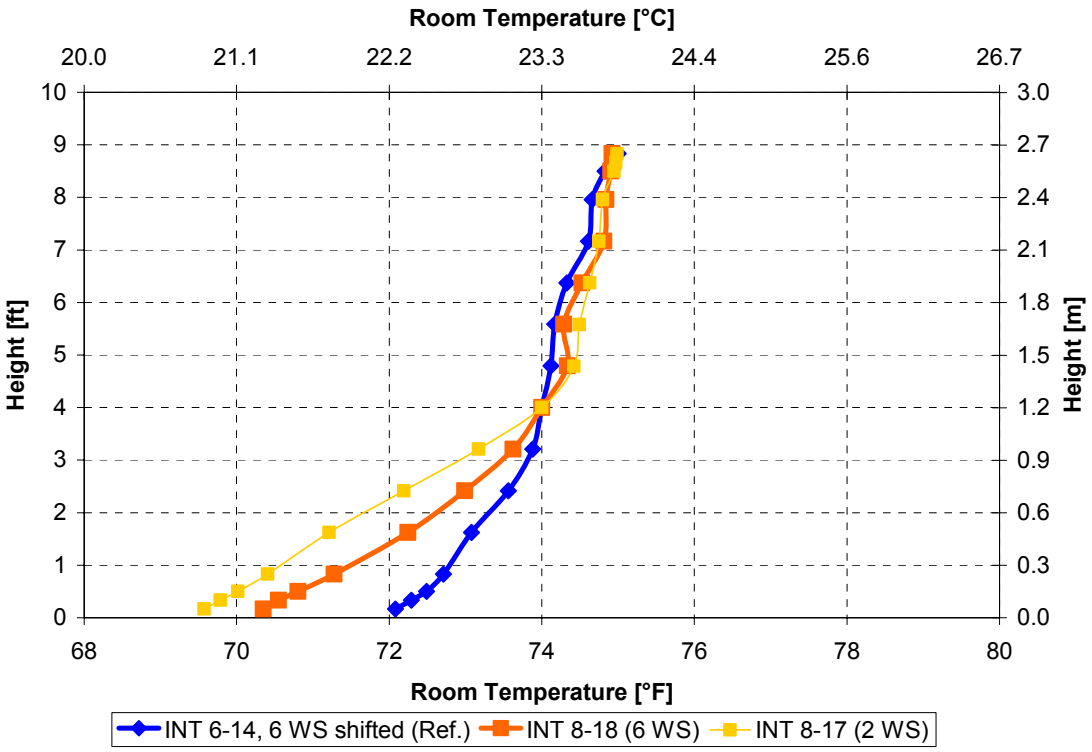

Figure 66: Leakage for York VA MIT diffusers under low and high internal load conditions

When we compare airflows and leakage rates for tests INT 8-18 and INT 6-14 with each other we see there are differences, i.e., the room airflows are not the same. This is most likely due to experimental and/or a normalization error since INT 6-14 was tested at a room set point of 22.2°C (72°F). However, this does not materially impact the comparison of the RAS profiles since we know from the results from previous sections above that VA diffusers have a consistent profile for a wide variety of operating conditions.

For all runs shown in Figure 66 the total floor leakage is equal because the plenum pressure is controlled to a fixed pressure of 12.5 Pa (0.05 iwc) for VA diffusers, although the room airflow was reduced for the lower load case. Both tests also show that the air going through the diffusers is *less* than the amount entering the room through floor panel leakage. In the higher internal load case, 51% of the total airflow is supplied through the leaking floor. As the internal load decreases (INT 8-17, 2 WS) the leakage rate increases to 88%. In this case, only 12% of the airflow enters through the diffusers. In fact for this test the diffusers were closed so that virtually all the airflow was supplied by leakage. This can lead to control problems in these low load cases since the diffusers will be virtually closed and the floor leakage becomes uncontrolled air entering the room.

In the case of VA diffusers these results indicate that the leakage itself is affecting the stratification, perhaps providing a displacement-like effect in the lower region of the room. The fact that this effect is more pronounced for VA diffusers indicates that as leakage becomes a greater percentage of the room airflow it has a greater impact on the stratification. Further research is warranted to understand the issue more fully.

To summarize, we can draw the following conclusions from these tests:

- There is a clear difference in how leakage affects room air stratification depending on the type and mode of operation of the diffusers.

- In VAV operation using plenum pressure modulation (e.g., passive swirl diffusers) the amount of leakage varies with underfloor plenum pressure just as the air volume through the diffusers does so the fraction of leakage is virtually constant.
- For constant plenum pressure systems (e.g., VA diffusers operated at constant pressure) the leakage rate is constant and the fraction of total room airflow made up by air leakage increases as load decreases. If leakage is excessive, control problems can result at low load conditions.
- For swirl diffusers, it appears that primary impact of leakage is due to a reduction of diffuser throw height and secondarily on the leakage itself. For VA diffusers it appears that the leakage itself is the primary cause. From these results we conclude that the cause of the change in stratification is split between the leakage itself and the reduced airflow through the diffusers; for pressure modulated swirl systems the emphasis is on the latter while for constant pressure VA systems the change is most likely due to the former.

4.3 PERIMETER ZONE TESTING

We conducted simulated perimeter zone tests in Sessions 7 and 8 to test how different diffuser types act under cooling operation for different perimeter load conditions (with blinds opened or closed) and different diffuser configurations. We describe the details of how these tests were performed in Section 3.3. In this testing we investigated two basic topics: 1) performance of linear bar grilles at the window, and 2) comparisons between linear bar grilles and other types of diffusers.

Perimeter zones operate somewhat like interior zones but in this case a thermal plume develops at the window due to the warm window surface temperatures. The strength of these plumes depends strongly on the window characteristics. Moreover, contrary to interior zones, since diffusers are normally positioned along the window, their airflow now interacts directly with the thermal plume. This practice complicates a theoretical understanding of this configuration.

4.3.1 LINEAR BAR GRILLES

Our objective for this testing was to determine the impact on room air stratification of linear bar grilles under typical solar and internal load conditions as that occur in open perimeter zones of office buildings. An example of the laboratory layout for this test series is shown in Figure 67. For this testing we used four swirl diffusers in the interior in addition to either 8 or 10 Titus linear bar grilles in the near vicinity of the window. Please refer to the layouts in Appendix A for the detailed lab layouts for this series of tests.

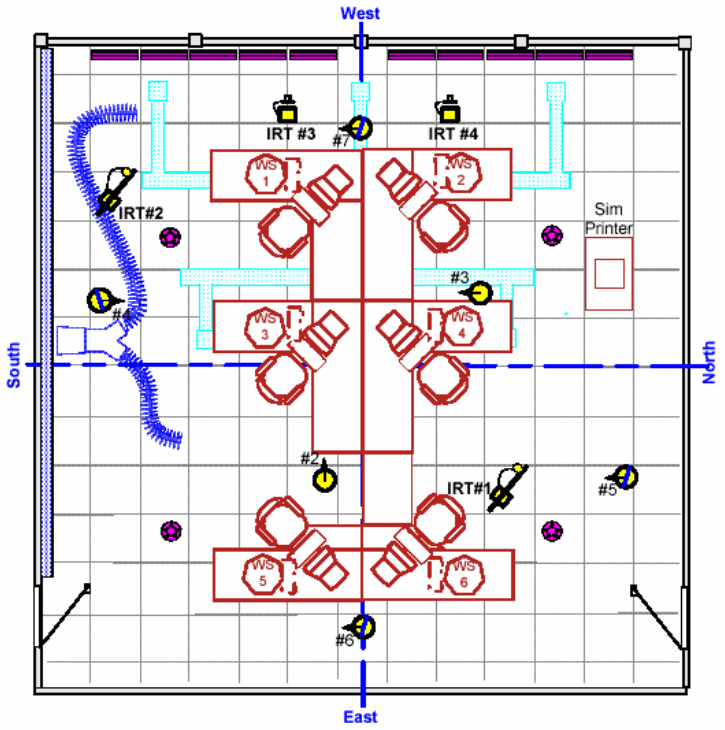

Figure 67: Lab layout for linear bar grille performance testing

All tests were controlled to a 24.4°C (76°F) setpoint using a VAV control strategy. All the results shown here we have normalized to 18.3°C (65°F) supply temperature and a 24.4°C (76°F) setpoint in the same manner as previous tests. We operated the four swirl diffusers in a manner to remove the internal gains from a 6 WS load condition. We did this by controlling the supply plenum to a pressure consistent with a diffuser airflow of 38 m³/s [80 cfm] per diffuser; their design condition. The additional cooling load due to solar gain was removed with the linear bar grilles. To simulate variable air volume fan coil units typically used in perimeter zones of actual buildings, we adjusted the dampers on the bar grilles for each test to balance the room airflow to accommodate the entire room load, while keeping the interior diffusers at their design airflow.

In Figure 68 two tests with peak load conditions are presented where 2 banks of the solar simulator were used to achieve a solar gain of approximately 70 W/m² (23 Btu/h-ft², 6.5 W/ft^2) (including conduction and convection at the window) plus an internal gain of 37.8 W/m² (12.5 Btu/(hft², 3.5 W/ft^2)) for a total of 107.8 W/m² (35.5 Btu/(hft², 10 W/ft^2)). In these tests we adjusted the vanes in the 8 bar grilles to produce either vertical airflow (90°, PER_8-21) or a sideways discharge of 53° from horizontal (PER_8-19) in an attempt to reduce the throw of the diffusers. For the interior loads we used the same 4 swirl configuration that we used for all of these tests. Summary data for these and other linear bar grille tests are shown in Table 20. In these tests, like for interior tests, the extraction rate of the room is less than the actual room heat gain because of the heat transferred to the plenum.

Table 20: Summary data for linear bar grille testing

Test ID	Diffuser Configuration	Solar	Blinds	Airflow		Extraction Rate		ΔToz	
				cfm/sf	l/(sm²)	Btu/(hft²)	W/m²	°F	°C
PER 8-18	8 LI, vanes at 90°	2 banks	Down	1.0	5.23	21.39	67.46	4.6	2.6
PER 8-19	8 LI, vanes at 90°	2 banks	Up	1.6	8.13	19.45	61.32	2.7	1.5
PER 8-20	8 LI, vanes at 90°	1 banks	Up	0.9	4.57	12.73	40.13	4.5	2.5
PER 8-21	8 LI, vanes at 53°	2 banks	Up	1.7	8.79	19.79	62.40	4.5	2.5
PER 8-22	10 LI, vanes at 53°	2 banks	Up	1.3	6.81	19.86	62.61	4.0	2.2
PER 8-23	10 LI, vanes at 90°	1 banks	Up	0.9	4.57	13.61	42.93	5.1	2.9

Figure 68 shows that there is virtually no difference in performance between the 53° and the 90° test for peak load conditions. Also the profile shape is the same for both runs.

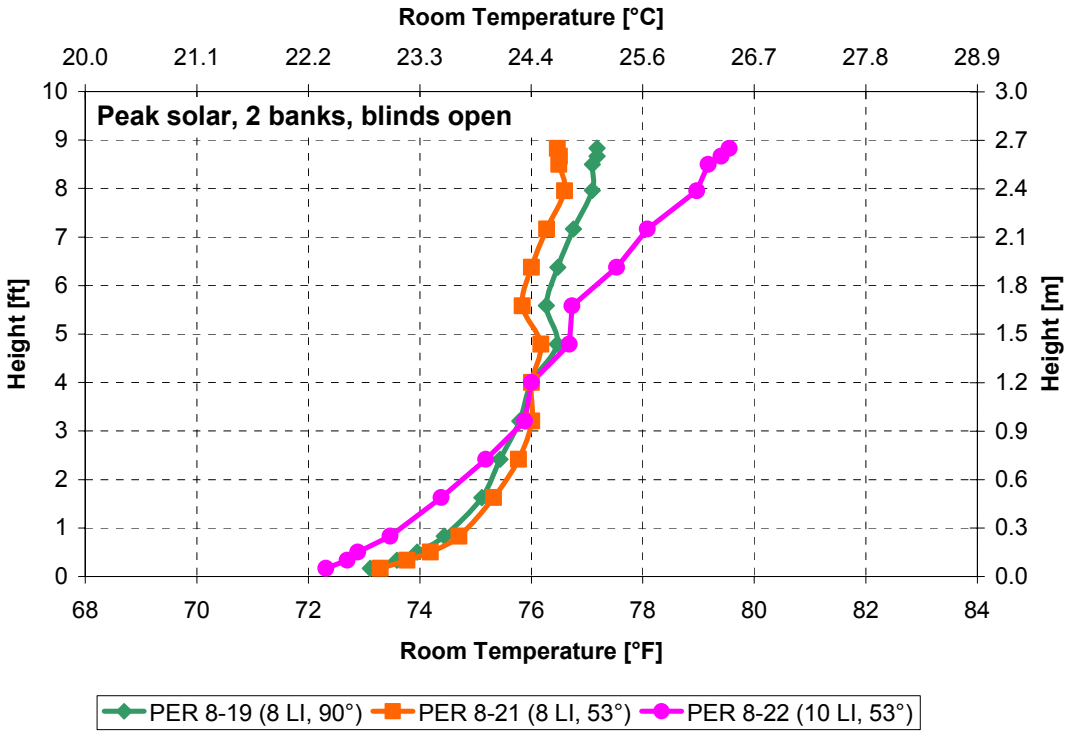

Figure 68: Linear bar grille performance comparing throw heights

Next we conducted experiments with 10 linear bar grilles to test the impact of lower throw for linear bar grilles. The results for full solar (2 banks) are shown in Figure 68 compared to the cases with 8 diffusers. In the case airflow is reduced about 23% due to the increased stratification caused by the lower diffuser throw for 10 diffusers. Note, however, that the occupied zone temperature difference is only 0.3°C (0.5°F) greater for the lower throw case indicating that the heat gain is confined predominately to the upper layer.

To understand the impact at lower solar loads we decreased the solar gain by turning off one bank of solar simulator lights for two cases; 8 diffusers at vertical discharge (PER_8-20) and 10 diffusers at 53° discharge (PER_8-23). Reducing the solar gain while keeping the same room setpoint, results in lower airflow through the diffusers (and thus the throw). In this case, as we

expected, the stratification increases as shown in Figure 69. Here it is shown that 10 diffusers with 2 banks of solar increased stratification by the same amount as reduced load with 8 diffusers. However, for 1 bank of solar, the stratification increased only slightly when 10 rather than 8 linear diffusers were used and the airflow did not change. This indicates that there may be an upper limit to what can be accomplished by reducing throw from linear bar grilles. Further study is warranted to verify this conclusion.

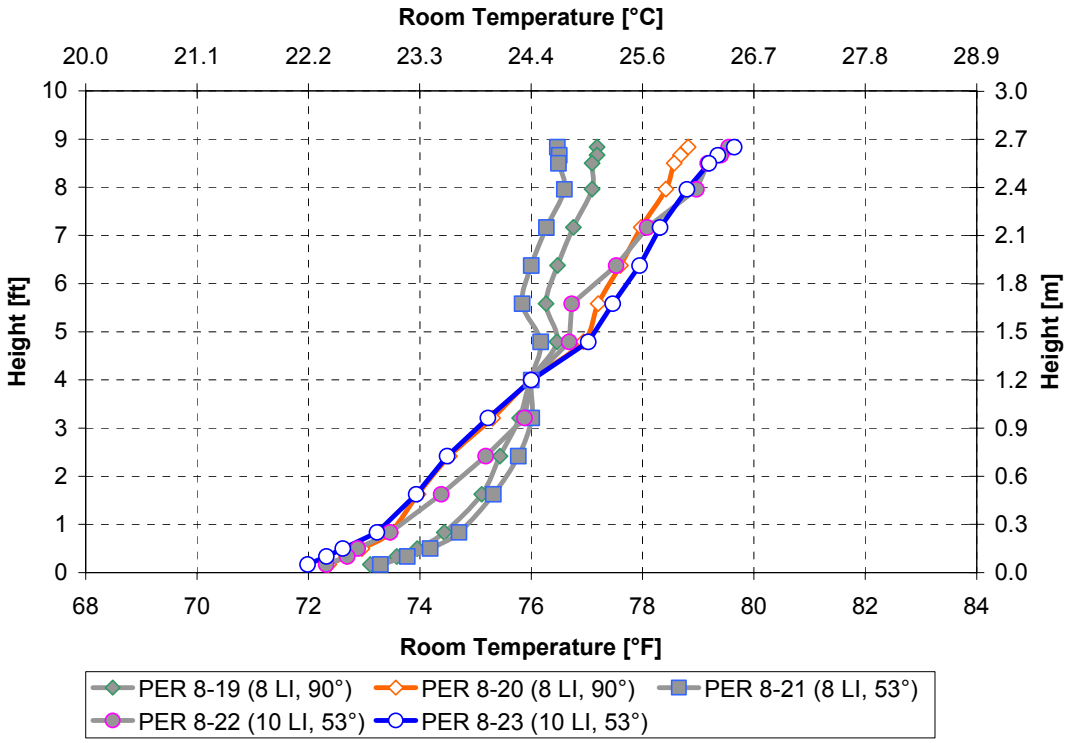

Figure 69: Linear bar grille performance with half solar, comparing to full solar (gray lines)

To sum up the performance of linear bar grilles, it can be said that the most significant difference in the temperature profiles (and airflow rates) can be found when linear bar grille throw is decreased by adding diffusers for a given load, or decreasing load (and airflow) for a given number of diffusers.

The impact of the vanes can not be determined since we did not conduct tests with 10 linear grilles at a 90° vane angle for 2 banks solar and 53° angle with 2 banks solar to compare against. Furthermore, the arrangement of vanes was different for the tests. With 8 bar grilles, the vanes of each diffuser were set to blow to the adjacent diffusers spaced one floor panel apart causing the supply air to mix to a certain amount. When 10 diffusers were used, the direction of air was divided in the middle of the window, blowing towards the south and north wall. Using this setup, the mixing may have been reduced as well.

4.3.1.1 Impact of blinds

We made an interesting discovery when the blinds were closed for a test with 8 linear bar grilles and 2 banks of solar. Based on a heat balance analysis (not included herein) we estimate that the total solar heat gain with 2 banks of simulator lights is about 25% (~15% reduction in total gain) less than with blinds open. However, as shown in Table 20 the extraction rate for PER_8-18 (blinds down test) is about 8% *greater* than for the other two tests, PER_8-19 and PER_8-21. This suggests that less heat entered the supply plenum from direct radiation to the floor due to the

shading. More importantly, Figure 70 shows that the room temperature difference is greater by almost 50% (return air temperature at ceiling increases from 77.2°F (25.1°C) to 83.5°F (28.6°C)) when blinds are down. This results in a reduction of airflow of about 40% as shown in Table 20, but if we factor in the 15% lower gain it would be about 25% less due to the increased stratification. Note that the occupied zone difference is virtually the same for this test and the others with blinds open. This may have significant implication on design, operation and energy performance of UFAD systems.

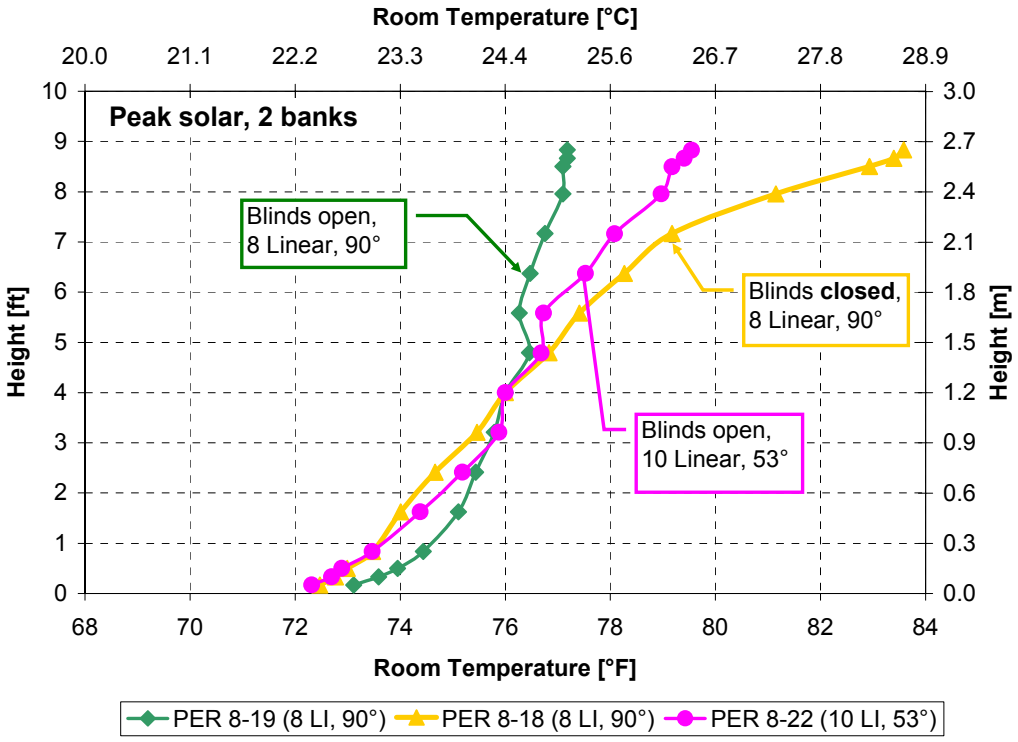

Figure 70: Linear bar grille performance with and without blinds

4.3.2 DIFFUSER TYPES

In this series of tests we evaluated the impact of different diffuser types on room air stratification. Specifically, we conducted tests to compare York MIT VA diffusers and no diffusers at the window with the linear bar grille tests described in the previous section. In typical office installations, the VA diffusers would be about 20 cm (8.5 in) closer to the window (west wall) than they were in the diffuser configuration tested. In the lab it was not possible to realize this because the arrangement of floor panels did not allow it (there was one half-floor panel next to the west wall where the MIT diffuser could not be mounted).

We tested the case with no diffusers at the window to evaluate how performance would be affected if we did not disturb the thermal plumes at the window. For these tests we increased the number of swirl diffusers in the room away from the window. By increasing the number of diffusers, the DDR (about 0.75) and throw height of the diffusers was also lowered.

The results shown in Figure 71 demonstrate room air stratification profiles for two tests with linear bar grilles (PER 8-21 and PER 8-22), a 9 York VA MIT diffuser case with 5 diffusers near the window and 4 in the interior (PER 8-2), and a 16 swirl diffuser case with no diffusers at the window (PER 8-11). Summary data for these tests is shown in Table 21.

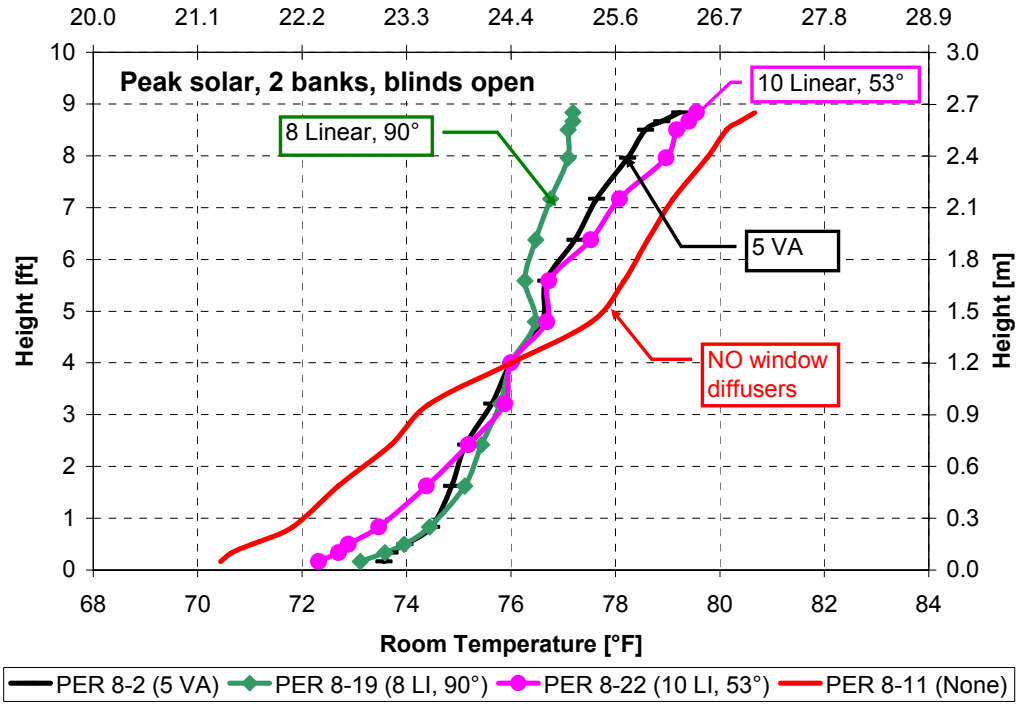

Figure 71: Diffuser type comparison for perimeter zones

Table 21: Data for diffuser comparison in the perimeter zone

Test ID	Diffuser Configuration	Solar	Blinds	Airflow		Extraction Rate		ΔToz	
				cfm/sf	l/(sm²)	Btu/(hft²)	W/m²	°F	°C
PER 8-2	5 VA at window	2 banks	Up	1.6	8.18	23.10	72.83	2.9	1.6
PER 8-11	16 SW, none at window	2 banks	Up	1.4	7.11	22.11	69.71	7.5	4.2
PER 8-19	8 LI, vanes at 90°	2 banks	Up	1.6	8.13	19.45	61.32	2.7	1.5
PER 8-22	10 LI, vanes at 53°	2 banks	Up	1.3	6.81	19.86	62.61	4.0	2.2

PER_8-19 is the linear bar grille test with 8 grilles at the window with vanes at a 90° angle and 4 swirl interior diffusers to remove the internal loads. PER_8-22 is similar to PER_8-19, except that it has 10 diffusers at the window with the vanes at a 53° angle.

The comparison of the VA diffuser performance (PER_8-2) with PER_8-22 shows that the VA diffuser operates at about 23% more airflow with a lower ΔT_{oz}. However, the extraction rate is about 16% greater for the VA diffuser so to first order there appears to be little difference in airflow between these two diffuser types. Further analysis is required to determine if the total heat gain was the same or not for these tests. In general, the charts confirm that the temperature distribution in the occupied zone is similar for all linear bar grille tests and the VA tests. Again, we should mention that VA diffusers behave similar under a wide range of testing conditions (refer to chapter 4.2.1.2). Therefore, only one VA test is shown in the chart above.

The highest temperature difference in the room of about 9K (16°F) is achieved when no diffusers are placed near the window, which was realized with the Krantz swirl diffuser layout (PER 8-11).

The average temperature in the occupied zone lies below that measured in other experiments, and also the return temperature is higher, thus the occupied zone difference is 4.2°C (7.5°F) for this test, and exceeds the ASHRAE Standard 55 limits of 3°C (5°F). For comparing airflows the differences in extraction rate complicate the analysis. If we assume that the performance is the same for 10 linear and 5 VA tests when operated at equivalent heat gains) then the airflow requirements for the swirl test (PER_8-11) would be approximately 12% lower. However, this test also needs to be further studied to determine the cause of the differences in extraction rate between test PER_8-22 and PER_8-2 before a final conclusion can be drawn.

5 SUMMARY AND CONCLUSIONS

In the following we summarize the significant findings and practical implications from the full scale room air stratification experiments.

5.1 FINDINGS BASED ON INTERIOR ZONE TESTS

5.1.1 DIFFUSER TYPE

The three diffuser types (four including linear bar grilles in perimeter zones) we studied have distinctly different characteristics and therefore provide a good representation of the range of characteristics we expect to find in practice. To summarize briefly: 1) Swirl diffusers come in two varieties. First there are the 'standard' designs which are the most prevalent and are passive (not physically controlled, although variants do exist that are actively controlled in some manner), have discharge patterns that impart a swirl motion to the vertically discharged airflow. Second, there are low throw or, as we refer to them in this paper, horizontal discharge swirls that impart a swirl but where the discharge pattern is horizontal rather than vertical. 2) Variable area diffusers represented best by York's MIT diffusers, where the outlet area is modulated by a moving damper.[8]

Our overall conclusions relative to diffuser type are:

- Standard swirl diffusers can produce large differences in stratification depending on design and operating conditions. HD swirls and VA diffusers, on the other hand have a relatively narrow range of stratification performance. See Table 22 for a summary of diffuser characteristics for the diffusers we tested. Another way we can express this is to say that variation in throw drives the performance of standard swirls, but does not with the other two. VA diffusers produce a very consistent profile over a broad range of design and operating conditions.
- At typical diffuser design conditions both standard swirl and VA diffusers operate the same for a given load and thermostat setting.
- When controlled at the same thermostat setting under VAV control using diffusers operating at their nominal design airflow, there is no difference in performance for VA and standard swirl diffusers. If the number of swirl diffusers is increased and the control setpoints remain the same, both diffuser types will require the same airflow. However, if in this latter case the system is operated at equivalent comfort conditions, the swirl diffusers will require less airflow.

[8] We should note that the testing reported on here used York's original design that has been largely replaced by the newer MIT 2 which is a different design that operates using a pulsed width modulated damper that discharges into a fixed discharge diffuser area. We have not compared the performance of this new product to the results shown herein.

Table 22: Diffuser characteristics summary

	Discharge area	Vertical throw	Nominal design airflow, cfm
Swirl, standard	Constant	Variable	80
Swirl, HD	Constant	Nearly constant	60
Variable area	Variable	Constant	150
Linear	Constant	Variable	250 (48")

5.1.2 SWIRL DIFFUSERS

5.1.2.1 Design conditions

As we have pointed out above, swirl diffusers have a greater potential for managing stratification because of the variation of throw with operating conditions. Our test results show how much the stratification in the occupied zone can be changed under the same load conditions and setpoint.

We also show that swirl diffusers produce the same profile independent of load condition when the throw height is the same. This result is useful for design but not for operations, because the throw varies as load changes in VAV systems. For constant volume systems the profile would stay the same with load (at its design condition), only the SAT varies to maintain the thermostat setpoint [Webster et. al. 2002]. When we change the throw height (by increasing diffusers or changing airflow (e.g., change the load or setpoint) for the same number of diffusers we see changes in the stratification.

When we combine these results with our preliminary analysis comparing airflow requirements based on equivalent comfort conditions, we see that swirl diffusers offer designers flexibility to optimize stratification (to reduce airflow while maintaining comfort) in a way that VA and HD swirl diffusers do not. For HD swirls, despite the fact that stratification is somewhat fixed, the stratification is maximized which results in minimizing the airflow. However, in some cases this can result in occupied zone temperature differences that exceed the ASHRAE Standard 55 criteria.

5.1.2.2 Operating conditions, load variation

The results obtained by the load variation study are somewhat mixed and further research needs to be done to corroborate our overall impression that the profile shape does not change as load is varied. If this is true it will have very interesting and important implications on practice: This would mean that during design, practitioners could "dial in" the stratification level they feel is appropriate and expect that it would remain consistent during load variations producing a reliable comfort environment. It also would allow optimization of stratification during commissioning at reduced loads, thereby saving cost and effort.

5.1.3 FLOOR LEAKAGE

This part of our testing produced some very important results and should prove helpful to design, commissioning and operations. The primary impact of floor leakage is on what we call Category 2 or "good" leakage -- leaks where the air enters the conditioned space. Although, in general, we used leakage rates greater (ranging from 0.12 to 0.3 cfm/ft^2 over all the leakage tests) than we

would expect to see in real systems they were not outside of the realm of possibility based on reports that we have received from commissioning studies on real buildings.

However, the effect on stratification appears to be different for swirl vs. VA diffusers. For pressure modulated swirl systems, stratification is increased due to two effects, the leakage itself causing a displacement like component to the airflow, and a reduction in airflow through the diffusers which decreases their throw. In addition for these systems;

- Leakage is proportional to the airflow reduction such that the ratio to total room airflow is constant
- The plenum pressure is reduced in proportion to how much floor leakage there is, thus potentially reducing the amount of Category 1 or "bad" leakage -- leakage out of the system that represents airflow lost.

For VA systems using constant pressure plenums, a similar increase in stratification with increasing leakage was observed. However, in this case the effect appears to be due to leakage alone since these diffusers are insensitive to airflow changes because they modulate. However, because the pressure is constant the relative proportion of leakage airflow increases as load decreases. This can lead to a loss of control at very low load conditions in combination with high leakage rates.

We tend to think of all leakage as undesirable but, based on these results, perhaps we are overly concerned about floor leakage in pressure controlled swirl systems; if the effect is to increase stratification and reduce Category 1 leakage, as long as it does not create local comfort problems, it may not be particularly deleterious.

5.2 FINDINGS FROM PERIMETER ZONE TESTING

For perimeter testing our results fall into three categories of studies; the effect on stratification performance of diffuser throw, diffuser type, and the impact of blinds closed vs. open.

5.2.1 DIFFUSER THROW

Although perimeter loads derived from peak solar gain can be larger than interior loads by a factor of 2 and the type of thermal plume is different than for internal loads, the stratification performance appears to be dominated by diffuser characteristics much as it is for interior zones. To study this impact we tested linear bar grilles, the predominant type if perimeter diffuser used today in most UFAD buildings (except of course, those with the York MIT system). In peak solar (2 banks of simulator lights) tests we decreased the throw characteristics by both increasing the number of diffusers and decreasing the (sideways from horizontal) angle of discharge of internal "flow-spreading" vanes. While we were unable to conduct enough tests to definitively determine the effect of vanes, our results clearly show that stratification is increased and airflow is reduced as throw is reduced. For example, airflow required for a load condition of ~10 W/ft^2 and 10 diffusers with 53° discharge versus 8 diffusers with vertical (90°) discharge is reduced by ~ 23%.

5.2.2 DIFFUSER TYPE

To compare the performance of different diffuser types we attempted to "bracket" this range by including the known diffuser types of VA and linear bar grille, but also adding a test using swirl diffusers located only in the interior so there were no diffusers near the window. This last case represents the ultimate possibility for reducing the interaction between the diffuser flow and the window thermal plume.

Results from these tests showed that linear bar grilles and VA diffusers performed comparably but for the case with no window diffusers we observed a large increase in stratification. In fact, the observed stratification exceeded the ASHRAE Standard 55 recommended limits. We estimate

that this larger stratification results in a nominal 12% lower airflow requirement for no window diffusers. This configuration deserves more study since optimizing the competing elements of occupied zone temperature difference and average temperature (i.e., equivalent comfort) would likely alter the conclusions from this single test. The final airflow requirements would be determined by a balance between increasing the setpoint to increase the occupied zone temperature and the effect produced by reducing the number of diffusers to increase throw and thereby reduce the stratification.

5.2.3 IMPACT OF BLINDS

Lowering blinds is a common practice in real buildings, especially under peak load conditions when direct solar gain and glare become intolerable. We tested the impact of lowering the blinds and found that this dramatically increases the temperatures near the ceiling, even though the total gain is reduced. We found that lowering the blinds (for the peak solar conditions tested) had the following impacts:

- Total heat gain (solar plus internal loads) reduced by about 15%
- room temperature difference increased by almost 50% (less heat transferred to the plenum)
- Occupied zone temperature virtually unchanged
- Estimated airflow (on equal heat gain basis) reduced by about 25%

These results indicate that lowered blinds has a substantial impact on the performance of perimeter zones that should be studied in more detail to develop a better understanding of its implications on design and energy performance, and its demand response possibilities.

6 RECOMMENDATIONS FOR FURTHER ANALYSIS AND RESEARCH

In this section we outline the work that remains unfinished due to lack of resources, as well as our "wish list" for further work that we view as important to advance UFAD toward the goal of a comprehensive understanding that we believer is necessary to fully develop the technology.

Remaining work (in order of importance)

- EnergyPlus models – Complete the semi-empirical models for interior and perimeter systems based on analysis of full scale and bench scale data.
- Validation – Using ADRF test chamber data complete the validation studies already begun using the final form of the UFAD models. Includes documentation of simplified heat balance analysis of full scale data.
- Overhead lighting – Complete overhead calibration testing analysis and comparison to OSU data [Fisher 2006] and document results.
- Comfort – Document preliminary comfort analysis.
- Uncertainty calculations – Complete the analysis and documentation of experimental uncertainty.
- Review preliminary findings presented in this report.

Further testing

- Window plumes and perimeter zone optimization studies; impact of blinds, reduced number of diffusers, etc.

- Load variation studies, interior and perimeter.
- Load characterization studies; load interactions, types of loads including newer more typical office equipment and window treatments.
- Linear bar grilles discharge angle effect on performance.

7 ACKNOWLEDGMENTS

This work was supported by the California Energy Commission (CEC) Public Interest Energy Research (PIER) Buildings Program under Contract 500-01-035. We would like to express our sincere appreciation to Norman Bourassa and Martha Brook of the CEC PIER Buildings Team, who expertly served as our current and original Commission Project Managers, respectively. We would like to acknowledge the invaluable assistance and guidance provided by our team members Paul Linden and Anna Liu at UC San Diego. In addition we would like to thank Allan Daly of Taylor Engineering for his insights and his contributions in creation of an EnergyPlus input utility for the chamber model and Ian Doebber of Arup for his help with the EnergyPlus input and solar gain analysis. We would also like to thank Fred Buhl from the Simulation Research Group at Lawrence Berkeley National Laboratory, who provided technical advice related to the implementation of the new UFAD module into EnergyPlus and Dan Fisher of Okalahoma State University who provided invaluable guidance about laboratory instrumentation and lighting heat gain. Our team members from York International; Jack Geortner, Jim Reese, Paul Trauger, Mike Filler, and Luke Dunton deserve special mention for their contribution in providing the laboratory facilities and support for testing without which this project would not have been possible.

8 REFERENCES

Agilent. 2005. Agilent Technologies, HP34970A Data Acquisition/Switch Unit website: http://www.metrictest.com/catalog/brands/agilent/pdfs/5965-5290EN.pdf (accessed on 06/05/2005)

Bauman, F. 2003. *Underfloor Air Distribution (UFAD) Design Guide.* Atlanta: ASHRAE, American Society of Heating, Refrigerating, and Air-Conditioning Engineers. 243 pp.

Bauman, F., T. Webster, and H. Jin. 2006. "Design Guidelines for Underfloor Plenums." *HPAC Engineering,* July.

Bauman, F., T. Webster, et al. 2006. Final Report to CEC PIER Buildings Team – "Energy Performance of Underfloor Air Distribution (UFAD) Systems." CEC Contract No. 500-01-035. Center for the Built Environment, University of California, Berkeley, December.

Benedek, C., T. Webster, F. Bauman, P. Linden, Q. Liu. 2006. Final Report to CEC PIER Buildings Team – "Part VI: UFAD Cooling Airflow Design Tool." CEC Contract No. 500-01-035. Center for the Built Environment, University of California, Berkeley, December.

Brandt MST. 2005. Loop Powered Multivariable SMARTFLOW transmitter, Thermo Electron Corporation, http://www.thermo.com/com/cda/product/detail/1,1055,14145,00.html (accessed on 7/26/2005)

Chromalox 2003. "QRT Quartz Tube Radiant Heater." Specifications. Chromalox, Ogden UT.

Epply (a). 2006.Epply Laboratories. Model PSP Pyranometer specifications website: http://www.eppleylab.com/PrdLabThermopile.htm

Epply (b). 2006.Epply Laboratories. Model PSP Pyranometer specifications website: http://www.eppleylab.com/PrdPrecSpectralPyrmtr.htm

Fisher, D. 2006. Personal communication, AHSRAE RP-1282, Oklahoma State University, Stillwater OK

IES. 1991. The Illuminating Engineering Society of North America (IESNA), "Photometric and Thermal Testing of Air-Cooled Heat Transfer Luminaires", IESNA LM-56-91, 8th of June 1991

Jin, H., F. Bauman, and T. Webster. 2006. "Testing and Modeling of Underfloor Air Supply Plenums." *ASHRAE Transactions,* Vol. 112, Part 2.

Krantz (a) 2005. Floor Twist Outlets, series DB-E website: , http://www.krantz.de/kunden/krantz-komponenten/internet/ProduktKatalog.nsf/main/99479FED60DB974F41256AB6003822DD/$file/3.1_1146a_s_11-02.pdf (accessed on 10/05/2005)

Krantz (b) 2005. Floor Displacement Diffusers, series Q-B-DN200 website: http://www.krantz.de/kunden/krantz-komponenten/internet/ProduktKatalog.nsf/main/CB54166DA77EF6CC41256AB5003ACF43/$file/3.6_4062e-l-s-2004-04.pdf (accessed on 12/05/2005)

Lin, Y., and Linden, P.F. 2005. "A model for an underfloor air distribution system." *Energy and Buildings*, 37, 399-409.

Lithonia Lightning. 2005. Paramax Parabolic Troffer, Product Number: 2PM3N website: http://www.lithonia.com/products/Family2.asp?Brand=LL&Family=PM3N&ProductType=Fluorescent%20Lighting&Category=Recessed&SubCategory=Parabolic%20Lighting (accessed on 08/05/2005)

Liu, Q, and P. Linden. 2005. "An Extended Model for Underfloor Air Distribution Systems", University of California, San Diego, Mechanical and Aerospace Dept.

Liu, Q.A. and P. F. Linden. 2006 "The fluid dynamics of an underfloor air distribution system." *J. Fluid Mech.*, 554, 323 - 341.

Mitchell, R., C. Kohler, D. Arasteh, and C. Huizenga. 2001. Window5 and Optics5 Software. Environmental Energy Technologies Division, Lawrence Berkeley National Laboratory. Berkeley, November. http://windows.lbl.gov/software/software.html

Ohio 2003. Model PC5 AC Watt Transducer. Ohio Semitronics, Inc. Hilliard OH.

Raytek. ,2005. Raytek Automation Products, MI Compact Series IRT website:, http://www.raytek-northamerica.com/admin/file_handler/2ae6092f570efab9e577de9b6820919c/1015439839/MI_DS_2-1702__Rev_F.pdf (accessed on 08/05/2005)

Setra 2006. Model 256 Specifications. Setra Systems, Boxborough MA.

Tate. 2005. Tate Access Floors, All Steel Panels, All Steel 1000 website: http://www.tateaccessfloors.com/all_steel_panels.html (accessed on 08/05/2005)

Titus. 2006. Titus CT-481 Electronic Product Catalog website: http://www.titus-hvac.com/ecatalog/

Webster, T., and F. Bauman, 2006. "Design Guidelines for Stratification in Underfloor Air Distribution (UFAD) Systems." *HPAC Engineering,* June.

Webster, T., F. Bauman, M. Shi, D. Dickerhoff. 2004. "Full Scale Testing Experimental Plan." Center for the Built Environment, University of California, Berkeley, July.

Webster, Tom, F. Bauman, and J. Reese, 2001. "UFAD Room Air Stratification Testing," CBE Internal Report, October.

Webster, T., F. Bauman, J. Reese and M. Shi, 2002. "Thermal Stratification Performance of Underfloor Air Distribution (UFAD) Systems." *Proceedings, Indoor Air 2002,* Monterey, CA, June.

York. 2005. York International, ISN Advantage Programmable Controllers, Facility Manager website: http://www.york.com/esglist/pdf/faciltymgr.pdf (accessed 08/05/2005)

York. 2005. Air Side Products, Underfloor Air Systems, Tech Guide website: http://www.york.com/products/esg/YorkEngDocs/847.pdf (accessed on 12/05/05)

Zhang, H., C. Huizenga, E. Arens, T. Yu, 2005. "Modeling Thermal Comfort in Stratified Environments," *Proceedings, Indoor Air 2005: 10th International Conference on Indoor Air Quality and Climate*, Beijing, China, September.